INTRODUCTION TO MORPHOLOGY

Ralph Abraham

"The next great era of awakening of human intellect may well produce a method of understanding the *qualitative* content of equations. Today we cannot see that the water flow equations contain such things as the barber pole structure of turbulence that one sees between rotating cylinders. Today we cannot see whether Schrödinger's equation contains frogs, musical composers, or morality - or whether it does not. We cannot say whether something beyond it like God is needed, or not. And so we can all hold strong opinions either way."

Feynman [403, p. 41-12]

CONTENTS

PREFACE

In recent years, the crises of the modern world have penetrated the scientific community with great force, and many have agonized over the question of the relevance of scientific research. Among mathematicians, this generally takes the form : is mathematics worth doing ? Buckminster Fuller writes that our species can survive only by means of a great evolutionary change [104]. René Guénon analyzes in detail the role of scientific materialism in the present crisis [105]. Oliver Reizer has outlined a reoriented, reintegrated science of the future, which could serve mankind in a crucial way [113].

During the past four years, I have devoted my time to these questions, and the search for ideas, especially in Eastern philosophy, which give some foundation for socially responsible and valuable scientific research. My position in these matters, at present, is represented by this paper, which is intended to open a door to the relatively inaccessible ideas of René Thom. The applications which interest me the most, described in the last chapter are close in spirit to the world view of Oliver Reiser.

My efforts to understand morphology and its potential applications to human life have been made possible by the great generosity of many colleagues and friends, who have given me all kinds of time, information, teaching and encouragement. Here I would especially like to thank :

Baba Hari Das
Baba Ram Das
Dick Bierman
Emilia Hazelip
Ralph Metzner
Jack Moore
Zdenek Rejdäk
Michael Saso

David Fowler
P.G. Gennes
John Guckenheimer
Klaus Jänich
Hans Jenny
Jerrold Marsden
Joel Robbin
David Ruelle

Russell Schofield	Floris Takens
Simon Vinkenoog	René Thom
Stan White	Chris Zeeman

In addition, I am grateful to the Institut des Hautes Etudes Scientifiques, and the Universities of Aarhus, Amsterdam, and Firenze for financial support this year, and to the University of Lyon for undertaking to publish this work.

Finally, I would like to thank William Barit, Joel Robbin, Floris Takens, and René Thom for reading the manuscript and suggesting several important improvements.

PART I

MATHEMATICAL FOUNDATIONS

This half of the survey is devoted to the basic constructs of Thom, for the morphometrization of phenomenological processes with controls : logos, morphos, and catastrophy. It ends with a zoo of the archetypal catastrophes presently known, for the morphostatic and morphodynamic schemes. Perhaps it is easier to read this after looking briefly at Part II.

CHAPTER I. MORPHOMETRY

The ideas of Thom's morphogenesis cross various levels of abstraction. At one extreme, there is a phenomenological philosophy of science of a classical type, which I call morphosophy. At the next more specific level, there is a scheme for parameterizing observations with mathematical structures, morphometry. Next, he defines some special cases of this scheme, the metamodels. For the most commonly used metamodels, there are the beginnings of a mathematical classification, catastrophe theory.

1. Morphosophy. While I feel that a satisfactory description of morphosophy is beyond my competence, I would like, at least, to place it in a historical context. Although not a prequisite for understanding morphology, I suppose it softens the blow of radical ideas to know they have precedents.

The earliest extant morphosophic text known to me is the Pêm Ching of the Chou Dynasty - from about 800 B.C. - which is preserved today as the core of the I Ching, or Chinese Book of Changes [107]. It is based on the idea that all life manifestations are realizations of archetypal forms and their mutations. Probably a prior version of this theory originated in Sumer or Egypt many centuries earlier, because it appears later in two branches of the river of knowledge from the ancient Near East in India, brought by the Vedic Aryans and expressed in the Rg Veda and in the Sankhya philosophy of Kapil, in the form of the theory of vibrations : all observed phenomena are manifestations of the akashic vibration - and in Greece, transmitted by Thales and Phytagoras, who studied in the Egyptian mystery schools, culminating in the theory of ideas of Plato and Aristotle : phenomena consist of substance and form, realizing abstract archetypes ($i\delta' \in \alpha$ = form [108]). An excellent survey of morphosophy from Thales to modern neurobiology can be found in Black [102]. Thom's book [201] is replete with quotations from Heraclitus, and references to European philosophers of recent centuries. In his manuscript, which has been floating around publishing houses for five years but has yet to appear, mathematics and morphosophy are reunited for the first time since Pythagoras. With the aid of mathematical metaphors, primarily from the qualitative theory of dynamical systems, Thom has raised phenomenology to unprecedented hights.

2. Logos and morphos. Probably the most basic innovation of Thom is a scheme for the mathematical description of form, as observed in phenomenological processes, which is implicit in his work. In this section, I will describe this scheme, somewhat generalized.

Suppose a process is observed repeatedly, and all its forms recorded. The most obvious parameterization of the observed forms would be to describe mathematically a set, Φ , such that each form observed was represented by a point of the set, $\varphi \in \Phi$. Thom rejects this method in favour of a more sophisticated one. Suppose that each observed state may be adequately labelled by a mathematical structure, φ . This will have an underlying set, D , which is the domain (or substance) of the state, on which φ specifies the observed form. For example, if we observe the second hand of a watch, and parameterize its position by a point on a circle $\theta \in S^1$, and its angular velocity by a real number, $v \in \mathbb{R}$, our observations may be recorded as a curve

$$\varphi : \mathbb{R} \to S^1 \times \mathbb{R} : t \mapsto \varphi(t) = (\theta(t), \gamma(t))$$

If it is a very good watch, this curve will be periodic, even though the function $x(t)$ is not constant. Then instead of recording the observation as point in a function space, $\varphi \in \Phi$, we may equivalently describe it as the function

$$V : S^1 \to \mathbb{R} : \theta \mapsto V(\theta)$$

such that $V(\theta(t)) = v(t)$. Then the domain is the circle, $D = S^1$, and the form is the mathematical structure on D given by the real valued fucntion V . In other situations, the form may be some other kind of structure, for example, a distance function, a topology, a vectorfield, and so on.

Now suppose that we have a <u>corpus</u>, or complete set of observations of a process, $\{\varphi_i | i \in I\}$, where I is some indexing set. For each state, φ_i , there is an underlying domain, a set, D_i . A <u>phase space</u> for the process is a set, P , containing all of these domains, $\cup D_i \subset P$. Usually this is suggested naturally, and points of P are actually observable, or measurable, in the experiment. A domain, $D_i \subset P$, may be a set of measurable phases of the process, occupied in succession in a way described by the form, φ_i , as in the watch example.

The next step is to take account of the fact that most experiments, or observed processes, have controls. We may suppose that the laboratory is like a television set. The experimentalist turns the control knobs, and for each setting of the controls, observes various forms on the screen. Suppose that the possible settings of these controls are parameterised the obvious way. Thus we have a set C, the <u>control space</u>, and each control value is represented by a point, $c \in C$. For each value, $c \in C$, only some of the forms of the process are observed, say $\{\varphi_i | i \in I_c \subset I\}$.

Now let's concentrate on the domains of the observed forms. For each control setting, $c \in C$, appear some of the domains, $\{D_i | i \in I_c\}$. These may be visualized in the product of the control and phase spaces, $C \times P$. For each $c \in C$, let $\alpha(c) = \cup\{D_i | i \in I_c\}$, the union of all the domains observed at this control. If 2^P denotes the set of all subsets of P, then we have defined a function, the <u>actual logos map</u>,

$$\alpha : C \to 2^P : c \mapsto \alpha(c)$$

which is a multiple-valued function from c to P. Recall that the <u>graph</u> of a function

$$f : C \to 2^P : c \mapsto f(c)$$

is the subset, $F \subset C \times P$, defined by

$$F = \cup \{\{c\} \times f(c) | c \in C\} \quad .$$

The graph, $A \subset C \times P$, of the actual logos map, $\alpha : C \to 2^P$ is called the <u>actual logos</u> of the parameterization scheme. For purposes of mathematical economy, it is usually convenient to enlarge this set, so the scheme may include a <u>logos map</u>, $\lambda : C \to 2^P : c \mapsto \lambda(c)$, with $\alpha(c) \subset \lambda(c)$ for all $c \in C$. The <u>logos</u>, Λ, is the graph of the logos map, λ, and contains the actual logos, $A \subset \Lambda \subset C \times P$, and a complement, $\Lambda \setminus A$, called the <u>virtual logos</u>.

At this point it must be acknowledged that there is no unique parametrization for any process. The description of the phases may be incomplete, due to ignorance of some of the internal parameters of the process. Even worse, one never knows how many controls to take account of - the temperature of the laboratory, the vibration due to passing trucks, the electromagnetic field of the experimentalist ? It does seem that the larger is the control space, C , the more drawn out is the structure of the logos, and finer detail of its geometry revealed. In the schemes elaborated to date, it turns out that enlargement of C leads to diminishing returns, while enlargement of P , past a certain point, is irrelevant. Once C and P have been chosen, the most important task of the experimentalist, from the point of view of morphosophy, is the charting of the actual logos, $A \subset C \times P$. Here I must confess that Thom gives a much more general interpretation of C , which he calls the space of external parameters.

Finally, we extend the scheme to the full parameterization of the observed forms, $\{\varphi_i | i \in I\}$. Each form, φ_i , is a structure on the domain, $D_i < P$. We could try to construct a set of structures, Φ , such that $\varphi_i \in \Phi$. At this point, mathematicians may jump at the chance to involve local categories or sheaves. But here, Thom makes a simplifying assumption , very restrictive, but adequate for many processes. So let us assume that each form, φ_i , is the restriction to its domain, $D_i \subset P$, of a similar structure, σ_i , defined on the whole phase space, P , or $\varphi_i = \sigma_i | D_i$. The structures used for the parameterization must be such, obviously, that restriction to a subset is defined. So let Σ be a set of structures on P - for example : real-valued functions, topologies, distance functions, sections of a bundle, or some such - and assume :

Restriction Axiom. For each $\sigma \in \Sigma$ and $D \subset P$, σ/D is defined.

Field Axiom. For each $c \in C$, there is a structure, $\sigma(c) \in \Sigma$, such that $\varphi_i = \sigma(c)|D_i$, for all $i \in I_c$.

These assumptions, especially the latter, are very restrictive, and one could easily imagine processes which cannot be morphometrized in this way. However, morphogenesis is the study of those that can be, and does admit a large number of important applications. The Field Axiom actually assumes a function

$$\sigma : C \to \Sigma : c \mapsto \sigma(c)$$

which is called the morphogenetic field. The complete parameterization of the corpus, $\{\varphi_i | i \in I\}$, is given by the two maps, $\alpha : C \to 2^P$, and $\sigma : C \to \Sigma$. Each domain of the logos, not only those of the actual logos, is given a form by the morphogenetic field. The logos and the field may be combined in a single graph, $M \subset C \times P \times \Sigma$, called the morphos of the scheme, defined by

$$M = \{(c,p,\ ) \mid p \in)(c),\ = \sigma(c)\}$$

This is the principal construction of morphometry.

3. Catastrophes. Points of the control space are classified in two categories : if, when the control is set at $c \in C$, and the process is observed in every achievable form $\varphi(c)$, a small change in the control produces no significant change in the form, then c is a regular point of the process. Otherwise, it is a catastrophe point. The catastrophe of the process is the set, $K \subset C$, of all catastrophe points. Plotting the catastrophe is the second basic goal of the experimentalist, from the morphosophic point of view.

Now suppose the observer moves the controls in a curve, $t \mapsto c(t)$, and at time t_o, this curve crosses the catastrophe, $c(t_o) \in K$. Then the observed morphology, $\varphi(t)$, jumps from one part of the actual logos to another. Suppose that over the point $c(t_o)$, the actual logos, $\alpha(c)$, contains several domains, $\{D_i \mid i \in I_{c(t_o)}\}$. Then another basic question for the experimentalist is : what jumps, φ_i to φ_j , are observed, and how does the process select the new state, φ_j ? In practice, this is related to the geometry of the logos, the way the curve $c(t)$ approaches the catastrophe, $K \subset C$, and various other considerations. When a simple rule can be given to describe the observations, it is called a <u>catastrophe convention</u>. It may also prescribe the division of the logos into its actual and virtual components. Here are some examples.

Let $C = P = \mathbb{R}$, Λ be two horinzontal lines, and $K = \{0\} \subset \mathbb{R}$. Suppose the actual logos, $A \subset \Lambda$, is the subset shown in heavy lines in figure 4-1. This is a model for a binary switch. The process must change phases each time the control passes zero.

Next let $A \subset \Lambda$ be as shown in Figure 4-2. As the control passes $K = \{0\}$ going from left to right, initially in the lower (only observed) state, a choice arises. We may observe that the process always jumps to the upper state. This is an example of the <u>saturation convention</u>. Or, we may observe that the process stays in the lower state. This is an example of the <u>delay convention</u>. If the control passes zero from right to left, the process has no choice but to choose the lower state. Now suppose that with the same logos, the catastrophe consists of two points, $K = \{0,1\}$, and the actual logos consists of two rays, as shown in figure 4-3. Then we may observe $K = \{0,1\}$, with a change of state at 0 for control moving from left to right, and at 1 for control from right to left. This is another example of the saturation convention. Alternatively, we may have $K = \{0,1\}$, with a change to the upper state as the control moves past 1 to the right, and a change to the lower state as the control passes 0 , moving to the left. This is another example of the delay convention.

Another rule, called the *Maxwell convention*, is discussed in the next chapter.

4. Morphogenetic fields. So far, all that has been accomplished is a peculiar mathematization of a routine empirical method. But now, I can state the two key ideas of Thom's morphosophy.

Principle of Universal Archetypes : The catastrophe, logos, and morphos are determined by the morphogenetic field.

Principle of Structural Stability : The catastrophe, logos, and morphos are stable under small perturbations of the morphogenetic field.

The first principle is achieved as follows.

There is to be, in the structure space, a subset, $\Theta \subset \Sigma$, the *universal archetypal catastrophe*, such that $\theta = \sigma^{-1}(\Theta)$ contains the catastrophe, $K \subset \theta$. Here, $\sigma : C \to \Sigma \supset \Theta$ is the morphogenetic field. The *Theoretical catastrophe*, θ , is to be the union of the *actual catastrophe*, K , and a complementary virtual catastrophe, $\theta \setminus K$. The catastrophe convention is to specify the partition of θ into actual and virtual catastrophes. In exceptional cases, we may have $K \not\subset \theta$, but K is derived from θ by a simple rule, contained in the catastrophe convention. An example of such an exception is given in Section 13.

Next, the logos is to be determined from the morphogenetic field by a *universal logos map*, $\tilde{\lambda} : \Sigma \to 2^P$. If $\sigma : C \to \Sigma$ is the morphogenetic field, then $\lambda = \tilde{\lambda} \circ \sigma$ is to be the logos map of the morphometric scheme.

Also, there should be a universal actual logos map, $\tilde{\alpha} : \Sigma \to 2^P$, such that the actual logos map is given by the composite, $\alpha = \tilde{\alpha} \circ \sigma$. Naturally, we should have $\tilde{\alpha}(\sigma) \subset \tilde{\lambda}(\sigma)$ for all $\sigma \in \Sigma$.

Finally, the morphos is trivially determined by the morphodynamic field, if the logos is. Thus, the Principle of Universal Archetypes presupposes a scheme :

$$\Theta \subset \Sigma \underset{\tilde{\lambda}}{\overset{\tilde{\alpha}}{\rightrightarrows}} 2^P$$

consisting of a set, Σ , of restrictable structures on the phase space, P , a distinguished subset, $\Theta \subset \Sigma$, and two special maps, $\tilde{\alpha}, \tilde{\lambda} : \Sigma \to 2^P$. Such a scheme is a morphometric metamodel.

The principle of Structural Stability is difficult to make precise at a stage.

CHAPTER 2. METAMODELS

In review, a morphometric metamodel assigns, to any appropriate set P , a scheme $\Theta \subset \Sigma \underset{\tilde{\lambda}}{\overset{\tilde{\alpha}}{\rightrightarrows}} 2^P$, where

- P is the phase space
- Σ is the structure space
- Θ is the universal archetypal catastrophe
- $\tilde{\alpha}$ is the universal actual logos map, and
- $\tilde{\lambda}$ is the universal logos map

A morphometric model is then given by adding a control space, C , a morphogenetic field, $\sigma : C \to \Sigma$, and a catastrophe convention, relating K to $\theta = \sigma^{-1}(\Theta)$, and to the actual and total logoi,

$$A = \mathrm{graph}(\widetilde{\alpha} \circ \sigma) \subset \Lambda = \mathrm{graph}(\widetilde{\lambda} \circ \sigma) \subset C \times P$$

In this chapter, I will describe the two basic metamodels introduced by Thom, the morphostatic and morphodynamic schemes.

5. Static models. The first and most extensively applied metamodel has for its structure space $\Sigma = C^{\infty}(P, \mathbb{R})$, the smooth functions on a manifold P . This is the static metamodel, and a morphogenetic field $\sigma : C \to \Sigma$ may be called a morphostatic field. The study of static models, morphostatics or classical catastrophe theory, relies heavily on the theory of singularities of mappings. The universal archetype $\Theta \subset \Sigma$ is defined as follows. Two functions, $f, g \in \Sigma$, are equivalent if there are diffeomorphisms, α of P and β of $\mathbb{R}$, such that $\beta f \alpha = g$. Give Σ the C^{∞} Whitney topology. Thus f and g are close if the values of all of their derivatives are uniformly close, for some appropriate definition of "uniformly". A function $f \in \Sigma$ is stable if it is in the interior of an equivalence class. It has been shown that stability is equivalent (at least if P is compact) to : all critical points are non-degenerate, and have distinct critical values. Let $\Theta \subset \Sigma$ be the set of unstable functions. For $f \in \Sigma$, let $\widetilde{\lambda}(f) \subset P$ be the set of all critical points of f , and $\widetilde{\alpha}(f)$ be the set of relative minima of f . This scheme, $\Theta \subset \Sigma \underset{\widetilde{\lambda}}{\overset{\widetilde{\alpha}}{\rightrightarrows}} 2^{P}$ is the static metamodel.

Here is how a static model works. For the observed process, we choose a control space, C , a phase space, P , and a morphostatic field, $\sigma : C \to \Sigma = C^{\infty}(P, \mathbb{R})$. This field is to satisfy the Principle of Structural Stability, which means in this context that the image of C , $\sigma(c) \subset \Sigma$, crosses the universal catastrophe, $\Theta \subset \Sigma$, in the nicest possible way - I will make this more precise in a moment. The catastrophe $K \subset C$ has been determined experimentally, and, if our model is successful, it is contained in the theoretical catastrophe, $\theta = \sigma^{-1}(\Theta)$.

Next, the total logos, $\Lambda \subset C \times P$, is determined as follows. To each point $c \in C$ corresponds a fictitious potential function, $\sigma(c)$, which need not have any physical significance. If $c \notin \theta$, then $\sigma(c)$ is stable, and the set of critical points of $\sigma(c)$, $\lambda(c) = \widetilde{\lambda}(\sigma(c))$, is a discrete set of points in the phase space, P . If $c \in \theta$, then $\lambda(c) \subset P$ may be more complicated. In any case, the total logos is

$$\Lambda = \text{graph}(\lambda) = \{\{c\} \times \lambda(c) \mid c \in C\} \subset C \times P$$

and similarly, the actual logos is

$$A = \text{graph}(\alpha) = \{\{c\} \times \alpha(c) \mid c \in C\} \subset C \times P$$

where $\alpha(c) = \widetilde{\alpha}(\sigma(c))$ is the set of relative minima of the function $\sigma(c)$, and $A \subset \Lambda$. From the experimental data, a catastrophe convention is concocted, which relates K to $\theta = \sigma^{-1}(\Theta)$ - hopefully $K \subset \theta$ - and relates the domains of observed states to the actual logos, A . Hopefully, they belong to A .

The process is governed by a minimum principle, and typical states minimize the fictitious pontential function, and are therefore described by a single point of the phase space, P , together with the (usually meaningless) value of the potential. As in each observed state, the phase is constant if the control is not changed, this model is called static. No stable oscillations in the phase arise as observed states.

Note that the theoretical catastrophe, $\theta = \sigma^{-1}(\Theta)$, locates unstable behavior of either (or both) of these types : (SS) - a critical point is degenerate, or (SM) - two critical points have the same value. These are called singular, and Maxwell catastrophes, respectively. We may therefore write θ as the union of two sets, $\theta = \theta_s \cup \theta_m$, where θ_s is the set of singular catastrophes, or singular set, and θ_m is the set of Maxwell catastrophes, or Maxwell set. Naturally, $\theta_s \cap \theta_m \neq \emptyset$ in general.

A typical catastrophe convention for static models is Thom's Maxwell convention. This specifies $K \subset \theta_m \subset \theta$, so all actual catastrophies are Maxwell catastrophes, and further : the process always chooses the lowest available relative minimum of the potential function.

Finally, I will try to clarify the Principle of Structural Stability in this context. This depends on the structure of $\Theta \subset \Sigma$, established by Thom [201] and Mather [309]. First, it is necessary to know that Σ is a vector space, and a topological space. By means of technical tricks, we may justify the pretense that Σ is a simple manifold. With this pretense, the structure of Θ in Σ may be described as a stratified set : a collection of submanifolds of Σ , called strata, partially ordered by increasing codimension, each contained in the topological boundary of a larger one, and satisfying some conditions of regular incidence, much like an algebraic variety [317]. Now the stability requirement for the morphogenetic field may be expressed as : $\sigma : C \to \Sigma$ must be transversal to the strata of $\Theta \subset \Sigma$. This implies that if $\theta = \sigma^{-1}(\Theta)$, $v_1 : C \to \Sigma$ is close to σ , and $\theta_1 = \sigma_1^{-1}(\Theta)$, then there is a diffeomorphism α of C , close to the identity, such that $\theta_1 = \alpha(\theta)$. In this sense, σ is "structurally stable". In addition, the transversality of σ to Θ implies that if the dimension of C is d , then $\sigma(c) \subset \Sigma$ can intersect only the strata of Θ of codimension less than or equal to d, as shown in Figure 5-1. This is the foundation of the extraordinary results of Thom and Mather : at any point in the logos, $(c,p) \in \Lambda$, with catastrophic control, $c \in \theta$, there is a neighborhood, $U \times V$ of $(c,) \in C \times P$, and a diffeomorphism of $U \times V$ onto a disk in Euclidean space, such that the local logos, $(U \times V) \cap \Lambda$, is carried onto one of a list of standard models. Thanks to the work of Thom [201], Mather [309], and Siersma [311], this list is explicitly known, for $\dim(c) \leq 8$. A list of the local models, for $\dim(c) \leq 4$, is given in Figure 5-2.

6. Dynamical interpretation. To motivate the definition of the dynamic metamodel, it will help to understand how a static model may be interpreted dynamically. Suppose for simplicity, that P is compact. Let $\Sigma_s = C^\infty(P, \mathbb{R})$, $\Theta_s \subset \Sigma_s$ the subset of unstable functions and $\Sigma_d = \mathfrak{X}^\infty(P)$, the smooth vectorfields on P. A morphostatic field, $\sigma_s : C \to \Sigma_s$, may be transformed to a morphodynamic field, $\sigma_d : C \to \Sigma_d$, by composition with a map $\nabla : \Sigma_s \to \Sigma_d$, $\sigma_d = \nabla \circ \sigma_s$. An appropriate map is defined as follows. Choose a Riemannian metric g on P. This induces a vector bundle isomorphism $g^\#$ from the cotangent bundle to the tangent bundle of P :

$$\begin{tikzcd}
T^*P \arrow[r, "g^\#"] \arrow[d] & TP \arrow[d] \\
P \arrow[r, "id"] \arrow[u, bend left=60, "-df"] & P \arrow[u, bend right=60, "\nabla f"']
\end{tikzcd}$$

For $f \in \Sigma_s$, let $df : P \to T^*P$ be the differential of f, as a section of the cotangent bundle. Then $\nabla f = -g^\# \circ df$ is a section of the tangent bundle, hence a vectorfield. The negradient operator

$$\nabla : \Sigma_s \to \Sigma_d : f \mapsto \nabla f$$

is a continuous linear transformation, its kernal consisting of the constant functions. Thus if $\nabla f = \nabla g$, the critical points and relative minima of f agree with those of g . For more details on such operators, consult any modern text of differential geometry, for example [302]. If P is ordinary Euclidean space, ∇f is the negative of the ordinary gradient of f .

Now we have transformed the morphostatic field, $\sigma_s : C \to \Sigma_s$, into a morphodynamic field, $\sigma_d = \nabla \circ \sigma_s : C \to \Sigma_d$. Let $\theta_s = \sigma_s^{-1}(\text{[illegible]}_s)$, suppose $c \notin \theta_s$, let $f = \sigma_s(c)$, and $X = \sigma_d(c) = \nabla f$. Then f has non-degenerate critical points, $\lambda(c) = \{p_i\}$, all of distinct critical values, $f(p_i)$, and $X(p_i) = 0$ for all i . Of these critical points, some are sources (corresponding to relative maxima), some saddle points, and the rest attractors (corresponding to relative minima), say $\{A_j\}$. At the remaining (regular) points, $p \in P$, $X(p)$ is a vector pointing in the direction of steepest descent of f , and through p passes a unique integral curve of X , which is a "fall-line", or curve of steepest descent for f . Let $In(S_i)$ denote the set of all points tending to S_i along integral curves of X . Then $In(S_i)$ is an immersed image of Euclidean k-space , $\mathbb{R}^k$, for an appropriate value of k between 0 and n = dimension of P . If S_i is a source, $k = 0$. If $S_i = A_j$ is an attractor, $k = n$, and $In(A_j) = B_j$ is an open subset of P , called the <u>basin</u> of A_j . Otherwise, $0 < k < n$. As P is compact, we have

$$P = \bigcup_i In(S_i)$$

Let $B = \bigcup B_j$, then $B \subset P$ is dense, and the complement of B consists of the union of the insets $In(S_i)$ of dimension less than n , that is, for S_i not an attractor. See Figure 6-1 for an example, with $P = T^2$, the 2-torus.

Now, to interpret the static model dynamically, suppose that the the control is left undisturbed at a non-catastrophic value $c \in C \setminus \theta_s$. Left to itself, the process can be observed only with a phase $p \in \Lambda(c) = \{A_1, A_2, \ldots\}$. But suppose that the process is forced, by external manipulation of the experimentalist, into an unnatural phase $p_o \in P \setminus (c)$, and then released. The process then moves from the initial non-equilibrium phase p_o , along the curve of steepest descent, seeking equilibrium. In a short time, t , it arrives at a point p_t close to an attractor A_j , if p_o is in the basin of A_j , B_j . Thus the process is in one of its observable states, $\sigma = (A_j, f(A_j))$. Almost every initial condition, p_o , is in the basin of one of the attractors of X .

Now that the process has arrived at a phase p_t very close to an attractor, suppose the control is changed, by abrubtly twisting the dial of the experimental apparatus, to a new value $d \in C \setminus \theta_s$. Then $f = \sigma_s(c)$ changes to a new function $g = \sigma_s(c)$. The gradient vectorfield $X=\nabla f$ changes to another, $Y = \nabla g$, there is a new set of attractors $\{A'_j\}$, and basins, $\{B'_j\}$. If the point $p_t \approx A_j$ is in a new basin, B'_k , then the process will hasten to the new equilibrium position, A'_k . If the control is changed further, by a continuous adjustment, slow with respect to the rate at which the process tends to its equilibrium phases, the observed state will follow a curve very close to the actual logos, A . When the control passes through the catastrophe, $\theta_s \subset C$, the observed state may very steeply rise or fall, approximating a discontinuity, to a different sheet of the logos, corresponding to a new attractor, as in the case of the sudden twist of the control dial discussed earlier. See Figure 6-2.

7. Dynamic models. The static metamodel does not allow oscillations as observable states, and this limitation of morphostatics is overcome by a more gene-

ral scheme, the dynamic (or metabolic) metamodel. Here, the structure space is taken to be the space of smooth vectorfields, $\Sigma = \mathfrak{X}^{\infty}(P)$. A morphogenetic field in this context, $\sigma : C \to \Sigma$, is called a morphodynamic field. In morphodynamics, the basic role of the theory of singularities of mappings is replaced by the theory of catastrophes (bifurcations) of families of vectorfields. As catastrophe theory is now barely in its infancy, it is impossible to describe morphodynamics as a mature theory. But here is its starting point, a first attempt at the scheme $\Theta \subset \Sigma \to 2^{P}$

Let P be a manifold, and $\Sigma = \mathfrak{X}^{\infty}(P)$, the space of smooth vectorfields on P. This is a real vector space, and a topological space, with the C^{∞} Whitney topology. Thus X, $Y \in \Sigma$ are close if the values of all their derivatives are uniformlyclose, for any of the appropriate definitions of "uniformly". If P is compact, Σ is a Frechet space. Two vectorfields, $X,Y \in \Sigma$, are conjugate if there is a homeomorphism α of P which takes integral curves of X onto integral curves of Y, preserving orientation, but not necessarily preserving parameter. This is an equivalence relation on Σ, and X is structurally stable if it is in the interior of an equivalence class. This means, if X is considered as a system of first order ordinary differential equations, that the qualitative behavior of its general solution is unchanged by small (in the C^{∞} sense) perturbations of its coefficients. A complete geometric characterization of structural stability is not yet known, but a long list of necessary conditions have been established. Historically, the first choice for the universal catastrophe $\Theta \subset \Sigma$, made by Thom,was the set of non-structurally stable vectorfields.

From the point of view of recent developments in dynamical systems theory, it might be better to choose a slightly different definition, which I can describe here only vaguely. It is the same as the preceeding definition, except that structural stability is replaced by absolute structural stability, in the sense of Franks and Guckenheimer. It is possible that the two definitions are equivalent. Details can be found in Robbin [310]. The reason for this suggestion is just a suspicion of mine, that this condition admits a complete geometric characterization, by means of Smale's spectral theory [312]. I may as well insert here, for those who know already the language of dynamical systems theory, a precise statement of this suspicion.

Spectral Conjecture. If $X \in \Sigma$ is absolutely structurally stable, then (1) the nonwandering set of X, Ω, is the closure of the set of critical points and closed orbits of X, (2) Ω has a countable set of components, $\{S_i\}$, (3) each S_i is topologically transitive, hyperbolic, and is a Cantor manifold, (4) the insets and outsets of the S_i have transversal intersections, without cycles, and (5) the union of the insets of the attractors among the S_i is dense in P.

Further modification of the definition of Θ in this metamodel may be expected to continue for some time to come. Unlike the static case, this universal catastrophe contains open sets ("chaos".)

To complet this scheme, we need to define the universal logoi maps, $\tilde{\alpha}, \tilde{\lambda} : \Sigma \to 2^P$, analogous to the relative minima and critical set of the static scheme.

For a morphodynamic field $\sigma : C \to \Sigma$, and a non-catastrophic control value $c \in C \setminus \theta$ where $\theta = \sigma^{-1}(\Theta)$, we imagine that the vectorfield, $X = \sigma(c)$, describes the striving of the process for equilibrium phases, which are to comprise the actual logos, as in the dynamical interpretation of the morphostatic field. Thus we need the analogous, for an arbitrary vectorfield, of the critical set, and the set of relative minima, of a gradient vectorfield. These analogues are the nonwandering set and the set of attractors, of the qualitative theory of dynamical systems. Here are their definitions.

For a given vectorfield, $X \in \Sigma$, and any initial point, $p_o \in P$, let $t \mapsto p_t$ denote the integral curve of X , starting from p_o . For simplicity in these definitions, I will assume that each integral curve is defined for all $t \in \mathbb{R}$, that is, X is complete. For a subset $U_o \subset P$, let $U_t = \{p_t \mid p_o \in U\}$. A point $p \in P$ is wandering if it has a neighborhood, U_o , and a positive number, $\tau \in \mathbb{R}$, such that for all $t \geq \tau$, $U_t \cap U_o = \emptyset$. Otherwise, p is a nonwandering point. Let $\Omega(X)$ denote the nonwandering set of X : the set of all nonwandering points. The total logos is defined by the universal logos map,

$$\tilde{\lambda} = \Omega : \Sigma \to 2^P : X \mapsto \Omega(X) \quad .$$

In case X is a gradient vectorfield, then $\Omega(X)$ is the set of critical points, as in the static metamodel.

Next let $0^+(p_o)$ denote the future integral curve starting at p_o , $0^+(p_o) = \{p_t \mid 0 \leq t < \infty\}$. Then the omega limit set of p_o is the intersection of the closures of the future orbits

$$\omega(p_o) = \bigcap \{\overline{0^+(p_t)} \mid 0 \leq t < \infty\}$$

and represents the smallest subset of P which is asymptotically approached by the future orbit of p_o . For all $p_o \in P$, $\omega(p_o) \subset \Omega(X)$. An attractor of $X \in \Sigma$ is a subset, $A \subset \Omega(X)$, which is closed, invariant under X (a union of full integral curves), such that there is a neighborhood U of $A \subset P$ with $\omega(u) \subset A$ for all $u \in U$ (in other words, every point sufficiently close to A is attracted by A), and minimal with respect to these conditions. For $X \in \Sigma$, let $\widetilde{\alpha}(X)$ be the union of all the attractors of X .

If X is a negradient vectorfield, $X = \nabla f$, then $\widetilde{\alpha}(X)$, as defined here, is the set of relative minima of f , as before.

The basic idea of Thom, on the structural stability of the morphogenetic field, is to be understood in the dynamic context in more or less the same way as in the static case, except that, at the moment, the necessary theorems on the stratified structure of Θ are not yet known. But it is hoped that Θ has some type of stratified structure, and a dynamic model should have a morphodynamic field $\sigma : C \to \Sigma$ which is transversal to the strata of $\Theta \subset \Sigma$. Some tentative definitions of structural stability for morphodynamic fields have been given by Sotomayor [313], Guckenheimer [305], and Takens [316].

At this point, I should warn you that the static and dynamic archetypal catastrophes are not perfectly analogous. Let $\widetilde{\Theta}_s \subset \Sigma_s$ denote the static metamodel, $\widetilde{\Theta}_d \subset \Sigma_d$ denote the dynamic metamodel, and $\nabla : \Sigma_s \to \Sigma_d$ be a negradient operator. Then

$$\nabla(\widetilde{K}_s) \neq \nabla(\Sigma_s) \cap \widetilde{K}_d$$

and, in fact, there is only a small intersection of the two archetypal catastrophes. This is the essence of "Guckenheimer's objection" [306]. I will try to clarify this further in the next chapter.

The interpretation of a dynamic model $\sigma : C \to \Sigma$ is similar to that of the previous section. Let $\theta = \sigma^{-1}(\Theta)$. Fix a non-catastrophic control value, $c \in C \setminus \theta$, and let $X = \sigma(c)$. Assuming the spectral conjecture, the nonwandering set, $\Omega(X)$, of X has a countable set of components, $\{S_i\}$. Some are sources, some saddles, and the rest attractors, say $\{A_j\}$, with basins $\{B_j\}$. If we suppose P is compact, then $B = \cup B_j \subset P$ is dense. This is exactly the same as the static case, with one crucial difference : the attractors are not necessarily points. Each attractor can be a point (critical point, or stationary solution), a circle (closed orbit, or periodic solution), a 2-torus (invariant torus, or almost periodic solution with two independent frequencies), practically any submanifold (admitting an Anosov flow, with a wide variety of possible topologically transitive dynamical systems), or a Cantor manifold (solenoid, or subset locally like the product of a Cantor set and a disk). Any of these, more complicated than a k-torus, is called a strange attractor.

This view of the qualitative behavior of the absolutely structurally stable dynamical system, $X = \mathcal{C}(c)$, may be summarized in a diagram, the Smale graph of X . Each basic set, S_i , is indicated by a vertex. A directed line segment from S_i to S_j is added if there is an orbit going (asymptotically) from S_i to S_j . This indicates an intersection of $\mathrm{Out}(S_i)$ and $\mathrm{In}(S_j)$. To each vertex is added a label, $(S_i , X|S_i)$ indicated the topology of the corresponding basic set, and the flow within it. The attractors are the vertices with arriving arrows, but no departing arrows.

With the control $c \in C \setminus \mathcal{B}$ fixed and experimental preparation for an nonequilibrium initial phase $p_o \in P$, the process evolves according to the dynamical system, X . Thus the phase, p_o , proceeds along an integral curve, $t \mapsto p_t$. As $B \subset P$ is dense, it is safe to assume that $p_o \in B$ to start with, hence in the basin of one of the attractors, say B_j . Thus after a short time, p_t is near the attractor A_j , and the integral curve follows very closely an orbit of $X|A_j$, dense in A_j , indefinately. The succession of phases is experimentally indistinguishable from an orbit within A_j . Thus the equilibrium motion of the process is adequately labelled by the state

$\varphi_j = (A_j, X|A_j)$. The different observable equilibrium states of the process are therefore $\{\varphi_j = (A_j , X|A_j)\}$, so the actual logos is contained in $\tilde{\alpha}(c) = \bigcup_j A_j \subset \tilde{\lambda}(c) = \Omega(X) \subset P$.

Now if the control is changed by the experimentalist gradually, the attractor will gradually move, and the phase p_t will follow it, until the control passes a catastrophic value. Then the configuration of attractors and basins is radically altered, the process finds itself far from equilibrium, and moves rapidly to a new attractor, depending on which new basin contains the old attractor which had previously caught the process, or perhaps some other convention. The experimentalist sees an apparently instantaneous jump from an equilibrium state, $\varphi = (A_j , X|A_j)$, to a new state, $\varphi' = (A'_k , X'|A'_k)$.

The morphodynamic field, $\sigma : C \to \Sigma$, is to be structurally stable in some sense. This is to assure that the theoretical catastrophe, $\theta = \sigma^{-1}(\Theta)$, is stable under perturbations. Hence the actual catastrophe, $K \subset \theta$, will also be stable in the same sense.

<u>8. Other models.</u> Three other metamodels must be mentioned. A <u>kymatic model</u> is simply a dynamic model, $\sigma : C \to \mathfrak{X}^\infty(P)$, in which P is an infinite dimensional manifold of mappings, and for each $c \in C$, $\sigma(c)$ is defined by a partial differential operator. An example is given in Section 15. This is a kind of nonlinear spectral theory.

A <u>self-regulation model</u> consists of two dynamic models, $\sigma : C \to \mathfrak{X}^\infty(P)$, and $\tau : P \to \mathfrak{X}^\infty(C)$. These may be considered as vectorfields on $C \times P$, the vertical vectorfield, or <u>internal dynamic</u>,

$$V : C \times P \to T(C \times P) : (c,p) \to (0,\sigma(c)(p))$$

and the horizontal vectorfield, or self-regulation dynamic,

$$H : C \times P \to T(C \times P) : (c,p) \mapsto (-(p)(c), 0)$$

The internal dynamic is interpreted exactly like a dynamic model, while the self-regulation dynamic, usually small with respect to the internal dynamic, is considered to automatically regulate the control parameters, in place of the experimentalist, or other external agent. The process actually follows integral curves of the sum of the two vectorfields, $H + V$. An example is given in Section 16.

A Hamiltonian model is a dynamic model, $\sigma : C \to \mathfrak{X}^\infty(P)$, with $\sigma(c)$ a Hamiltonian vectorfield, for all $c \in C$. Let $\mathcal{H}^\infty(P) \subset \mathfrak{X}^\infty(P)$ denote the subspace of Hamiltonian vectorfields. That is, P is a symplectic manifold, with symplectic form, ω, and

$$\mathcal{H}^\infty(P) = \{X_H : H \in C^\infty(P, \mathbb{R})\}$$

where X_H is the symplectic gradient of H with respect to ω, $X_H = \omega^\# \circ dH$ where $\omega^\# : T^*P \to TP$ is the vector bundle isomorphism induced by ω (see [302] for details).

As $\mathcal{H}^o(P) \subset \mathfrak{S} \subset \mathfrak{X}^\infty(P)$, a new definition of the universal archetypal catastrophe is needed. So far, no satisfactory definition has been made. However, in case C is a single point, and the Hamiltonian model consists of a single vectorfield $X_H \in \mathfrak{X}^\infty(P)$, the energy function $H : P \to \mathbb{R}$ is an invariant function of X_H, so its level surfaces $\{\Sigma_e = H^{-1}(\{e\})\}$ are invariant sets. We may consider $e \mapsto X_H|\Sigma_e$ is a dynamical model with control space $C \subset \mathbb{R}$, as the energy of the system can be manipulated externally by the experimentalist, by heating the process, for example. In this case, the catastrophe $K \subset C$ may be taken to be the set of critical values of H, or the set of energies where bifurcations of closed orbit cylinders occur (see [301]). Such a model has been used by Thom in psycholinguistics [213]. There remains the question of the universal logos map. Thom has suggested that, as attractors do not occur in Hamiltonian systems, the actual logos be constructed of "vague attractors". A satisfactory definition has yet to be given. Thus the Hamiltonian metamodel, $\mathscr{E}_H \subset \mathscr{H}^{\infty}(P) \to 2^P$, still awaits definition.

A totally different scheme, for catastrophes of partial differential equations, based on a suggestion of Thom [201], has been beautifully elaborated by Guckenheimer [307].

CHAPTER 3 : ARCHETYPAL CATASTROPHES

The goal of catastrophe theory is to classify the possible geometries of logoi, in the neighborhood of a catastrophe point. This theory is well developed in morphostatics, but barely started in morphodynamics and the other metamodels. This chapter is a collection of examples of known local archetypes, to give a better intuition for the logos morphometry.

9. Static catastrophes of codimension one. The local structure of morphostatic logoi is fully known, for codimension less than or equal to eight. Lets consider, first, codimension one. Thus we have a structurally stable morphostatic field, $\sigma : C \to \Sigma_s = C^{\infty}(P, \mathbb{R})$, where we may as well have $C = \mathbb{R}^m$, and $P = \mathbb{R}^n$, so $\Lambda \subset C \times P \approx \mathbb{R}^{m+n}$, $\theta_s = \sigma^{-1}(\mathscr{E}_s) \subset \mathbb{R}^m$. The morphostatic field may be interpreted dynamically, via the negradient operator $V : \Sigma_s \to \Sigma_d = \mathfrak{X}^{\infty}(\mathbb{R}^n)$ of the standard metric, and the derived morphodynamic field, $V \circ \sigma : C \to \Sigma_d$, may be visualized as a vertical vectorfield on $C \times P$,

$$V : C \times P \approx \mathbb{R}^{m+n} \to T(C \times P) \approx \mathbb{R}^{m+n} \times \mathbb{R}^{m+n} \to \mathbb{R}^{m+n}$$

$$: (c,p) \mapsto ((c,p) , (0, -\mathrm{grad}(\sigma(c))(p)))$$

To study catastrophes of codimension one, we set $m = \dim(C) = 1$, and consider small values of $n = \dim(P)$, so the logos and negradient field may actually be visualized in $\mathbb{R}^{n+1}$. The original morphostatic field, $\sigma : C \to \Sigma_s$, may be visualized as a master potential function,

$$\varphi : C \times P \to \mathbb{R} : (c,p) \to \sigma(c)(p)$$

or its graph, $\varphi \subset \mathbb{R}^{n+2}$. Then the derivative of $\sigma(c)$ at p is the partial derivative with respect to the second factor of φ at (c,p) , $\sigma(c)'(p) = D_2\varphi(c,p)$, and therefore the logos, $\Lambda \subset C \times P \approx \mathbb{R}^{n+1}$ is the set of zeros of the function $D_2\varphi : C \times P \to \mathbb{R}$. With these notations, lets consider some examples.

Example 9A . Let $n = 1$, and

$$\varphi : \mathbb{R}^2 \to \mathbb{R} : (c,p) \to \varphi(c,p) = \frac{1}{2} p^2 + cp$$

Thus $D_2\varphi(c,p) = p + c$, so $\Lambda \subset \mathbb{R}^2$ is the line : $p + c = 0$. As $D_2^2\varphi(c,) = 1$, $\Lambda = \Lambda$, as shown in Figure 9-1. This static model is essentially equivalent to the constant field, $\sigma(c)(p) = \frac{1}{2} p^2$, shown in Figure 9-2. In these cases, $\sigma(c) \subset \Sigma_s$ does not meet the universal catastrophe, $\Theta_s \subset \Sigma_s$, as $\sigma(c)$ is stable for all $c \in \mathbb{R}$. Hence there is no catastrophe, and $\theta \subset C$ is empty. For any control setting, $c \in \mathbb{R}$, there is exactly one possible state for the process, which is therefore determined, and morphologically constant.

Example 9B . Again let $n = 1$, and $\varphi(c,p) = \frac{1}{3} p^3 + cp$. Then

$D_2\varphi(c,p) = p^2 + c$, $D_2^2\varphi(c,p) = 2p > 0$ for $p > 0$, so we obtain the configuration shown in Figure 9-3. At the origin, $D_2\varphi(0,0) = D_2^2\varphi(0,0) = 0$, so $\sigma(0)$ is not right-stable, and $\theta = \{0\}$. As the control c passes through 0 , $\sigma(c)$ passes through $\mathfrak{S}_s$, from a region of no critical points, to a region of two critical points. Perturbation of σ leaves this situation unchanged, so this static field is a structurally stable one, representing a curve piercing a stratum of $\mathfrak{S}_s$ of codimension one. It is called the <u>fold</u>. As the control is decreased through zero, there is no stable state, to begin with , but one suddenly appears at $0 \in P$, as the control passes the catastrophic value $0 \in C$. This persists, and moves slowly upwards, as $c \in C$ continues to decrease.

<u>Example 9C</u> . Let $n = 1$, $C = (-\varepsilon,\varepsilon) \subset \mathbb{R}$, for some small $\varepsilon > 0$, $P = \mathbb{R}$, and $\varphi : C \times P \to \mathbb{R} : (d,p) \mapsto \varphi(d,p) = \frac{1}{4} p^4 - \frac{1}{2} p^2 + dp$. Then $\sigma(0)(p) = \varphi(0,p) = \frac{1}{4} p^4 - \frac{1}{2} p^2$ has two relative minima of the same hight, and one relative maximum. The effect of the linear term, dp , is to tilt the graph, raising one minimum and lowering the other, see Figure 9-4. The function $\sigma(d)$, for $d \in C$, is stable except for $d = 0$, and the curve $\sigma : C \to \Sigma_s$ crosses a stratum of $\mathfrak{S}_s \subset \Sigma_s$ of codimension one, corresponding to violation of the stable property of distinct critical values. This is called a <u>Maxwell catastrophe</u>.

<u>Example 9D</u> . Again with $n = 1$, consider

$$\varphi : \mathbb{R}^2 \to \mathbb{R} : (c,p) \mapsto \varphi(c,p) = \frac{1}{4} p^4 + cp$$

This is geometrically similar to the simple minimum, Example 9A, but $\sigma(c) \in \mathfrak{S}_s$ for every $c \in C$, so it is a very unstable static field, and $\theta = C$.

Example 9E . With $n = 1$ still, consider

$$\varphi : \mathbb{R}^2 \to \mathbb{R} : (c,p) \mapsto \varphi(c,p) = \frac{1}{4} p^4 + \frac{1}{2} cp^2$$

Then $D_2\varphi(c,p) = p(p^2 + c)$, and $D_2^2\varphi(c,p) = 3p^2 + c$, positive for $c > 3p^2$. Thus we have the logos and catastrophe shown in Figure 9-5. With the control set at $c > 0$, there is one observable state, A_o . As c is wound down, this persists until the catastrophe at $c = 0$. There then appears two competing states, A_1 and A_2 . If the process was initiated with phase $p_o > 0$, it may be assumed that the phase p_t has approached very closely the initial attractor, A_o , but still has $p_t > 0$. Therefore as c is moved past zero to the left, p_t finds itself in B_1 , the basin of A_1 , and therefore will follow the upper attractor, A_1 , upward as c continues to decrease. The source acts as the separator of the two basins of attraction.

When $c \leq 0$, the two relative minima of $\varphi(c)$ have the same value, hence $\sigma(c)$ is not stable, so Ξ is the non-positive ray in C corresponding to a curve of Maxwell catastrophe and φ is a highly unstable static field.

Example 9F . Now we try to stabilize the previous example, by twisting φ so that the relative minima, for $c \leq 0$, have different values. Let $d \in \mathbb{R}$ be a small positive number, and consider

$$\varphi : \mathbb{R}^2 \to \mathbb{R} : (c,d) \mapsto \varphi(c,d) = \frac{1}{4} p^4 + \frac{1}{2} cp^2 + dp$$

Then $D_2\varphi(c,p) = p(p^2 + c) + d$, $D_2^2\varphi$ is unchanged, and the logos becomes the cubic curve shown in Figure 9-6. The lower attractor, A_o , behaves exactly like the simple minimum, Figure 9-2. The upper part of the logos behaves exactly like the fold, Figure 9-3. In the dynamic interpretation, if the process is begun with $c > 0$ and $p_o > 0$, the process evolves swiftly to $p_t > 0$ close to A . As c is moved to the left, p follows A slowly downwards

When c passes the catastrophe, $\mathcal{S}$, a single point, a new attractor, A_1, appears. But p_t is in the basin, B_o, of A_o, so it remains near A_o, and no change of phase is observed. Depending on the details of the model, some other logos and catastrophe convention may be required. For example, with Thom's Maxwell convention, $K = \mathcal{S}$, and the process prefers the lower of the two minima, for $c < K$. Thus again, no change is observed. With the saturation convention, $K = \mathcal{S}$, and as soon as the new attractor, A_1, appears, it is preferred, so a jump of p_t from near A_o to near A_1 occurs, against the force of the gradient field.

If in this example, the stabilizing term dp is added, with a small negative coefficient, $d < 0$, a similar configuration arises, as shown in Figure 9-7.

According to the theory of stable functions, any structurally stable static field, with $m = n = 1$, must have its logos and catastrophe locally equivalent to one of these examples. A typical global configuration is shown in Figure 9-8.

10. Static catastrophes of codimension two. Consider $C = \mathbb{R}^2$. Any of the previous examples may be extended to this context by trivial suspension:

$$\mathbb{R}^2 \to \mathbb{R} \to \mathcal{F}_s : (c,d) \mapsto c \mapsto \varphi(c)$$

Example 10A. For example, the fold is defined by

$$\varphi(c,d) = \frac{1}{3}p^3 + cp$$

with the logos shown in Figure 10-1.

An irreducible example of codimension two is provided by extending Example 9F for all values of the stabilizing coefficient, d .

Example 10B . Let $m = 2$, $n = 1$, and

$$\varphi : \mathbb{R}^3 \to \mathbb{R} : (c,d,p) \mapsto \varphi(c,d,p) = \frac{1}{4} p^4 + \frac{1}{2} cp^2 + dp$$

As the graph is in $\mathbb{R}^4$, it is no longer visible, but the logos, in $\mathbb{R}^3$, defined by

$$D_3\varphi(c,d,p) = p^3 + cp^2 + d = 0$$

is shown in Figure 10-2. This is the Cusp, or Riemann-Hugoniot logos, which appears in many of the applications of Zeeman, in economics, ecology, psychology, and so on [318]. If we take sections of it, with vertical planes defined by $d = 0$, $d = \varepsilon$, and $d = -\varepsilon$, where $\varepsilon > 0$ is small, we get the logoi of Figures 9-5, 9-6, and 9-7, respectively.

This morphostatic field, $\sigma : \mathbb{R}^2 \to C^\infty(P, \mathbb{R})$ is actually structurally stable, transversal to a stratum of $\mathcal{E}_s \subset \Sigma_s = C^\infty(P, \mathbb{R})$ of codimension two, so a perturbation of σ makes no significant change in the logos. It meets the stratum of codimension two at a single point, $\sigma(0,0)$ the function $p \mapsto \frac{1}{4} p^4$, which is called the organising center of the field, σ , which is the universal unfolding of $\sigma(0,0)$. This point, $\sigma(0,0)$, is a function with a degenerate critical point, or "triple point". The remainder of the catastrophe, θ , consists of three rays. The external ones, making the "cusp", are singular catastrophes : transversal crossings of σ with strata of $\mathcal{E}_s \subset \Sigma_s$ of codimension one, at functions with an inflection point. Crossing these creates (or destroys) a pair of critical points, one a maximum, the other a minimum. For controls, (c,d) , inside this cusp, the gradient field has two attractors. The internal ray of θ is the Maxwell set, corresponding to transversal crossings of a stratum of $\mathcal{C}_s \subset \Sigma_s$ at which the relative hights of these two attractors interchange, as in Example 9C.

The dynamic interpretation of this morphostatic field is identical to the previous two examples, when the control is moved along a curve (c_t, d), with d fixed. Now consider a change of control along a low horizontal curve, (c, d_t), with $c < 0$. As d_t increases (dotted line in Figure 10-2), the phase, p_t, closely follows the attracting surface, A. As (c, d_t) passes the catastrophe, θ, for the first time, at (c, d_1), $d_1 < 0$, a new sheet of the attracting surface suddenly appears below the phase, p_t. But the phase is above the separatrix (unshaded surface), hence in the basin of the upper sheet of the attractor, so no change of phase is observed. As (c, d_t) passes the catastrophe for the second time, at (c, d_2), $d_2 > 0$, the upper sheet abrubtly dissappears, and p_t finds itself suddenly in the basin of the lower sheet. It then moves swiftly donward, approximately on an integral curve of the gradient field, as in Figure 6-2, and approaches the lower attractor asymptotically. The experimentalist observes a catastrophic change of equilibrium phase at (c, d_2), but nothing at (c, d_1). Then turning the control back, so that the curve (c, d_t) is transversal backwards, no change is noticed at the first crossing, (c, d_2), but a jump occurs at the second crossing, (c, d_1). This hysteris behavior corresponds to the <u>delay convention</u>.

In the dynamical interpretation, the Maxwell set (center ray of θ) does not have any qualitative significance, hence it is shown dashed in Figure 10-2. With the <u>Maxwell convention</u>, the process changes states (attractors) as this ray is crossed by the control.

According to the theory of stable functions, the fold and the cusp are the only local configurations which can arise with $m = 2$ and $n = 1$. A typical global logos is shown in Figure 10-3. The dynamic interpretation is similar to that of Example 10B.

These examples give a complete picture of the structurally stable morphostatic fields with control dimensions $m = 1$, or 2, and phase dimension $n = 1$. According to the theory of stable functions, nothing new is encountered by allowing n to be larger than 1. Thus a typical logos in $C \times P$, for $\dim(C) = 1$, or 2, and $\dim(P) = n$, is locally, just a suspension of these examples. For example, $\varphi(c,d,p_1,\ldots,p_n) = \frac{1}{4} p_1^4 + \frac{1}{2} cp_1^2 + dp_1$.

For $\dim(C) > 2$, new logoi arise for stable gradient fields, a complete list is given in Figure 5-2, for $\dim(C) \leq 4$.

11. Basin catastrophes. As described previously, the universal static catastrophe, $\Theta_s \subset \Sigma_s$, consists of functions failing to be stable, because of either of the atomic catastrophes,

(SS) a critical point is degenerate (singular catastrophe)

(SM) two critical points have the same value (Maxwell catastrophe)

or because of a molecular catastrophe, compounded of several of these atoms. However, the universal dynamic catastrophe, $\Theta_d \subset \Sigma_d$, consists of vectorfields failing to be stable, because of

(DS) a critical point or closed orbit (or other basic set) is not hyperbolic (singular catastrophe), or

(DB) insets and outsets are non-transversal (basin catastrophe),

or because of a combination of these reasons. Under a negradient operator, $\nabla : \Sigma_s \to \Sigma_d$, the unstable conditions (SS) and (DS) correspond, but the conditions (SM) and (DB) are totally unrelated. Thus if $\Theta_{ds} = \nabla^{-1}(\Theta_d)$, we have neither $\Theta_s \subset \Theta_{ds}$ nor $\Theta_{ds} \subset \Theta_s$. I have already referred to this, as the Guckenheimer objection. To clarify the difference, let us consider the DS metamodel, $\mathcal{B}_{ds} \subset \mathcal{F}_s \xrightarrow[\tilde{\gamma}]{\tilde{\alpha}} 2^P$, where $\tilde{\alpha} = \tilde{\alpha}_d \circ \nabla = \tilde{\alpha}_s$ assigns to a function its minima, and $\tilde{\gamma} = \tilde{\gamma}_d \circ \nabla = \tilde{\gamma}_s$ assigns to $f \in \mathcal{F}_s$ its critical set, which is the same as the nonwandering set of its negradient vectorfield, $\Omega(\nabla f)$. where $\nabla : \mathcal{F}_s \to \mathcal{X}_d$ is fixed throughout. In other words, this is precisely the static metamodel, with $\mathcal{B}_{ds}$ in place of $\mathcal{B}_s$ as universal archetypal catastrophe. This is the metamodel in which the dynamic interpretation of Section 6 is the most natural. A morphostatic field, $\sigma : C \to \mathcal{F}_s$, may be structurally stable with respect to this model, without being structurally stable with respect to $\mathcal{B}_s$, the unstable functions. Suppose C is one-dimensional, and σ is structurally stable with respect to $\mathcal{B}_{ds}$. Then it pierces strata of $\mathcal{B}_{ds}$ of codimension one transversally, so at points of $\mathcal{B} = \sigma^{-1}(\mathcal{B}_{ds})$, either a singular or a basin catastrophe takes place. The singular catastrophes are identical to those of Section 9. Here are some examples of basin catastrophes.

Example 11A. Let $T^2 \subset \mathbb{R}^3$ denote the 2-torus, embedded as shown in Figure 11-1, and $f : T^2 \to \mathbb{R}$ denote the hight from the (x,y)-plane, or $f = z|T^2$. Then f has four critical points, all nondegenerate, and four distinct critical values, and hence it is stable. The negradient vectorfield $\nabla f = -\text{grad}(f)$ has four critical points, as shown in the figure. At the bottom is an attractor, $A_o = S_o$, so the outset is trivial, $\text{Out}(S_o) = \{S_o\}$, and the inset $\text{In}(S_o) \subset T^2$ is open,

$$\text{In}(S_o) = T^2 \setminus (\text{In}(S_1) \cup \text{In}(S_2) \cup \text{In}(S_3))$$

Next is a saddle, S_1 , with one-dimensional inset and outset. $\text{In}(S_1)$ is the closed geodesic around the hole, with a point, S_2 , deleted, and $\text{Out}(S_2)$ is the closed geodesic around the lower waist, with a point, S_o , removed. Then there is another saddle point, S_2 , with similar one-dimensional inset and outset. At the top is a source, S_3 , with $In(S_3) = \{S_3\}$, and $Out(S_3) \subset T^2$ open. Both $In(S_o)$ and $Out(S_3)$ are the whole torus, with two intersecting cycles removed. As $In(S_1)$ and $Out(S_2)$ have a one-dimensional intersection, ∇f is not absolutely structurally stable, $\nabla f \in \Sigma_{ds} \setminus \mathcal{S}_s \cap \mathcal{S}_{ds}$. To embed ∇f in a curve of negradient vectorfields as a catastrophe, lets consider another example, obtained from this one by a perturbation.

Example 11 B. Let $g_d : T^2 \to \mathbb{R}$, for a small real number d , be the function defined by the hight above a plane near the (x,y)-plane, through the y-axis, and inclined by an angle $(\tan^{-1} d)$ to the x-axis, as shown in Figure 11-2. The function, g_d , has four critical points exactly like $f = g_o$, but rotated around the waists of the torus by this single. For $d \neq 0$, the insets and outsets are all transversal. Especially, $In(S_1) \cap Out(S_2) = \emptyset$, as shown in the figure. Thus, for $d \neq 0$, g_d is a stable function, and, ∇_{gd} is an absolutely structurally stable vectorfield. Now let $C \subset \mathbb{R}$ be a small interval around zero, and $c : C \to \Sigma_d = \mathcal{X}^r(T^2) : d \mapsto V_{g_d}$. This curve is a structurally-stable morphodynamic field, piercing a stratum of $\mathcal{S}_d \subset \Sigma_d$ of codimension one transversally at $d = 0$. Suppose $d > 0$, and decreases. The insets and outsets are as shown in Figure 11-2. $In(S_1)$ on the left side of the torus, $Out(S_2)$ on the right side. The critical points rotate clockwise around the waists of the torus. Suddenly , at $d = 0$, $In(S_1)$ coincides with $Out(S_2)$, an unstable configuration. Then the momentary catastrophe is over, $d < 0$, $In(S_1)$ is on the right side of the torus, and $Out(S_2)$ is on the left side. Perhaps this should be called an inset-outset catastrophe, but I call it a basin catastrophe. The reason will become clear in the next examples.

Example 11 C. Let $f : \mathbb{R}^2 \to \mathbb{R}$ be a smooth function, whose graph is an undulating surface, with hill-tops, rounded valleys, and saddle passes, as shown in Figure 11-3. There are six critical points, which we will assume to be non-degenerate, and of distinct critical values, so f is a stable function. But as shown in the figure, the outset of the higher saddle has a one-dimensional intersection with the inset of the lower saddle. Thus, the gradient vectorfield, ∇f, is not absolutely structurally stable. This situation is exactly analogous to the toral case, Example 11 A, shown in Figure 11-1.

Example 11 D. Let f be as in the previous example, and perturb it by tilting, as in Example 11 B. Thus we have a morphostatic field $\sigma : C \subset \mathbb{R} \to \Sigma_s$; $d \mapsto g_d$, with C a neighborhood of zero, and $g_o = f$. The function g_d is obtained by tilting g_o an angle $(\tan^{-1} d)$, for example, by adding a linear term, $g_d(p,q) = g_o(p,q) + dp$. Then for $d > 0$, the outset of the higher saddle, $\mathrm{Out}(S_1)$, passes to the left of the inset of the lower saddle, $\mathrm{In}(S_2)$, as shown in Figure 11-4 A, and ∇g_d is a strongly-structurally-stable vectorfield. As d decreases, they move closer together, coinciding at $d = 0$, as shown in Figure 11-4 B. For $d < 0$, the part again, with $\mathrm{Out}(S_1)$ to the right of $\mathrm{In}(S_2)$, as shown in Figure 11-4 C. The curve $\nabla \circ C$ passes a stratum of $\mathcal{E}_d \subset \Sigma_d = \mathfrak{X}^\infty(T^2)$ of codimension one at $d = 0$, while $\sigma : C \to \Sigma_s$ completely misses $\mathcal{E}_s$.

A similar example may be made from Example 11 B, by putting two bumps (attractors) on the bottom of the torus.

12. Dynamic catastrophes. At the moment, little is known about the dynamic catastrophes which occur when $\mathcal{E}_d \subset \Sigma_d$ is crossed by a morphodynamic field, $\sigma : C \to \Sigma_d$. If the Spectral Conjecture is true (see Section 1) these catastrophes may be expected to be like those of morphostatic fields, with critical points replaced by basic sets. We might expect, then, catastrophes of three types :

(DS) Singularities in the logos, due to creation or explosion (or annihilation or implosion) of basic sets, or changes of the dimensions of their insets and outsets.

(DB) Basin catastrophes due to changes of the inset-outset intersections, with basic sets fixed (actually, many basin catastrophes are accompanied by basic set explosions).

(DM) Morphos catastrophes due to changes of type of the dynamical system restricted to a fixed basic set, affecting the vertex labels of the Smale graph.

For the present, we must be satisfied with a few examples of codimension one catastrophes, of the first type, (DS). Throughout, $C = \mathbb{R}$. We will consider, in sequence, basic sets which are critical points, closed orbits, etc., or other (strange) sets. To begin, I will recall the theory of <u>characteristic multipliers</u> (or CM's).

Suppose $p \in P$ is a critical point of a vectorfield, or $X(p) = 0$, $X \in \mathfrak{X}^{\infty}(P)$. Then in a neighborhood of $p \in P$, X is approximated by a linear endomorphism, $A \in L(T_pP, T_pP)$, of the tangent space to P at p , T_pP . The complex eigenvalues of A are called the characteristic exponents of X at p , their exponentials, which are eigenvalues of $\exp(A)$, are the CM's of X at p . The critical point, p , is <u>elementary</u> if none of its CM's are on the unit circle. For a closed orbit, $\gamma \subset P$, choose a point, $p \in \gamma$, and a subspace of T_pP complementary to $X(p)$, S_p , so

$$T_pP = S_p \oplus \langle X(p) \rangle \quad .$$

By a construction due to Poincaré, a linear automorphism, B , of S_p is found which approximates the assymptotic behavior of the orbits close to γ. The eigenvalues of B are called the CM's of X at γ, or the CM's of γ. If $\dim(P) = n$, there will be n CM's for each critical point, and $(n-1)$ CM's for each closed orbit. A closed orbit is <u>elementary</u> if none of its CM's are on the unit circle. According to a classic result, the Kupka-Smale Theorem, the critical points and closed orbits are generically elementary. But within a structurally stable morphodynamic field, $\sigma : C \to \Sigma_d$, non-generic phenomena may occur at the universal catastrophe, $\Theta_d \subset \Sigma_d$.

Now for the singular (SD) catastrophes of critical points, of codimension one, we have a complete catalog of the generic cases, as only two phenomena appear. In each, the change takes place at a single critical point, for which the CM's are moving with the control, $c \in C$. At the catastrophic value, $c_o \in \mathcal{G} = \sigma^{-1}(\Theta_d)$, either a real eigenvalue arrives at the unit circle, (the <u>static creation catastrophe</u>, Figure 12-1), or a complex conjugate pair crosses the unit circle (the Hopf excitation catastrophe, Figure 12-2).

For codimension two, the singular (DS) catastrophes of critical points have been classified by Takens [315], fourteen cases occur.

For closed orbits, there are five structurally stable singular catastrophes of codimension one. The first, the <u>blue sky catastrophe</u> mentionned by Ruelle and Takens [411, p. 174], consists of a closed orbit, γ_c of $X_c = \sigma(c)$, $c \in C$, whose period goes to infinity as c approaches a catastrophic value $c_o \in \mathcal{G}$. When $c = c_o$, γ_c has vanished (into the clear blu sky, Figure 12-3). Meanwhile, a CM of γ_c approaches the unit circle. Next are three catastrophes studied by Brunovsky [303], corresponding to the passage of a real CM through $+1$ (the <u>dynamic creation catastrophe</u>, Figure 12-4), through -1 (<u>subtle division</u>, Figure 12-5, and <u>murder</u>, Figure 12-6).

These occur also in Hamiltonian systems [301]. Finally, the passage of a complex conjugate pair of CM's through the unit circle produces a logos similar to the Hopf catastrophe, as shown by Ruelle and Takens [A11] (the Neumark catastrophe, Figure 12-7).

The structurally stable singular (DS) catastrophes for closed orbits, of codimension two, have not yet been systematically studied. But one very instructive example, due to Zeeman, is given in Section 14.

After closed orbits, the next more complicated basic sets are the invariant tori. Recall that a submanifold $M \subset P$ is invariant under $X \in \mathfrak{X}_d$ if for every point $m \in M$, $X(m) \in T_m M < T_m P$, so $X|M$ may be considered a vectorfield on M. An invariant torus simply means an invariant manifold of X, $M \subset P$, with M diffeomorphic to a torus, T^k, $2 \leq k \leq \dim(P)$. Like the more complicated basic sets, the singular catastrophies of tori are largely unknown at present, but one case has been studied by Ruelle and Takens [A11]. This is similar to the Hopf and Neumark catastrophes. As c passes $c_o \in C$, the inset and outset of the invariant torus, T^k_c, of $X_c = \xi(c)$, change dimension by one, and from $T^k_{c_o}$ grows an invariant torus, T^{k+1}_c, surrounding T^k_c, the Ruelle-Takens excitation catastrophe. The central torus, T^k_c, $c > c_o$, may become wandering, and drop out of the logos.

This is about all that is known of the dynamic singular (DS) catastrophes at present. For the basin (DB) catastrophes, the examples of the previous section give some idea of what to expect for general morphodynamic fields. Any inset of a basic set may drift into the outset of any other basic set. But in this context, a further complication arises, which is impossible with morphostatic fields. If a basic set, B, is a closed orbit, or bigger, then its inset may drift into its own outset, becoming a homoclinic set. This is a catastrophe of compound type, as it causes a basic set explosion.

Suddenly, B becomes one component of a Cantor set of copies of itself, and this mess (a strange basic set) comprises a basic set for the post-catastrophic vectorfield. I call this the Smale horseshoe catastrophe, although the skeleton of the idea was known to Poincaré and Birkhoff.

Finally, lets consider a single example of a morphos (DM) catastrophe. Lets follow a single invariant torus, $T_c^2 \subset P$, of $X_c = \pi(c)$, $c \in C = \mathbb{R}$. Suppose that as the control is changed, the vectorfield, X_c, changes only in a neighborhood of T_c^2, which itself does not move. Further, suppose that the inset and outset of T_c^2 are also motionless. Thus the only part of the Smale graph of X_c which changes is the label, $X_c | T_c^2$, of the vertex corresponding to the basic set, T_c^2. The logos is unchanged, but the morphos changes. Let $Y_c = X_c | T_c^2$ be the restricted morphodynamic field on the torus. This context has been thoroughly studied by Sotomayor [313]. As in this case Y_c has no critical point, Y_c is a Peixoto field, with an even number of closed orbits, half attractors, half repellors, alternating around the torus, each wound around it the same way. If $c \in \hat{C}$, Y_c corresponds to an irrational rotation of the torus, and all orbits are dense (an almost periodic motion). Thus as c changes, Y_c is a Peixoto field for a time, then after a momentary almost periodic motion for $c \in \hat{C}$, Y_c becomes again a Peixoto field, with a different number of closed orbits. The catastrophe, $\hat{C} \subset \mathbb{R}$, may be a set of relatively large measure. Further, the non-catastrophic intermediate tori may be wandering, and drop out of the logos. Thus, the logos, as well as the morphos, may change. This is the Sotomayor vascillation catastrophe.

The catastrophes of strange basic sets, of both singular and morphos types, are still unknown. Also, it must be admitted that the classification of catastrophes into three types (DS, B3, DM) is, even in the case of codimension one, fictitious. A singular catastrophe may change the basins of attraction, and the inset-outset intersections, and the restricted vectorfield. Altogether, the future development of the subject looks arduous. It might be simpler to look only for those catastrophes of special significance in the dynamic interpretation of morphodynamic fields : those of the attractors and basins. Thus we could envisage a theory as follows (optional digression).

A vectorfield, $X \in \Sigma_d$, is crested if it has a countable number of attractors, $\{A_i\}$, with basins, $\{B_i\}$, dense in P, $\overline{\cup B_i} = P$. Two crested fields, X and Y, are A-equivalent if there is a homeomorphism of P, taking attractors of X onto attractors of Y, preserving oriented orbits within attractors, but not parameter, and they are B-equivalent if there is a homeomorphism taking attractors to attractors, basins to basins, but not preserving orbits, and AB-equivalent if both A- and B-equivalent. Then the goal is to classify the interiors of the equivalence classes (attractor-stable basin-stable, and AB-stable vectorfields) within the set of crested vectorfields. Unfortunately, this program is probably not easier than the current one (the spectral conjecture).

In any case, this brings us to the current frontier of morphodynamic catastrophe theory, obviously a nascent subject of great difficulty.

PART II

APPLICATIONS

At present, morphology is an infant science, developing as a collaboration of mathematicians and experimentalists of various specialties. In this half, I will give a sketch map for a few segments of this new frontier of applied mathematics. Unfortunately, I must omit the most spectacular applications, Thom's schemes for embryology and psycholinguistics, for they are beyond my competence. I do hope, however, that Part I makes the published papers of Thom more accessible.

CHAPTER 4 : EXEMPLARY MODELS

Our next step is to see how a morphometric model is adapted to a specific experimental corpus. Here is one example each, of a static,dynamic, kymatic, and a self-regulating model, abstracted from the recent literature. It will help, at this point, to experiment with a model of Zeeman's catastrophe machine, described in Figure 13-0.

13. Phase transitions (Fowler). Early in the history of mathematical morphogenesis, Thom realized that the van der Waal's surface of the gas-liquid phase transition was a static cusp catastrophe - hence his name, Maxwell convention, for the transitions at the central ray. The details of this model have been studied by David Fowler, and here I will give the highlights of his forthcoming paper [405]. I will ignore the fact that, van der Waal's surface is not a good model for the phase change near the critical point.

The experimental apparatus consists of a hollow cylinder, closed on both ends, with a sliding piston inside which seals perfectly against the wall of the cylinder, dividing it into two sealed chambers. One is evacuated, and filled with one grain of a particular gas. The other is connected to a hydraulic device which maintains a fixed, adjustable pressure, P , against the piston, and therefore on the gas in the first chamber. The whole cylinder is immersed in a thermal bath, of adjustable temperature, T . The position of the piston is registered on an external gauge, calibrated for the volume of the first chamber, V . The experimentalist can control P and T with knobs, and observes only the gauge, V .

Holding the T knob fixed, he turns the P knob slowly back and forth, and records V graphically, obtaining the isotherms shown in Figure 13-1, and the corresponding actual logos (state surface) shown in Figure 13-2. For some settings of the controls, he must wait a few minutes for the process to reach equilibrium, before recording the volume, but a static value of V always results. The actual logos, he observes, fits very closely the van der Waal's surface, defined by

$$\left(P + \frac{a}{V^2} \right) (V - b) - rT = 0$$

if the constants a,b, and r are well chosen, as shown in Figure 13-3.

Later, a morphogeneticist (Fowler) looks at the logos. He reasons : "no oscillation, should try a static model. Two dimensional control, $C \subset \mathbb{R}^2$, the positive quadrant, one dimensional phase space $P \subset \mathbb{R}$, the positive ray, the logos must be either a fold or a cusp. Looks just like a cusp. There must be a change of coordinates to put the van der Waal equation into Thom's standard form. The actual catastrophe, $K \subset C$, looks like the Maxwell set of the cusp". Very cleverly, he divides the van der Waal's equation by V , and introduces a new coordinate, $X = V^{-1}$ ($V > 0$ in this process) , the absolute density of the gas. This is to eliminate to nonstandard steepness of the state surface. Then, an affine translation, to slide the critical point (P_c, T_c, X_c) to the origin, so $(P,T,V) \rightarrow (p,t,x)$, where

$$\begin{cases} p = P - P_c \\ t = T - T_c \\ x = \frac{1}{V} - \frac{1}{V_c} = X - X_c \end{cases}$$

As $(P_c, T_c, X_c) = \left(\frac{a}{27\, b^2}, \frac{8a}{27\, br}, \frac{1}{3b} \right)$, the van der Waal's surface of Figure 13-3 is transformed into the logos, shown in Figure 13-4, defined by

$$x^3 + cx + d = 0$$

where

$$c = \frac{1}{a} \left(\frac{r}{b} t + p \right) = \frac{1}{a} \left[\frac{r}{b} T + P - \frac{a}{3b^2} \right]$$

$$d = \frac{1}{3ab} \left(\frac{r}{b} t - 2p \right) = \frac{1}{3ab} \left[\frac{r}{b} T - 2P - \frac{2a}{9b^2} \right]$$

Making the further transformation : $(p,t) \rightarrow (c,d)$, we obtain the standard cusp logos of Figure 10-2. This is the logos of the morphostatic field

$$\sigma_o : \mathbb{R}^2 \rightarrow \Sigma_s : (c,d) \rightarrow \sigma_o(c,d)$$

defined by $\sigma_o(c,d)(x) = \frac{1}{4} x^4 + \frac{1}{2} cx^2 + dx$. Returning to the original coordinates, we obtain a morphostatic field for the van der Waal logos,

$$\sigma : \mathbb{R}^2 \rightarrow \Sigma_s : (P,T) \rightarrow \sigma(P,T)$$

defined by

$$\sigma(P,T)(V) = \frac{1}{4V^4} - \frac{1}{3bV^3} + \frac{1}{2a}\left(\frac{r}{b}T + P\right)\frac{1}{V^2}$$

$$- \frac{P}{ab}\frac{1}{V} - \frac{1}{18ab^2}\left\{\frac{r}{b}T - 5P - \frac{a}{6b^4}\right\}$$

Could this potential, with units like twelve-dimensional volume, have any physical significance ? If it helps, the term independent of V could be dropped, or arbitrarily changed. The van der Waal's equation may be recovered from this static field by differentiating with respect to V , multiplying by V^3 , and equating to zero.

Now, lets consider the catastrophe. The theoretical catastrophe, $\theta_o = \sigma_o^{-1}(\Theta_s)$ in the (c,d)-control space, consists of a cusp (the singular catastrophes) defined by

$$\theta_s : 4c^3 + 27\, d^2 = 0$$

together with a central ray (the maxwell set) defined by

$$\theta_m : c < 0 \ , \ d = 0$$

as shown in Figure 13-5. Transformed to the original coordinates in C , we have $\theta = \sigma^{-1}(\Theta_s)$, with the cusp

$$\theta_s : \frac{4}{a^3}\left[\frac{r}{b}T + P - \frac{a}{3b^2}\right]^3 + \frac{3}{a^2b^2}\left[\frac{r}{b}T - 2P - \frac{2a}{9b^2}\right]^2 = 0$$

and Maxwell set

$$\theta_m : \frac{r}{b}T + P - \frac{a}{3b^2} < 0 \ , \ \frac{r}{b}T - 2P - \frac{2a}{9b^2} = 0$$

or equivalently,

$$\theta_m : P < P_c \ , \ \frac{r}{b} T - 2P - \frac{2a}{9b^2} = 0$$

as shown in Figure 13 - 6. The experimentally observed catastrophe, $K \subset C$, is a ray like θ_m, but apparently not exactly the same. Thus here we have an exceptional application, in the sense discussed in Section 3. The catastrophe convention needed is : K is obtained from θ_m by a certain perturbation (apparently the equation for K is not well known, but is calculable , in principle, from Maxwell's theory of the critical point) and the system changes sheets of the logos whenever the control crosses K . If it actually were found that $K = \theta_m$, then this would be exactly the same as Thom's Maxwell convention : $\theta_m \subset \theta$ is the actual catastrophe, and the system always prefers the lower of the two minima.

Perhaps this topic is not yet finished. It is possible that a different morphostatic field could provide the same logos and singular catastrophe, but a different Maxwell set, so that $\theta_m = K$. This field would differ from σ , probably, only in the terms independent of V . A further, less trivial modification would be required to fit the real experimental data [404].

14. Forced vibrations (Zeeman). Now I will give an example of a dynamic catastrophe of codimension two, due to Zeeman [318]. For the sake of exposition, I will replace his original application - to short-term memory - by another (fictitious) experimental corpus.

Suppose an electronic watch is constructed as follows. A small, ferromagnetic tuning fork, with a natural resonant frequency of one kilohertz, ω_o is placed in the field of small electromagnets, connected to a miniature electronic system which provides positive feedback, so that the oscillation is stable, and does not decay. If x denotes the linear displacement of one end the Duffing equation,

$$x'' + ax' + 4\pi^2\omega_o^2\, x = 0 \quad , \quad a > 0$$

which has a stable solution of frequency ω_1 , close to ω_o . The tuning fork is mechanically coupled to an escapement mechanism, which drives the watch. The coupled system is governed by the same equation, with the coefficient a decreased by the resistance of the escapement. The watch controlled in this way, turns with an angular velocity, ω_1 , of satisfactory stability, constant to a high degree of accuracy, depending on both the amplitude and frequency of the tuning fork. But the almost constant rate may not be the correct one for keeping time. So a speed control is added, to make small adjustments of the frequency. This consists of a small supplementary electronic oscillator, with a quartz regulated variable frequency control, coupled to the arms of the tuning fork by additional miniature coils. The speed control is accomplished by delicate adjustments of two screws, tuning the amplitude and frequency of this oscillator. The combined system is governed by the Duffing equation with a sinusoidal forcing term,

$$x'' + ax' + 4\pi^2\omega_o^2\, x = F \cos 2\pi\omega t$$

where F and ω are the controls, and should be set at $F \approx 0$, $\omega \approx \omega_1$. The engineers designing this system have computed that the accuracy and stability of this system are unsurpassed in the industry, but it takes them months to set the controls (F,ω) so that the potential accuracy is obtained. Zeeman's analysis of the Duffing equation with forcing term shows why, and also provides a scheme for adjusting the watch more rapidly.

First, we display the Duffing equation as a morphodynamic field. Let $C = \mathbb{R}^2$ with coordinates (F,ω) , and $P = \mathbb{R}^2 \times S^1$, with coordinates

(x,y,t). Here S^1 is identified with the reals mod 1, $S^1 = \mathbb{R}/\mathbb{Z}$, and t is actually the standard coordinate in the covering space, $\mathbb{R}$. Then the Duffing equation becomes a dynamical system on P, for fixed (F,ω),

$$\begin{cases} x' = y \\ y' = -ay - 4\pi^2\omega_o^2 x + F \cos 2\pi t \\ t' = \omega \end{cases}$$

and this defines a morphodynamic field

$$\sigma : C \to \Sigma_d = \mathfrak{X}^\infty(P) : (F,\omega) \to \sigma(F,\omega)$$

$$\sigma(F,\omega) : P = \mathbb{R}^2 \times S^1 \to TP = (\mathbb{R}^2 \times S^1) \times (\mathbb{R}^2 \times \mathbb{R})$$

$$: (x,y,t) \to (((x,y),t),((y,Y),\omega))$$

where $Y = -ay - 4\pi^2\omega_o^2 x + F \cos 2\pi t$. According to the analysis of Zeeman, this morphodynamic field has a structurally stable catastrophe, at $(F,\omega)=(0,\omega_1)$, of codimension two. Since here, $C \times P$ is five dimensional, it is not possible to visualize the logos directly. But the catastrophe involves the trifurcation of a nonelementary closed orbit of $\sigma(0,\omega_1)$, which has frequency close to ω_1. Lets visualize $\mathbb{R}^2$ as a small disk, so $P = \mathbb{R}^2 \times S^1$ is seen as a solid ring. The closed orbit of $\sigma(0,\omega_1)$, $\gamma(0,\omega_1)$, traverses this ring once, as shown in Figure 14-1A. While $\sigma(0,\omega_1)$ may have many closed orbits, this is the only one circling the ring once. As $(F,\omega) \in C = \mathbb{R}^2$ is moved away from $(0,\omega_1)$ in some directions, this closed orbit moves slightly in the ring, and becomes an attractor. But in other directions, it trifurcates into three closed orbits traversing the ring once, two attractors and a saddle, as shown in Figure 14-1B. The catastrophe, $\theta = \sigma^{-1}(\Theta_d) \subset C = \mathbb{R}^2$, contains a cusp, as shown in Figure 14-2. When the control passes one of the rays of the cusp, from inside to outside, two closed orbits, a saddle and an attractor, come together and vanish, much like critical points in the static cusp catastrophe.

To extract a visible aspect of the logos of this catastrophe, Zeeman introduces a ficticious phase variable, $A \in \mathbb{R}$, denoting the amplitude of once-traversing closed orbits, and derives the graph shown in Figure 14-2, precisely the static cusp catastrophe. Presumably, the frequency of the closed orbits has a similar trifurcation. Thus, we call this the dynamic cusp catastrophe.

We may suppose that the watch mechanism described above follows the delay convention. Thus if the control is moved from a position of large amplitude and frequency by decreasing the amplitude only, (dotted curve in Figure 14-2) the system is initially in an orbit very close to a once-traversing attractor, and stays near this attractor as the control passes the first ray of the catastrophe, and a second attractor is created. When the control passes the second ray of the catastrophe, the old attractor vanishes, and the system is attracted swiftly to the remaining attractor. A discontinuity in the amplitude and frequency of the watch is observed.

Perhaps the best strategy for the watch manufacturer would be to supply Figure 14-2 with each new watch sold, to facilitate its adjustment by the owner.

This model can also be applied to certain mental and erotic processes.

15. Turbulence (Ruelle and Takens). Next we consider an experiment in which a fluid is observed in a transparent chamber, while subjected to external forces controlled by the experimenter, with a single knob, $c \in C = \mathbb{R}$. At $c = 0$, the fluid is at rest. As c is increased, the fluid moves, and reveales a re-

cognizable pattern of motion. At catastrophic values of the control, the morphology of this pattern suddenly changes. Eventually, the fluid becomes so chaotic it looks like write froth, turbulence has begun. The onset of turbulence has troubled hydrodynamicists for years, but finally, a plausible explanation has been given by Ruelle and Takens [411].

Let B denote the container of the fluid, and suppose $B \subset \mathbb{R}^3$ is a reasonable set, for example, a manifold with corners, and the closure of a bounded open set. Let $P = \mathfrak{X}_0^\infty(B)$, the vectorfields on B vanishing on its boundary. A point in the phase space, P, is a possible instantaneous velocity field for the fluid. As P is infinite dimensional, the nature of $\Sigma_d = \mathfrak{X}^\infty(P)$ and $\Theta_d \subset \Sigma_d$ are little understood. The fluid motion is governed by the Navier-Stokes equation, with a forcing term depending on the control, which may be interpreted as a vectorfield on P. Suppose that this vectorfield is smoothed, so that at each $c \in C$, the fluid motion is described by a vector-field $\sigma(c) \in \Sigma_d = \mathfrak{X}^\infty(P)$, and $\sigma(0)$ is the Navier-Stokes equation. Thus we have a morphodynamic field (not precisely known), $\sigma : C \to \Sigma_d$.

For $\sigma(0)$, we suppose that, as in the Navier-Stokes equation, the zero vectorfield of P is an attracting critical point, the only attractor in fact, and that this is supported by the experimental corpus : any observable motion of the system quickly subsides when the control is shifted to zero.

As the control is gradually increased, the attracting critical point moves slowly away from zero, but remains an attractor for a time. A steady motion of the fluid is observed, revealing this attractor. Eventually, the control passes a catastrophic value. As we always suppose a morphodynamic field must be structurally stable to correspond to an observable phenomena, we must now observe (assuming $\Theta_d \subset \Sigma_d$ behaves as if P were finite dimensional) one of the canonical dynamic catastrophes of codimension one : annihilation (followed by a jump to another attractor) or Hopf excitation (followed by a gradually growing oscillation). Suppose the latter occurs. Then the fluid motion is caught in the basin of attraction of a closed orbit attractor, and the observer sees the fluid oscillating in a cycle of velocity vectorfields. As c passes the next catastrophic value, we must observe one of the canonical dynamic catastrophes of codimension one : annihilation, disappearance into the blue, or murder (followed by a jump to another attractor), subtle division (observable as a loss of frequency), or Neumark excitation (observable as a compound vibration with two frequences). Suppose the latter occurs. Then the two frequencies gradually change through rational and irrational rations, and the Sotomayor vascillation catastrophes occur in rapid succession, as the control is increased further. This may be observable only as a slight jitter, or trembling, in the observed compound oscillation. Eventually, there may be Ruelle-Takens excitation catastrophe, and the attractor changes from a 2-torus to a 3-torus, observed as a compound oscillation with three frequencies, or vibrational modes. Then a sequence of unknown catastrophes may take place on the attracting 3-torus, until finally, through another excitation, another mode of oscillation is activated, and the motion follows an attracting 4-torus. Then another sequence of unknown catastrophes for vectorfields on the 4-torus may be observed, until, finally, a Smale horseshoe catastrophe takes place, and the 4-torus is replaced by a strange attractor, within the 4-torus, that looks like a heap of spaghetti (one-dimensional Cantor manifold). This is the onset of turbulence, according to Ruelle and Takens, and also an example of a kymatic model.

This context suggests that the universal catastrophe of the kymatic model can be studied experimentally.

16. Neurons (Zeeman). As an example of a self-regulation model, we consider an experiment of the Hodgkin-Huxley type. A neuron is tacked to the table, and electrodes attatched to the inside and outside of the axon. The experimentalist controls conductance of the cell membrane to potassium ions, g_k, and the voltage across the electrodes, b, (from outside to inside) and observes the conductance of sodium ions, q_{Na}. His goal is to understand the mechanism of the nerve impulse, the spike of activity of these three parameters produced by triggering the nerve, shown in Figure 16-1. He finds, of course, that the process adjusts its own controls, and all he is able to do is vary the voltage. When he increases the voltage from its resting value to a certain trigger value and releases the control, a nerve impulse results.

In Zeeman's self-regulation model, we have $C = \mathbb{R}^2$, with coordinates (a,b), and $P = \mathbb{R}$, with coordinate x. Representing the two morphogenetic fields by horizontal and vertical vectorfield on $C \times P = \mathbb{R}^3$, as described in Section 8, the combined field is an ordinary dynamical system on $\mathbb{R}^3$, Zeeman's local nerve impulse equations :

$$\dot{x} = -1\ 25(x^3 + ax + b)$$
$$\dot{a} = (x + 0{,}06(a + 0{,}5))(x - 1.5a - 1.67)(0.054(b - 0.8)^2 + 0.75)$$
$$\dot{b} = -g_k(b + 1.4) - g_{Na}(b - 4.95) - 0.15(b - 0.15)$$

where a,b, and x determine g_k, V, and g_{Na}, respectively, as shown in Figure 16-2. Near the origin in $\mathbb{R}^3$, these equations are (rounding off the coefficients)

$$\dot{x} = -1.25(x^3 + ax + b)$$
$$\begin{aligned}\dot{a} \approx {} & (\tfrac{3}{4}x^2 - x - \tfrac{3}{100}) \\ & - (x + \tfrac{1}{10})\,a - (\tfrac{8}{100}x^2 - \tfrac{1}{10}x - \tfrac{3}{1000})b \\ & - \tfrac{1}{13}a^2 + (\tfrac{1}{10}x - \tfrac{1}{100})\,ab + (\tfrac{1}{20}x^2 - \tfrac{1}{15}x + \tfrac{1}{500}) \\ & + \tfrac{1}{100}a^2b - (\tfrac{1}{10}x + \tfrac{1}{160})\,ab^2 - \tfrac{1}{200}a^2b^2\end{aligned}$$
$$\dot{b} = -2 - 3a - b - 2ab$$

The interpretation is best understood by consideration of a simplistic model, Zeeman's "Example 8" :

$$\dot{x} = -B(x^3 + ax + b)$$
$$\dot{a} = -2a - 2x$$
$$\dot{b} = -1 - a$$

where $B \in \mathbb{R}$ is very large. Here, for additional simplification, we identify (a,b,x) with $(g_k, V, -g_{Na})$.

Consider, first, the dynamic model defined by $\sigma : C \to \Sigma_d = \mathfrak{X}^\infty(P)$, where $C = \mathbb{R}^2$ and $P = \mathbb{R}$, where

$$\sigma(a,b)(x) = (x, -B(x^3 + ax + b))$$

This is a version of the static cusp catastrophe, interpreted dynamically. The logos is the graph of critical points of the negradient vectorfields $\sigma(a,b)$. As we interpret this field dynamically, we have the singular catastrophe only, as shown in Figure 16-3. For given control values (a,b) of potassium conductance and action potential, the sodium conductance, x , will change swiftly from an arbitrary initial condition to an equilibrium value, or attractor. If (a,b) is outside the cusp, θ , there is only one attractor. But if (a,b) is inside the cusp, it will approach one of the two attractors, depending on whether the initial sodium conductance is above or below the separatrix of the basins of attraction, which is the virtual logos.

If the control is slowly moved, by external manipulation of the potassium conductance and the action potential (electrode voltage), the sodium conductance will follow the actual logos. That "slowly" here may be interpreted reasonably, the large constant, B, has been inserted in the sodium equation, which is therefore called the fast equation. As moving the control slowly produces a slow shift of the phase variable, x, along the logos, it is called in this context, the slow manifold.

Next, we add, to the control by the experimentalist, a representation of the effect the Neuron has on the controls through an internal (biochemical) process of self-regulation. This, in the simplistic model, is given by the horizontal vectorfield defined by the slow equations,

$$\dot{a} = -2a - 2x$$
$$\dot{b} = -1 - a$$

which give a vectorfield on each horizontal plane, x = constant, which may be considered as a dynamical system on the control space, $C = \mathbb{R}^2$, of variables (a,b). But the self-regulation varieswith the hight of this plane. So if the sodium conductance, x, could be fixed, the "controls" would then evolve according to this slow equation. The dynamic interpretation of the combined system is the same as if the controls were adjusted by the experimentalist, according to the slow equation. From an arbitrary initial point in $C \times P = \mathbb{R}^3$, the phase variable, x, zooms to the slow manifold. Only there does the vertical motion slow to such an extent that the action of the slow self-regulation dynamic becomes significant. The orbit of the combined system then drags along near the slow manifold, occasionally passing through, as it is not an invariant set of the total dynamic. So the eventual behavior of the system is described by orbits of the slow equation, near the slow manifold or logos, and projected upon it, as shown in Figure 16-4. There is an attracting critical point of the total system on the slow manifold at $(a,b,x) = (-1,0,1)$. Suppose the neuron parameters are at equilibrium near these values, when the experimentalist suddenly increases the voltage, then releases it. The point in $C \times P$ represents the parameters of the neuron moves to the right, past the right-hand ray of the cusp catastrophe, is caught by the last equation, zoomed downward to the lower attracting sheet of the logos, then slowly returned to equilibrium by the slow equations, spiraling around behind the cusp, so no further fast action is observed, as shown in Figure 16-5.

Qualitatively, the simple model gives the basic features of the nerve impulse, as shown in Figure 16-1. For a more precise agreement with actual experimental results, Zeeman adjusted the slow equations to fit the data. The portrait of the qualitative behavior near the slow manifold is slightly different, due to an added saddle point, as shown in Figure 16-6.

This is one of the most impressive applications of catastrophe theory, and it is well worthwhile to read Zeeman's paper. It is also a pioneer example of collaboration of mathematical and empirical morphologists, as Zeeman has recommended experiments suggested by his model, which have been performed, verifying his predictions.

CHAPTER 5. EXPERIMENTAL MORPHOLOGY

Next, I would like to describe a few experimental situations where catastrophic changes of morphology are observed, and kymatic models might be helpful to provide a global overview of the process. As such models have not yet been studied, this is all speculation, and borders on science fiction. But mainly I would like to indicate haw the collaboration of mathematical and experimental morphologists might be mutually profitable.

17. Hydrodynamics. A general scheme for hydrodynamical catastrophes has been given in Section 15, due to Ruelle and Takens. The observation of real fluid morphological catastrophes has a long history. A book of excellent photographs has been published by Schwenk [111], showing morphogenesis observed in nature. Theoretical discussion of various phenomena is given in numerous texts, for example, Eckhaus [402]. In the laboratory, the most studied phenomena are those of Taylor and Bénard, which I will briefly describe.

Couette flow refers to a fluid between concentric rotating cylinders. Let ω_1 and ω_2 denote their velocities. For each point $c = (\omega_1, \omega_2) \in C = \mathbb{R}^2$, the flow evolves according to the Navier-Stokes equation, with forcing term, $\sigma(c) \in \Sigma_d = \mathfrak{X}^\infty(P)$, the kymatic model described in Section 15, but having two-dimensional control. If the control is moved along a curve, $t \mapsto c(t)$, starting at the origin, the fluid is observed first motionless, then in uniform rotational flow, then suddenly changes to a stack of annular circulations, shown in Figures 17-1 and 17-2, called Taylor cells. This is still, a point attractor, and no catastrophe has taken place to explain the breakdown of symmetry. Later, the boundaries of the Taylor cells begin to oscillate, revealing a Hopf excitation catastrophe. Then follow a series of catastrophes such as Ruelle and Takens describe, and finally, turbulence is observed. For more details, see Coles [401], Feynman, Leighton, and Sands [403], or Snyder [413, 414]. By now, so many experiments have been done, that it should be possible to extract from the corpus a complete graph of the actual catastrophe, $K \subset \mathbb{R}^2$. I don't know if this has been done. But if the experimentalist had a morphosophic orientation, this graph would be his first objective.

The phenomenon of Bénard is observed in a fluid sandwiched between two horizontal glass plates, heated from below. The static fluid suddenly breaks into hexagonal cells, in which convection currents flow torally, as shown in Figure 17-3. For details, see Velarde, Schecter, and Kiockemeister [415]. A Kymatic model for this phenomenon would be very similar to that of Ruelle and Takens, described in Section 15.

Here it must be admitted, that morphogenesis, as currently concieved, does not explain the Taylor or Bénard cells, but only models the catastrophes, during which one morphology changes to another, especially through the excitation of additional modes of vibration.

18. Kymatics. Now I would like to give a short survey of some experimental work of Hans Jenny [103] and Theodore Schwenk [112], and I cannot recommend highly enough the reading of the original reports of these pioneer experimental morphologists.

Hans Jenny - who coined the word "kymatics", meaning wave-like, which I have adopted - photographs hydrodynamical vibrations. The apparatus devised by him consists of a thin plate or diaphragm, driven by a piezoelectric crystal or loudspreaker from a sinewave generator with two controls, amplitude and frequency, as in Zeeman's Duffing equation, Section 14. On the vibrating surface is placed a small amount of sand, powder, or liquids of various viscosities. The resulting pattern undergoes morphogenetic catastrophes as the control is varied. The highly evolved photographic technique records, in motion, the most incredible patterns, some resembling very familiar morphotypes occuring in nature, others like the computer graphic films of the Whitney family. Two stills, from Jenny's book, are shown in Figures 19-1 and 18-2. The first shows sand on a metal plate, in a series of five consecutive patterns. The sand collects on the Chaldni nodal lines, where the amplitude of the plate vibration is minimal.

Here I may propose some ideas for a model for this corpus. Let $D \subset \mathbb{R}^2$ represent the plate, a disk, and $f_t = D \to \mathbb{R}$ denote the deflection of the disk, in a normal direction. Suppose that $N_t : D \to \mathbb{R}^3$ represents the normal vectorfield to the deflected disk, which is the graph of f_t, and that the force moving the sand is proportional to the horizontal component of the acceleration, $\frac{\partial N_t}{\partial t}$. Thus $F = ma$, where a is the vectorfield on D defined by

$$a(x,y) = \nabla(\frac{\partial f_t}{\partial t})$$

the negradient of the vertical velocity function, $\frac{\partial f_t}{\partial t} = p_c(t)$. The kymatic model, $\sigma : C = \mathbb{R}^2 \to \Sigma_d = \mathfrak{X}^\infty(P)$, where $P = C^\infty(D, \mathbb{R})$, and $\sigma(c)$ is a wave operator, has an attractor A, for $c \in C$, $t \mapsto f_t$ is an orbit close to this attractor, and $t \mapsto p_c(t)$ is the velocity of this orbit. Then $p_c : \mathbb{R} \to P$ may be considered as a static model with one-dimensional control. The logos of this field, $\mathcal{L}_c \subset \mathbb{R} \times D$, projected into D, is the Chaldni nodal set. As $c \in C$ is changed, the nodal set changes, and reveals a catastrophic change when c crosses the catastrophe, $\mathfrak{S} = \sigma^{-1}(\mathfrak{S}_d) \subset C$, as shown in Figure 18-1. This particular example looks very much like a static basin catastrophe, compare Figure 11-4.

The second example, Figure 11-2, shows a still from one of the most interesting films I have seen, in which the only actor is a drop of water. Pulsating spatial symmetry of the boundary, hydrodynamic oscillation within, density condensation along the nodal lines, and optical caustics dance together in a compound oscillation of several modes, and catastrophic changes of the complete pattern result from slight adjustments of the two controls. It would be interesting to try to graph the complete catastrophe, $K \subset C = \mathbb{R}^2$, with the original apparatus, using human observation as the catastrophe detector.

The experiment of Theodore Schwenk, elaborating earlier work of Helmholtz and others [114, p.70], is even more difficult to morphometrise, but I suppose it admits a Kymatic model. A glass disk of transparent liquid is held over a very sophisticated photographic apparatus. A drop of the same liquid falls into the disk from above. The density rarefactions of the fluid motion are revealed in sharp contrast in the photograph. Examples are shown in Figures 18-3 and 18-4. This experiment can be crudely repeated at home, by releasing a drop of ink into a glass of still water, from a hight of two or three inches. Schwenk's apparatus was so precisely made that the same patterns could be reproduced many times. He observed that hidden controls, such as planetary conjunctions, or infinitesimal impurities in the fluid, produced catastrophic changes in the observed morphology. Thom suggests that a static model can be made for this phenomenon [201, § 5.5].

These pioneers have shown how discoveries in the mathematical theory of dynamic catastrophes may be made with experimental methods. This is experimental morphology, which Thom has called the science of the future.

19. Liquid crystals. Discovered in 1888, liquid crystal denotes a group of physical states between liquid and solid : nematic, cholesteric, smectic A , C , and B . Nematic and cholesteric materials are more like liquid, smectics closer to solid. Each changes to ordinary (isotropic) liquid when sufficiently heated, and to ordinary solid when cooled. The extraordinary properties of these materials are due to the elongated shape of their large molecules, and many biological materials belong to this class. For details, see Gray [406].

While liquid crystals display many morphogenetic phenomena of special interest to morphologists, I will describe briefly only two here.

In the Williams effect, a thin layer of oriented nematic is observed through transparent electrodes, which maintain an electrostatic field. As the experimentalist increases the strenght of this field, the liquid crystal forms cells of convection, as shown in Figure 19-1. The fluid motion is very similar to the Bénard phenomenon, and when I observed this effect through a microscope in Orsay, I thought I recognized several catastrophes.

In the Meyer flexoelectric effect, an alternating electric field is applied to a similar preparation. For small values of the amplitude and frequency, waves transverse to the electrodes are observed, very similar to sound waves. If the nematic is replaced by a cholesteric, these may display many different colors. For higher values of the controls, there appear various catastrophes, an oscillating Williams effect, and finally, turbulence. There is a considerable similarity to the experiments of Hans Jenny. I suspect that kymatic models for these phenomena should be similar to those of the Ruelle-Takens model, but in place of the Navier-Stokes equation, one would have to deal with the very cumbersome magnetohydronamical equations currently being discussed by theoreticians of liquid physics. So far as I know, there has been no attempt yet to graph the catastrophe, $K \subset \mathbb{R}^2$.

The theory of disinclinations of liquid crystals looks like a very interesting problem for the mathematical morphologist. But as it does not seem to me that it can be morphometrized by Thom's scheme, I will not go into it here. Similar patterns are observed in chemical waves [416].

<u>20. Video</u>. Now I would like to describe a fascinating phenomenon shown to me by Jack Henry Moore, a pioneer of video technique. A video camera is aimed at

a video monitor, to which it is connected, in a dark room. The screen is black. A match is struck briefly in front of the screen, which immediately shows an image of it. The match goes out, but the image remains on the screen, and grows, bifurcates, multiplies. The video feedback system goes on a self-regulation voyage, exhibiting frequent catastrophies of morphology, continuing for hours. In other variations, the room is lit, and some action takes place in front of the screen. Or, a time-delay device, consisting of two videotape decks, is inserted in the feedback loop. Or, the lens is zoomed at the start, and the zoom continues indefinately, through level after level of microscopic implosion. A typical sequence of forms is shown in Figure 20-1.

Preliminary analysis of the mechanism at work here reveals the system as an analog computer for dynamic catastrophes of codimension one, a laboratory tool of enormous potential for experimental mathematics.

CHAPTER 6. PSYCHOMORPHOLOGY

The mechanism of the mind is one of the great frontiers of science today. Recent advances in neurobiology, perceptual psychology, paraphychology, and other fields have opened this frontier to a possible understanding of thought, perception, and communication - presently the greatest of mysteries. Morphometric models for some mental functions have been discussed by Thom and Zeeman, and it seems concievable that morphogenesis could be the catalyst to combine isolated, specialized results into a new understanding. Here I outline my own dreams on this subject.

21. Biological materials and fields. An engineer might describe biological material naively in terms of its gross physical properties. Thus, flesh is a material state between liquid and solid, very heterogeneous, a large variety

of complicated structures involving large molecules of irregular shapes, membranes consisting of smectic liquid crystalline material, stridded with proteins, ionized plasmas moving here and there, many of them nematic or cholesteric liquids mixed with isotropic liquids; many continuous chemical reactions in progress, some of them periodic, metabolic and respirational processes in interaction with the environment, etc. Inspection with an electronic stethescope reveals mechanical vibrations in the audio range. Magnetometry and radio frequency spectroscopy reveal oscillations of the ambient electromagnetic field through most of the measurable spectrum. Electrical probes indicate electrical conduction and convection currents throughout the spectrum, and stationary direct currents as well. While some of the processes generation these oscillations are identifiable, the bulk of the physical observations are unexplained. He concludes his description with the observation that flesh is a heterogeneous highly structured form of matter, in which chemical, mechanical, hydrodynamic and electromagnetic vibrations are strongly coupled, maintained in amplitude by unknown metabolic processes, and regulated by interior and exterior controls, via neuroelectrical circuits. When different samples are in contact or close proximity, weak coupling of the various oscillatory manifestations may be observed.

In addition to this view, what, if anything, can be added by a more sophisticated observer ? Besides the details of numerous microcosmic components of the system, elaborated by biochemists and neurobiologists, little has been added to this naive picture so far. But two subtle observations deserve mention. One consists of the cycle of ideas called biological morphogenesis, concerning the growth and form in which this kind of material is found in nature. Here we may recall the ancient Greek theory of ideas - concerning substance and form. The study of form is a step beyond the study of substance. The second consists of psychotronics and cosmobiology, concerning the interaction of live forms with each other, and with inert material, in microcosmic and macrocosmic dimensions. Here, numerous refined experiments by reputable scientists over many centuries lead to a strong suspicion that the energetic interactions of biological material are not explainable through coupling of gravitational, electromagnetic, weak and strong interactions, only. So speculation, and serious scientific exploration of a fifth interaction continues to accumulate. Known variously as bioplasmic energy, odic force, orgone energy, elan vital, entelechy, psychotronic field, fifth interaction, third energy, an many other names, it is postulated by different authors as the essence of life, the carrier of telepathy, clairvoyance, and psychokinesis, the cause and cure of cancer, the motivation for sexual activity, the field photographed by the Kirlian process, the force of time, and so on ad infinitum.

Concerning biological morphogenesis, see Thom [201, 203, 204, 206, 207, 210], Thompson [114], Turing [503], and Waddington [504, 505]. For an introduction to psychotronics, see Barnothy [601], Certok [607], Cohen [608], Kolin [613], Volkers and Candib [620], and most importantly, Reizer [113], and Ostrander and Schröder [615].

<u>22. Retina and cortex.</u> As the retina is obviously a bit of cortex extruded to the boundary of the body, I will discuss these two extraordinary biological materials together. Naively, we have a more-or-less two dimensional surface of smectic crystalline form, $C \subseteq \mathbb{R}^2$, containing a one-dimensional neuroelectric graph as control mechanism. At each vertex of the graph there is a fluid droplet of great biochemical complexity, containing various hormones, some of them indubitably nematic and cholesteric liquids. The concentrations of the components of the hormone droplet are controlled by the electrical activity of the synapse at its center. The droplets at the various vertices of the neural graph presumably overlap, so we have a heterogeneous layer of bioplasmic fluid,

much like the key element in the kymatic experiments of Hans Jenny. Each droplet, and in fact the whole layer, is in a state of mechanical, chemical, and electromagnetic oscillation, presumably an attractor of a dynamical system, as yet unknown. It seems safe to assume that cells of Taylor, Bénard, Williams, and flexoelectric phenomena abound. Considering time as a control variable, the catastrophe is a set $K \subset C \times \mathbb{R}$. External control is effected by the neural net,as well as the manipulation of the ambient mechanical, chemical, and electromagnetic environment. There appears to be a strong self-regulation dynamic as well, and feedback from the bioplasmic oscillation to the neural net. Local models for the logoi of kymatic models, discovered by mathematical catastrophe theory or by experimental morphology, could be used to model functionssuch as memory, learning, visual perception, stream of conciousness, and so on. Some efforts in this direction have been reported by Thom [201], Buneman and Zeeman [606], and Zeeman [318, 621]. More conventional brain models - for example, Black [102], Blum [604], de Bono [623], or Pribraum [617] - can easily be incorporated in the kymatic model suggested here. And should it be established that a psychotronic field exists, and is coupled to the fields already accounted for in this model, it would make little difference in the logos of the model. Telepathy, planetary influence, and other "paranormal" phenomena, such as are established by numerous reliable experiments, have a "normal" explanation in this scheme, perhaps even without the intervention of a psychotronic field.

Similar kymatic models for the glial body, brain stem, and other components of the central nervous system can easily be made, as soon as one such model has been elaborated successfully.

Further, this type of model admits mathematical archetypes as parameters of thoughts, visual perceptions, and so on, which are the same archetypes manifested in the external phenomena being perceived or thought about.

Hence Plato's theory of ideas, Jung's archtypes, and other constructs of phenomenology may be given a particularly precise mathematical formulation. The Hindu Sankhya philosophy may be the closest precedent to the viewpoint of this scheme.

<u>23. Sense perception</u>. For visual perception, we have already the beginning of a morphogenetic model, in the discussion of the retina above. As the control net of the retina is excited photoelectrically, an optical morphology incident on the retina produces an attractor in the logos of the kymatic scheme, by a process of morphological resonance. This is transported, by the optic nerve, to a control net in the brain stem, which is excited to an attractor in its own actual logos of a corresponding morphology, and similarly, the visual cortex, and its processed feedback to the retina and visual motor apparatus.

For auditory perception (excluding bone conduction) we may propose a surprisingly similar kymatic scheme. Here the impress of the external morphology on the sense organ is modelled exactly by the kymatic scheme, as Hans Jenny has observed [103]. The sound waves activate, through a mechanical linkage, the cochlear window, and thus the perilymph fluid in the cocklea. This fluid is thus excited to an attractor in the actual logos of a kymatic model. The hydrodynamical motion, as shown in Figure 23-1, reveals features of Jenny's photographs, and the eddies of von Bekesy, which are analogous to Taylor cells [602]. Variation of the amplitude and frequency - or property frequencies, that is Fourier coefficients - produces catastrophes of this attractor, or hydrodynamical motion. I do not know if the perilymph or endolymph fluids are liquid crystal, or even if their properties have been studied, or if its chemical composition is changeable by the central nervous system. They are coupled to the electromagnetic field, however, and their electrical activity has been extensively studied. See, for example, von Bekesy [602]. Both the hydrodynamic and electromagnetic vibrations are probably involved in the perception of sound by the organ of Corti, and the hearing nerve.

The sense of feeling is very analogous to hearing, as von Bekesy has shown [603], and I will not speak about the other senses.

Of course a lot of work must be done to precise this fantasy about morphogenetic models for sense perception, and the mathematical results, on dynamic catstrophes, which will be needed may not be known for decades. However, this point of view suggests simple experimental studies of a basic nature which differ in a fundamental way from most of the sophisticated research in progress at the present time.

24. Communication. Since communication is an aspect of sense perception, together with an agreed and common symbolical vocabulary or language, there is not a great deal to add here. However, I would like to simply mention some ideas of Thom on this subject.

Communication usually involves simultaneous perceptions by the various senses, and a series of translations of symbolical systems, via speech, visual cues, intermediate instruments, sense organs, mental processes, and so on. Thus a message M_1 is emitted from system A_1 , and later a message M_2 is received by system A_2 . According to morphosophy, each translation of the message sequence involved should have a morphogenetic model, the attractor of one activating the control of the next, and so on. When dynamic models are involved, we can think of each transition as a resonance phenomenon, of coupled oscillating systems. The information is coded in the form of the attractors, as Platonic ideas. In an accurate system, such as human perception or speech, M_1 and M_2 are related by an excellent correspondance, analogous to a Fourier transform, or hologram, and represent different manifestations of the same mathematical archetypal idea.

In the case of a speech description, M_2 , of an observed phenomenon, M_1 , Thom provides startling evidence of this correspondance. The message, M_1 , is a real physical phenomenon is space-time, realiszing a static morphogenetic model. After developing a catastrophe theory of language, Thom shows that the verbal description of the event, M_2 , realizes the same catastrophe as M_1 . Meanwhile, numerous transformations - retina, brain stem, visual cortex, speech analysis, vocal motor control, and so on - each presumeably described by an unknown morphogenetic model - most have preserved the archetypal catastrophe of M_1 , without error. Thom's papers on psycholinguistics present a number of related, fascinating ideas [202, 203, 212, 213].

CONCLUSION

Morphosophy is not an easy subject. The adequate description of its basic ideas (Part I) will probably be the subject of a simple exposition in a few years. But its applications (Part II) require a knowledge of enormous breath, possessed by few people, least of all me. I am sorry to take so much space, to say so little. But I do feel that the crisis of our world, described so well by Guénon and Fuller, involves technology both as cause and cure. The morphosophy of Thom is a new direction in technology and understanding. While failing somewhat short of the awakening envisionned by Reizer, or Feynman, I do believe it is a potential step toward the reintegration of wisdom so badly needed for our survival, and social evolution. I am also painfully aware of the awful potential in the misuse of knowledge of such power, but it seems to me better to go ahead, rather than stay here.

Therefore, I have tried to create an opening to a new science with this introduction to Thom's ideas. I hope it will help some to go on, and thus also all of us.

BIBLIOGRAPHY

I. Morphosophy

[101] J. Bergier and L. Pauwels, Morning of the Magicians.

[102] S. Black, Mind and Body, London (1969)

[103] H. Jenny, Kymatics, Basel (1967)

[104] B. Fuller, Operating Manual for Spaceship Earth, New York (1970)

[105] R. Guénon, The Crisis of the Modern World, London (1962)

[106] R. Landau, The arabesque, San Francisco (1955)

[107] J. Needham, Science and Civilization of China, Vol II, Cambridge (1962)

[108] Plato, Parmenides

[109] E. Schrödinger, What is life, Cambridge (1944)

[110] K. Szilard, Reduction in entropy of a thermodynamic system caused by the interference of intelligent beings, Z. Physik, 53 (1929) 840

[111] T. Schwenk, Sensitive Chaos : The creation of Flowing Forms in Water and Air, London (1965)

[112] ———, Formes de l'Eau en Mouvement, Paris (1968)

[113] O. Reizer, Cosmic Humanism, Cambridge, Mass. (1966)

[114] d'A. Thompson, On Growth and Form, Cambridge (1969)

[115] F. Toth, Regular Figures, London (1964)

[116] J. Uexkull, Théorie de la Signification, Paris (1956)

2. By René Thom.

[201] Stabilité Structurelle et Morphogenèse (to appear ?)

[202] Topologie et signification, l'Age de la Science 4 (1968) 219-242

[203] Topological models in biology; Topology 8 (1969) 313-336, or in [207], Vol. 3, 89-116.

[204] A mathematical approach to morphogenesis : archetypal morphologies, Wistar Institute Symposium Monograph No 9 (1969) 165-174

[205] Topologie et linguistique, Essays on Topology and Related Subjects, Heidelberg (1970) 226-248.

[206] Une théorie dynamique de la morphogenèse in [507] Vol.1, 152-166

[207] Structuralism an biology, to appear in [207], Vol. 4.

[208] Modèles mathématiques de la morphogenèse, Ch. 1-3, mimeographed, I.H.E.S. (1970/71)

[209] Les symétries brisées en physique macroscopique et la mécanique quantique (to appear)

[210] A dynamical scheme for vertebrate embryology (to appear)

[211] Sur les équations différentielles multiformes et leur intégrales singulières (to appear)

[212] Sur la typologie des langues naturelles : essai d'identification psycholinguistique, in Menton (ed) , Formal Analysis of Natural Languages (Proc. I.R.I.A. Congress, April, 1970), Janua Linguarium (to appear)

[213] Language et catastrophes, M. Peixoto (ed.), Salvador Symposium on Dynamical Systems, Academic Press, 1973.

[214] La théorie des catastrophes : état présent et perspectives (to appear).

3. Mathematics

[301] R. Abraham, Foundations of mechanics (this volume)

[302] ———— and J. Marsden, Foundations of Mechanics, New York (1967)

[303] P. Brunovsky, One-parameter families of diffeomorphisms. Symposium on Differential Equations and Dynamical Systems, Heidelberg (1971) 29-33.

[304] A. Godwin, Three dimensional pictures for Thom's parabolic umbilic, Publ. Math. I.H.E.S., 40 (1972) 117-138.

[305] J. Guckenheimer, One parameter families of vectorfields on two-manifolds : another non-density theorem (to appear).

[306] ————, Bifurcation and catastrophe (to appear)

[307] ————, Catastrophes and partial differential equations (to appear)

[308] E. Hopf, Abzweigung einer periodischen Lösung von einer stationären Lösung eines Differential systems, Ber. Math.-Phys. Kl. Sächs. Akad. Wiss. Leipzig, 94 (1942) 1-22.

[309] J. Mather, Right equivalence (manuscript)

[310] J. Robbin, Topological conjugacy and structural stability for discrete dynamical systems (to appear in Bull. Amer. Math. Soc.)

[311] D. Siersma, Singularities of right codimension less than or equal to eight (to appear)

[312] S. Smale, Differentiable dynamical systems, Bull. Amer. Math. Soc., 73 (1967) 747-817.

[313] J. Sottomayor, Generic one-parameter families of vectorfields, Bull. Amer. Math. Soc., 74 (1968) 722-726.

[314] ————, ————, (to appear in Topology)

[315] F. Takens, Singularities of vectorfields (to appear)

[316] ————, Singularities of functions and vectorfields (to appear)

[317] R. Thom, Ensembles et morphismes stratifiés, Bull. Amer. Math. Soc., 75 (1969) 240-284.

[318] C. Zeeman, Applications of Thom's catastrophe theory (to appear in Proc. Lon. Math. Soc.)

[319] I.R. Porteous, Normal singularities of a submanifold, J. Diff. Geom. (1971)

[320] T. Poston, The plateau problem, in P. de la Harpe (ed.), Proc. Summer College on Global Analysis and its Applications, Trieste, 1972 (to appear).

4. Physics and Chemistry.

[401] C. coles, Transition in circular Couette flow, J. Fluid Mech. 21 (1965) 385-425.

[402] W. Eckhaus, Studies in Nonlinear Stability, Berlin (1970)

[403] R. Feynman, R. Leighton, M. Sands, The Feynman Lectures in Physics, Vol. 2, Reading (1964)

[404] M. Fischer, The nature of critical points, Lectures in Theoretical Physics, Vol XII C, Boulder (1965)

[405] D. Fowler, The Riemann-Hugoniot catastrophe and van der Waal's equation (to appear in [506] Vol. 5)

[406] G. Gray, Molecular Structure and the Properties of Liquid Crystals, London (1962)

[407] P. Glandsdorff and I. Prigogine, Thermodynamic Theory of Structure, Stability, and Fluctuations, New York (1971)

[408] E. Hopf, A mathematical example displaying features of turbulence, Comm. Pure Appl. Math. 1 (1948) 303.

[409] D. Joseph and D. Sattinger, Bifurcating time-periodic solutions and their stability (to appear)

[410] I. Prigogine, Introduction to Thermodynamics of Irreversible Processes New York (1967)

[411] D. Ruelle and F. Takens, On the nature of Turbulence, Comm. Math. Phys., 20 (1971) 167-192, and 23 (1971) 343-344.

[412] E. Sel'kov, Self-oscillations in glycosis, European J. Biochem., 4 (1968) 79-86.

[413] H. Snyder, Phys. Fluids, 11 (1968) 728-734.

[414] ————, Phys. Fluids, 11 (1968) 1599-1605.

[415] M. Velarde, Schecter, and Kiockemeister, a survey of Bénard-Rayleigh problems (to appear in Adv. Chem. Phys.)

[416] A. Winfree, Spiral waves of chemical activity, Science, 175 (1972) 634-636.

[417] C. Zeeman, Breaking of waves, Symposium on Differential Equations and Dynamical Systems, Heidelberg (1971) 2-6.

5. Biology

[501] K. Goldstein, Der Aufbau des Organismus, den Haag (1934)

[502] R. Rosen, Dynamical System Theory in Biology, Vol 1, Stability Theory and its Applications, New York (1970).

[503] A. Turing, A chemical basis for biological morphogenesis, Phil. Trans. Roy. Soc. (London), Ser. B., 237 (1952) 37.

[504] C. Waddington, Organisers and Genes, London (1940)

[505] ————, Introduction to Modern Genetics, London (1957)

[506] ————, ed., Towards a Theoretical Biology, Vol. 1-3, Edinburgh (1970), Vol. 4,5 (to appear)

6. Psychology and Neurobiology

[601] M. Barnothy, ed., Biological Effects of Magnetic Fields, Vol. 1,2, New York (1969)

[602] G. von Békesy, Experiments in Hearing, New York (1960)

[603] ——————, Sensory Inhibition, Princeton (1967)

[604] H. Blum, A new model of global brain function, Perspectives in Biology and Medecine 10 (1967) 381-408.

[605] ———, Biological shape and visual science, Part I (to appear)

[606] O. Buneman and C. Zeeman, A topological model for the brain, in [506], Vol. 2.

[607] L. Certok, ed., Psychophysiological Mechanisms of Hypnosis, Berlin (1969)

[608] D. Cohen, Magnetoencephalography, Science 175 (1972) 664-666.

[609] W. Ellis, A Source Book of Gestalt Psychology, London (1938)

[610] D. Hepp, The Organization of Behaviour, New York (1949)

[611] K. Koffke, Principles of Gestalt Psychology, New York (1935)

[612] W. Köhler, Gestalt Psychology, New York (1947)

[613] A. Kolin, Magnetic fields in biology, Physics Today (1968) 39-50

[614] J. von Neumann, The Computer and the Brain, New Haven (1958)

[615] S. Ostrander and N. Schroder, Psychic Discoveries Behind the Iron Curtain New York (1969)

[616] K. Pribram, The brain, Psychology Today,(Sept. 1971)

[617] ——————, Languages of the Brain (to appear)

[618] W. Rosenblith, ed., Sensory Communication, Cambridge, Mass. (1961)

[619] S. Stevens, ed., Handbook of Experimental Psychology, New York (1951)

[620] V. Volkers and W. Candib, Detection and analysis of high-frequency signals from muscular tissues with ultra-low-noise amplifiers, Intern. Conv. Radio Eng. (1960)

[621] C. Zeeman, Topology of the brain, Mathematics and Computer Science in Biology and Medicine, London (1965)

[622] ———, Differential equations for the heartbeat and nerve action (to appear in M. Peixoto, ed., Salvador Symposium on Dynamical Systems, Academic Press, 1973)

[623] E. de Bono, The Mechanism of Mind, Middlesex (1969)

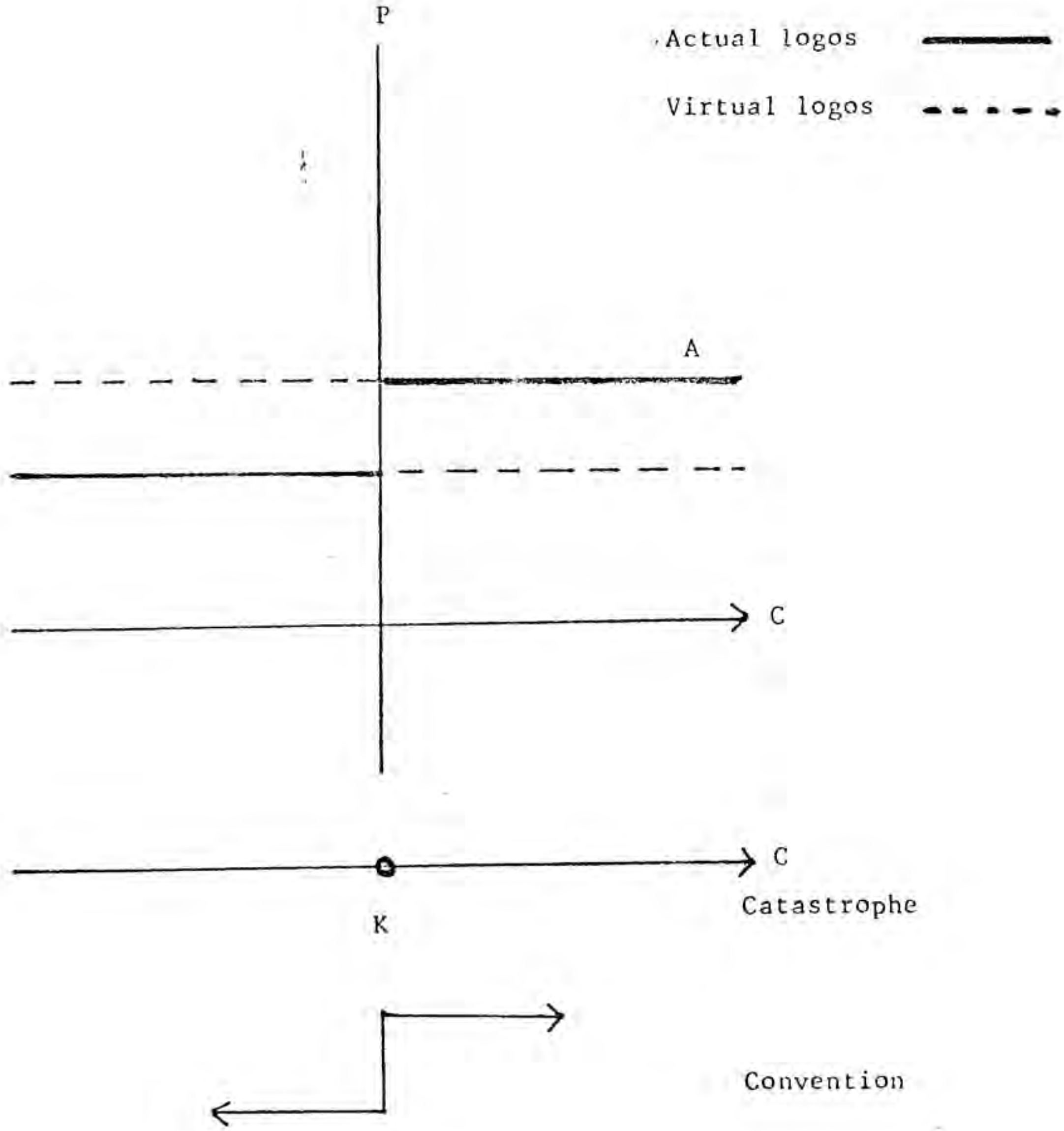

FIGURE 3-1 : SWITCH CONVENTION

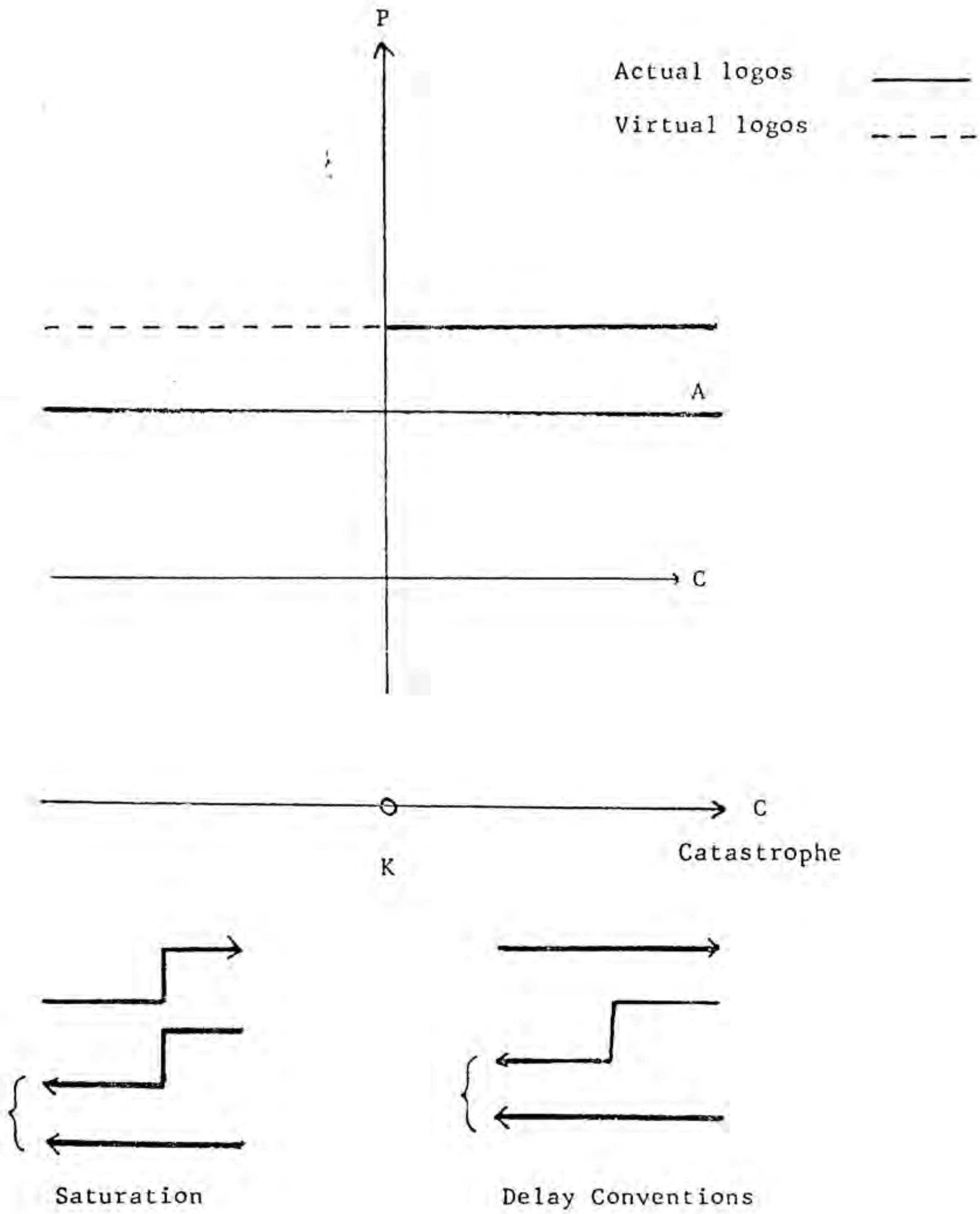

FIGURE 3-2 : SATURATION AND DELAY CONVENTIONS

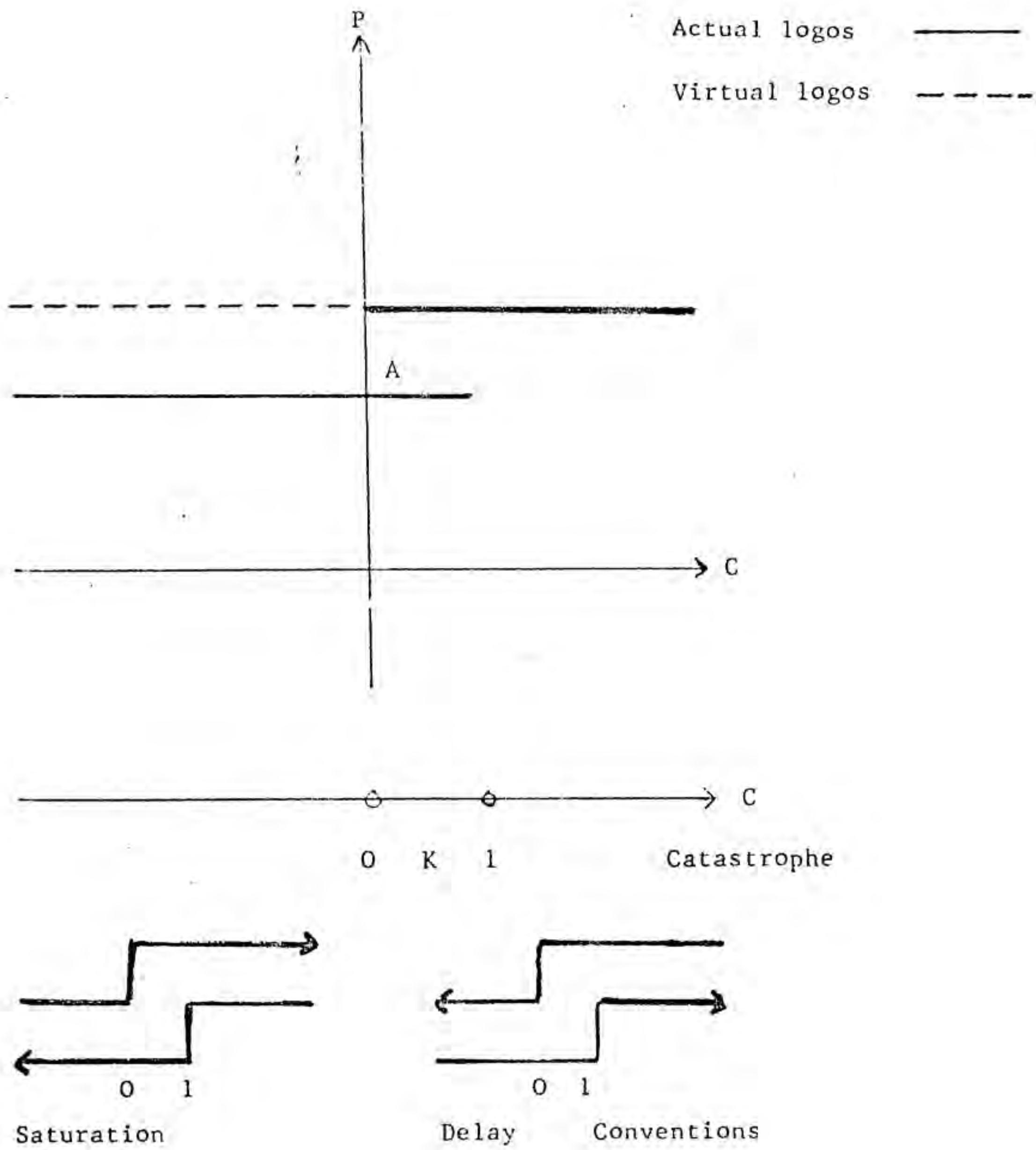

FIGURE 3-3 : SATURATION AND DELAY CONVENTIONS

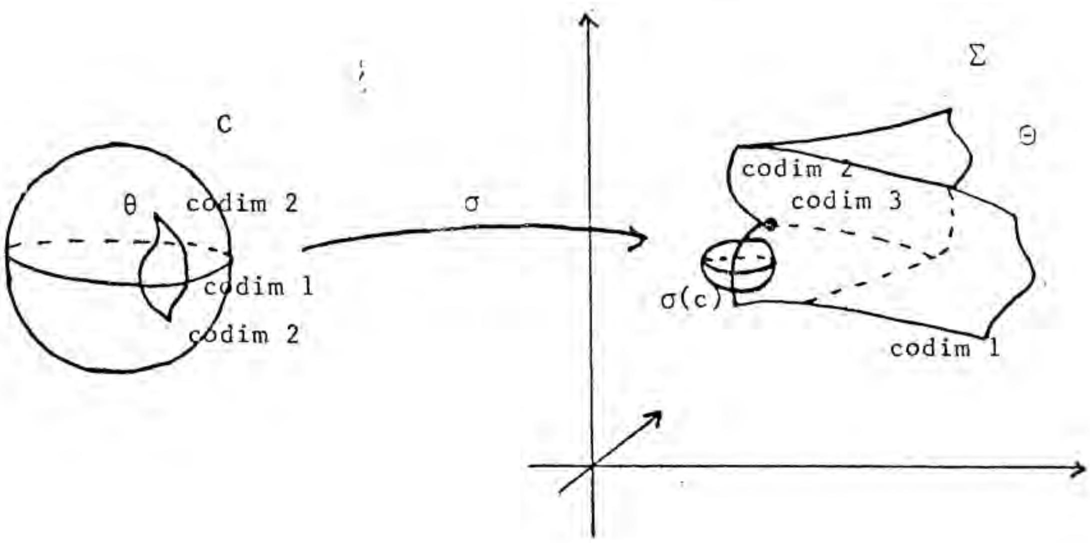

FIGURE 5-1 : STRUCTURALLY STABLE MORPHOGENETIC FIELD

Pictorial sketch, showing transversal intersection of a morphostatic field with three strata of the universal catastrophe, with preservation of codimension in the theoretical catastrophe, $\theta = \sigma^{-1}(\Sigma)$. Here, the control space is the two-sphere.

m	n	field	$\sigma(c,d\ldots)(p,q\ldots) =$
1	1	fold	$(p^3) + cp$
2	1	cusp	$(p^4) + cp^2 + dp$
3	1	swallow's tail	$(p^5) + cp^3 + dp^2 + ep$
3	2	hyperbolic umbilic	$(p^3 + q^3) + cp^2 - dp - eq$
3	2	elliptic umbilic	$(p^3 - 3pq^2) + c(p^2 + q^2) - dp - eq$
4	1	butterfly	$(p^6) + cp^4 + dp^3 + ep^2 + fp$
4	2	parabolic umbilic	$(p^2q + q^4) + cp^2 + dq^2 - ep - fq$

$\sigma = \mathbb{R}^m \rightarrow \Sigma_s(\mathbb{R}^n, \mathbb{R})$

m = codimension

n = minimum phase dimension

FIGURE 5-2 : THOM'S CANONICAL FIELDS

The local models for structurally stable morphostatic fields for control dimension less than five.

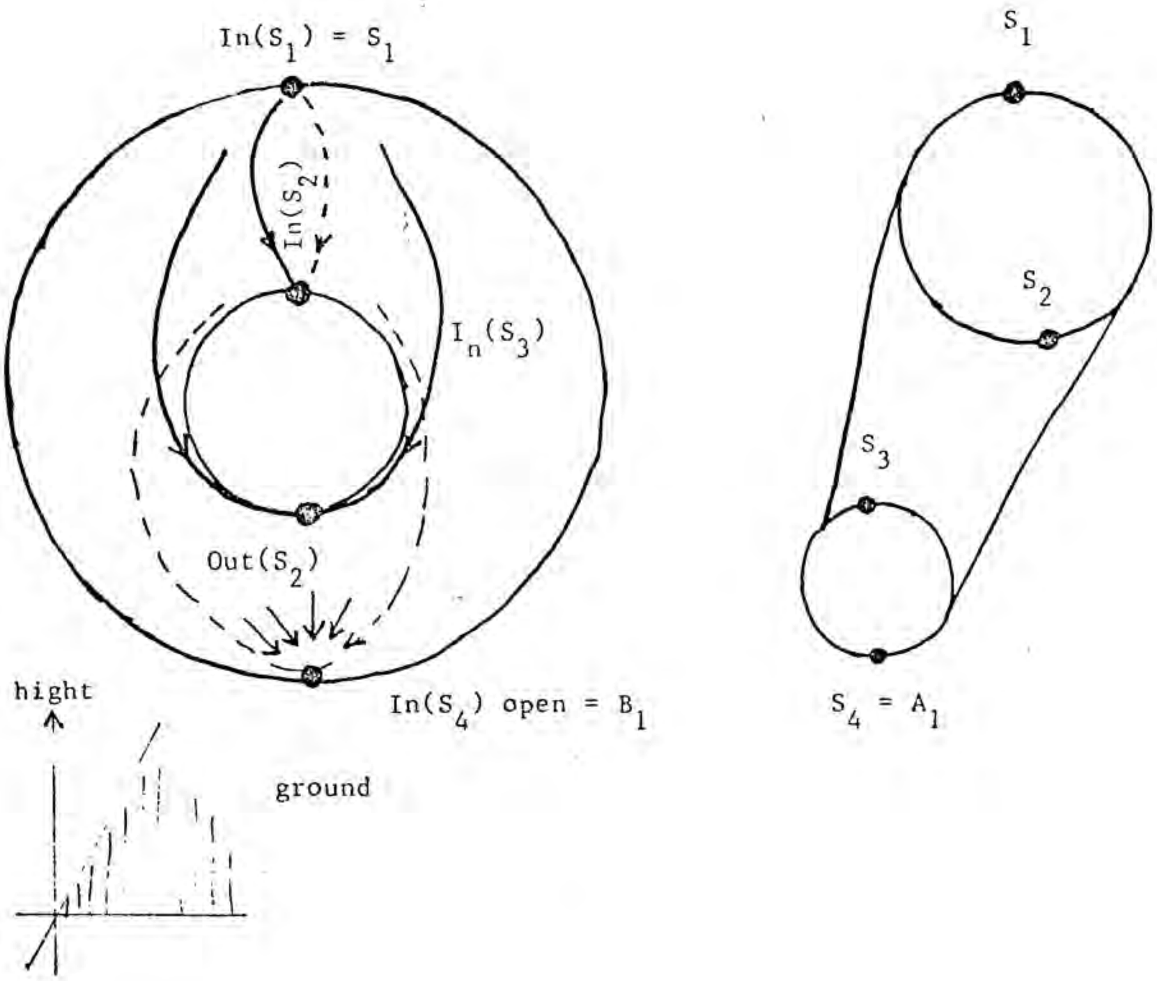

FIGURE 6-1 : INSETS

A negradiant vectorfield, $X = \nabla f$, where f is the hight above ground of the tilted torus, showing the critical points and their insets. Front and side views.

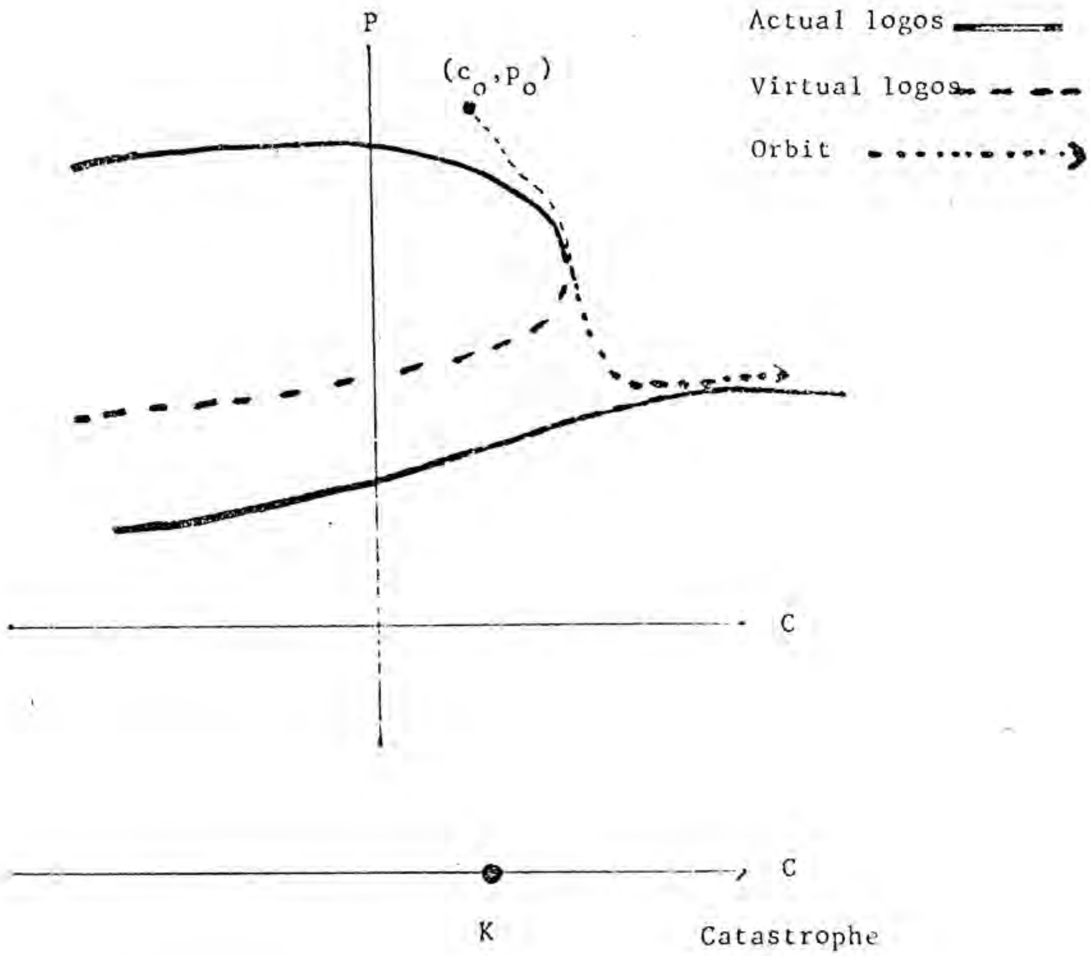

FIGURE 6-2 : DYNAMIC INTERPRETATION

Orbit of a point in phase space, subject to a controlled negradient vectorfield. As the control, c_t , moves past the catastrophe, K , an attractor dissappears and the orbit moves rapidly toward the remaining attractor.

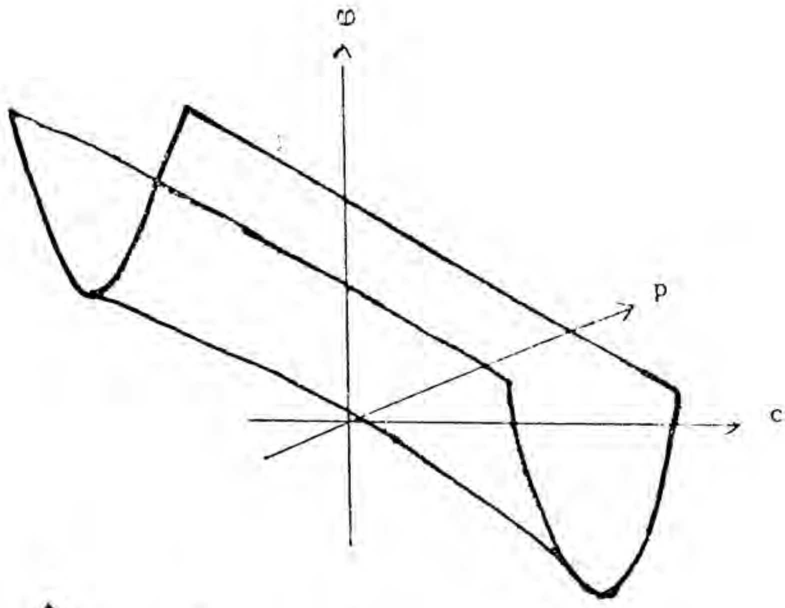

Graph of φ

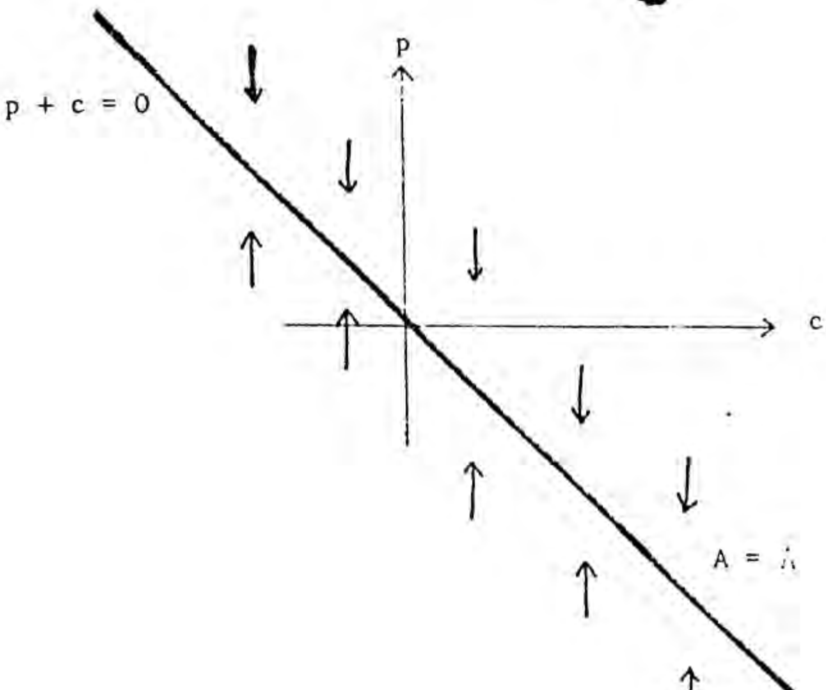

Negradient field
and logos

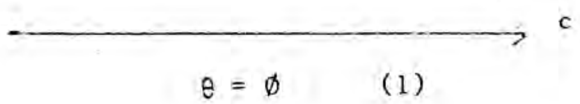

Theoretical
catastrophe

FIGURE 9-1 : SIMPLE MINIMUM

Morphostatic field defined by $\sigma(c)(p) = \frac{1}{2} p^2 + cp$ does not meet $\mathcal{C}$, there is no catastrophe. Number of attractors in parenthesis.

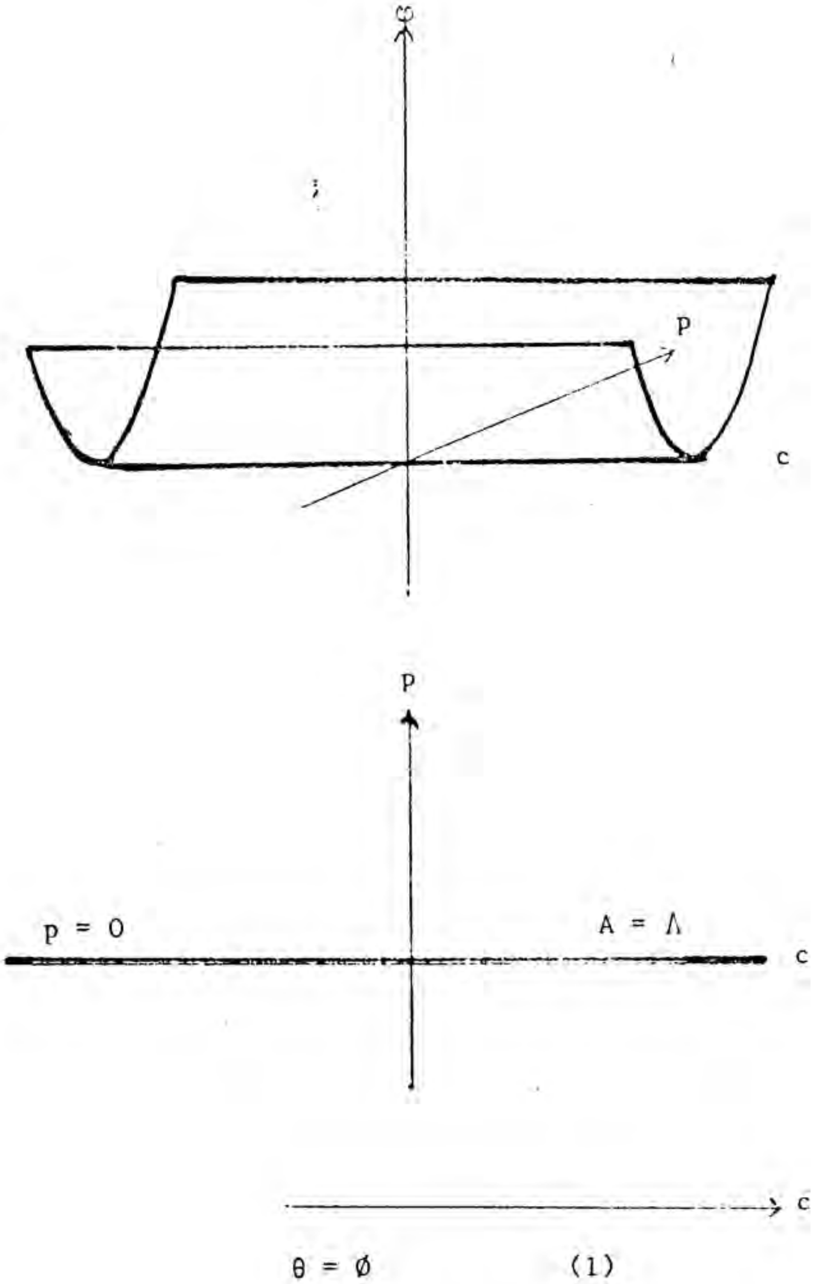

Graph of φ

Negradient field and logos

Theoretical catastrophe

FIGURE 9-2 : STANDARD SIMPLE MINIMUM

Field defined by $\sigma(c)(p) = \frac{1}{2}\,p^2$ does not meet [illegible], there is no catastrophe.

Number of attractors in parantheses.

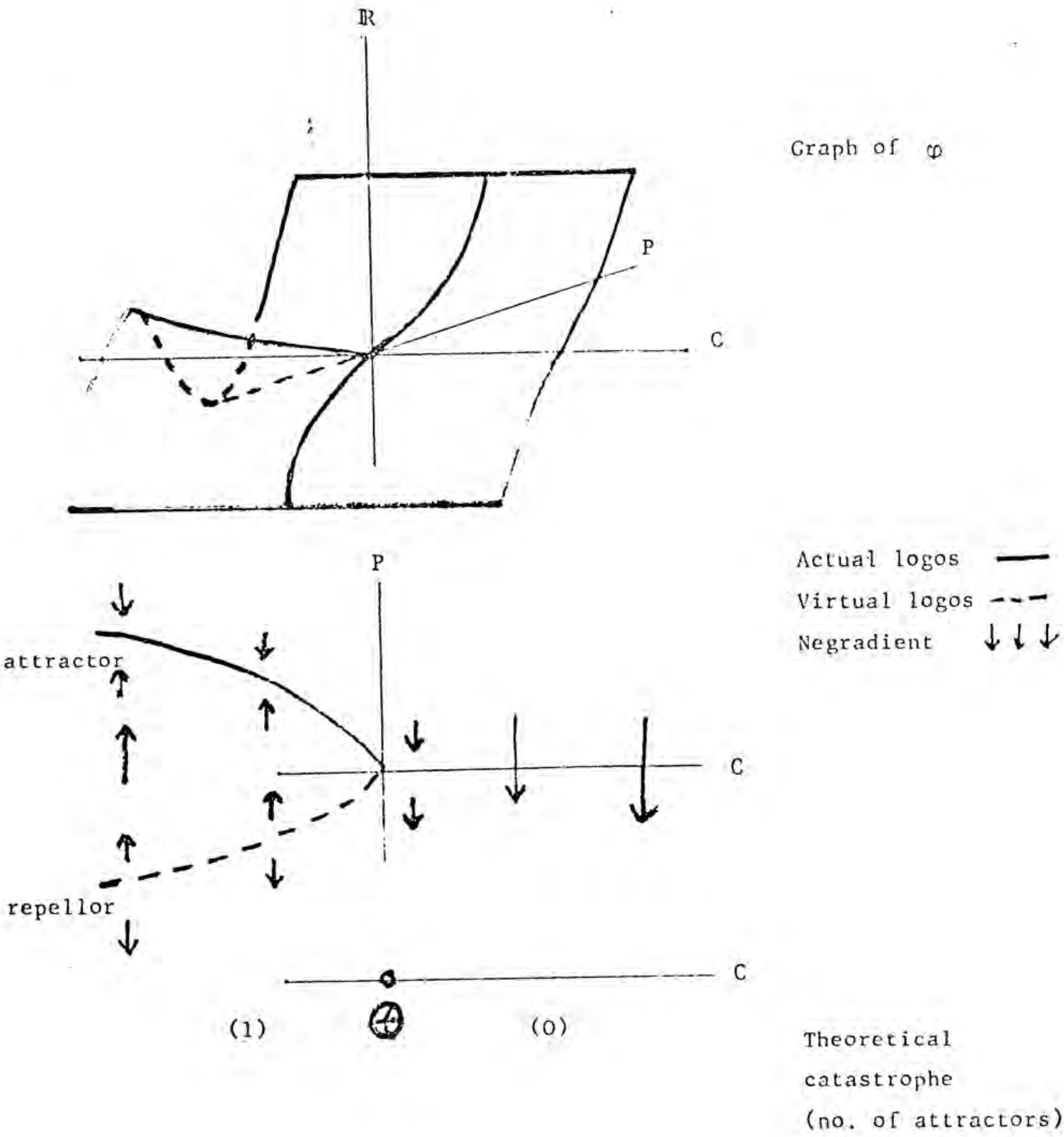

FIGURE 9-3 : THE FOLD

Field defined by $\sigma(c)(p) = \frac{1}{3}p^3 + cp$ meets universal catastrophe of codimension one, so catastrophe is a point. Virtual logos is the boundary of the basin of attraction.

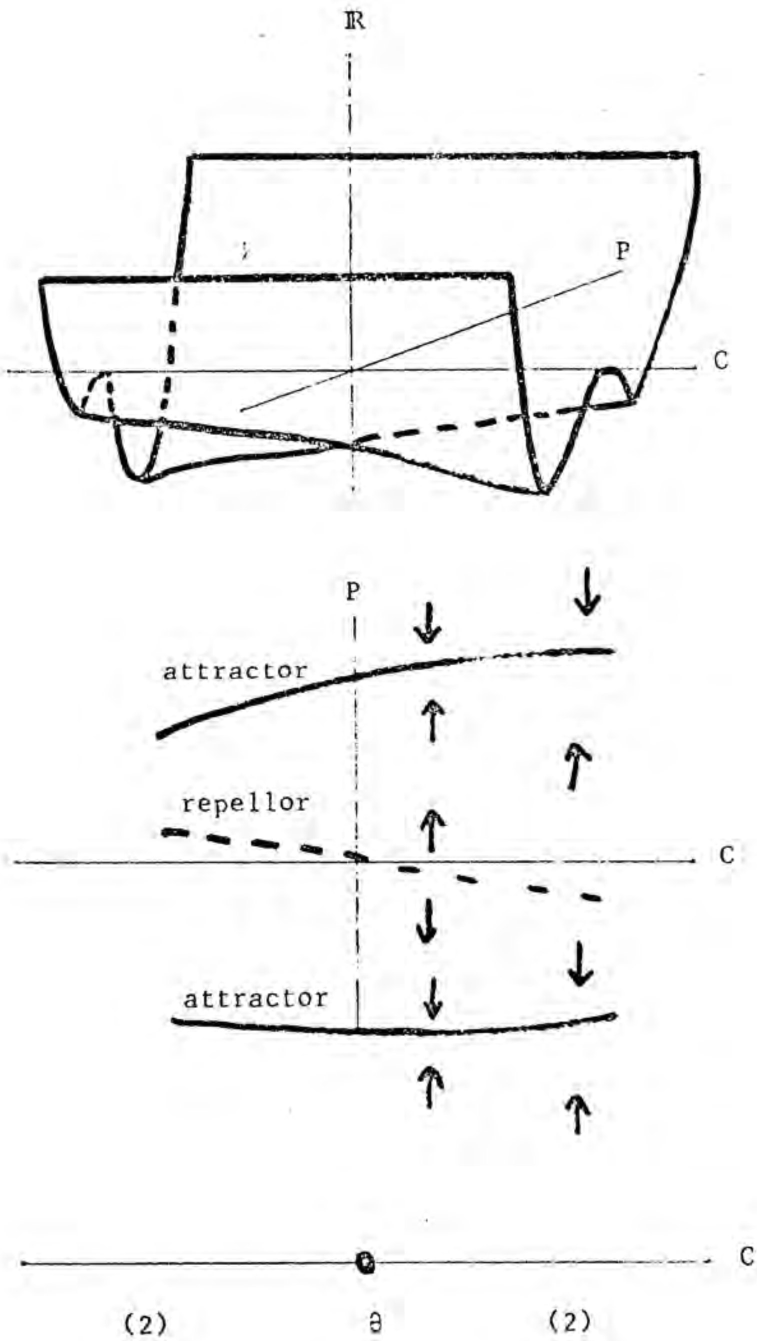

Graph of φ

Negradient and logos

Catastrophe (no. of attractors)

FIGURE 9-4 : MAXWELL CATASTROPHE

Field defined by $\sigma(d)(p) = \frac{1}{4}p^4 - \frac{1}{2}p^2 + dp$ has two minima, which cross values at $d = 0$. The virtual logos is the separatrix of the two basins of attraction.

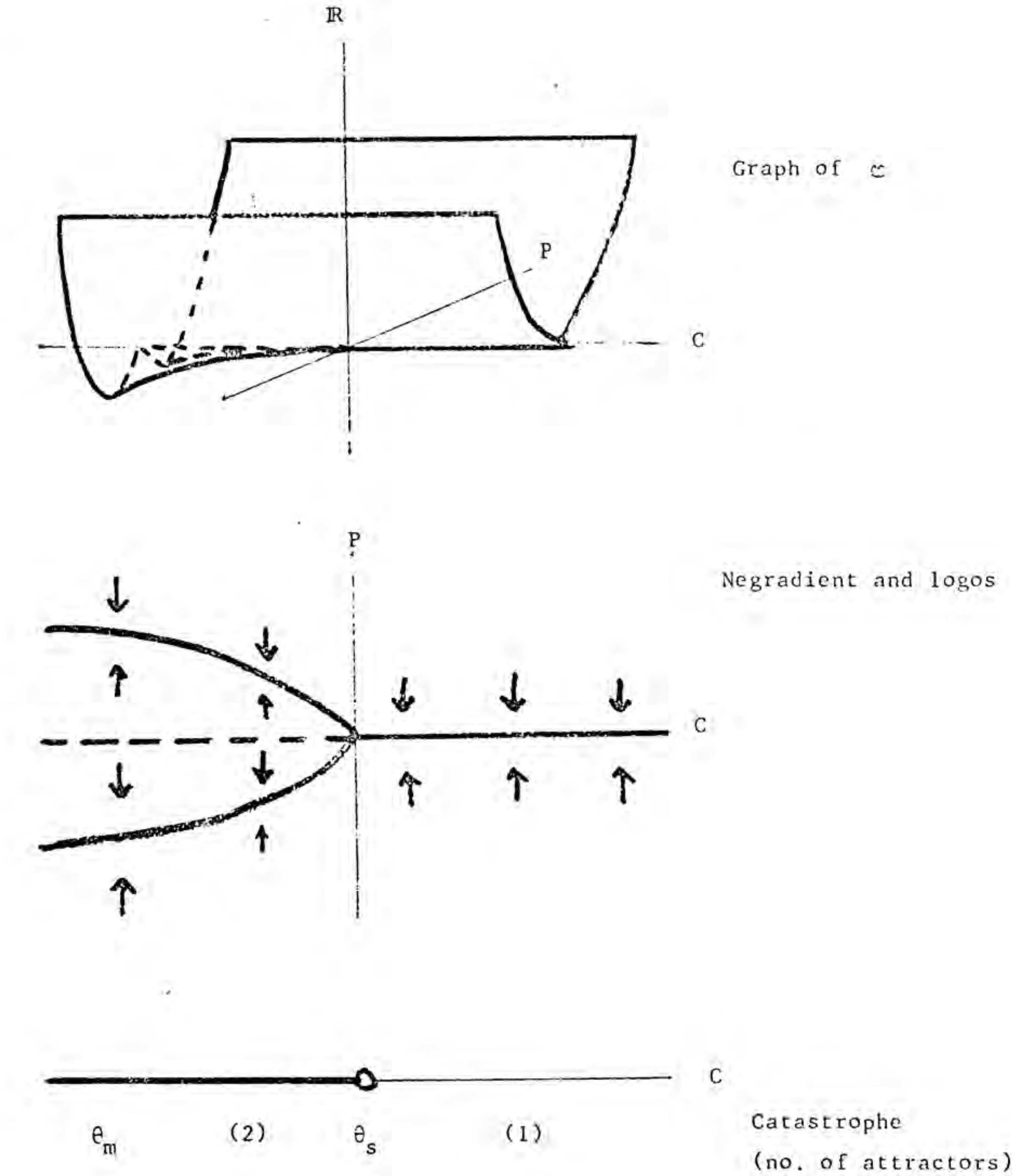

FIGURE 9-5 : UNSTABLE PARABOLIC CATASTROPHE

Static field defined by $\sigma(c)(p) = \frac{1}{4} p^4 + \frac{1}{2} cp^2$ has a singular catastrophe, $\theta_s = \{0\}$, and a ray of Maxwell catastrophes, $\theta_m = \{c < 0\}$, hence is not structurally stable.

Graph of σ

Negradient and logos

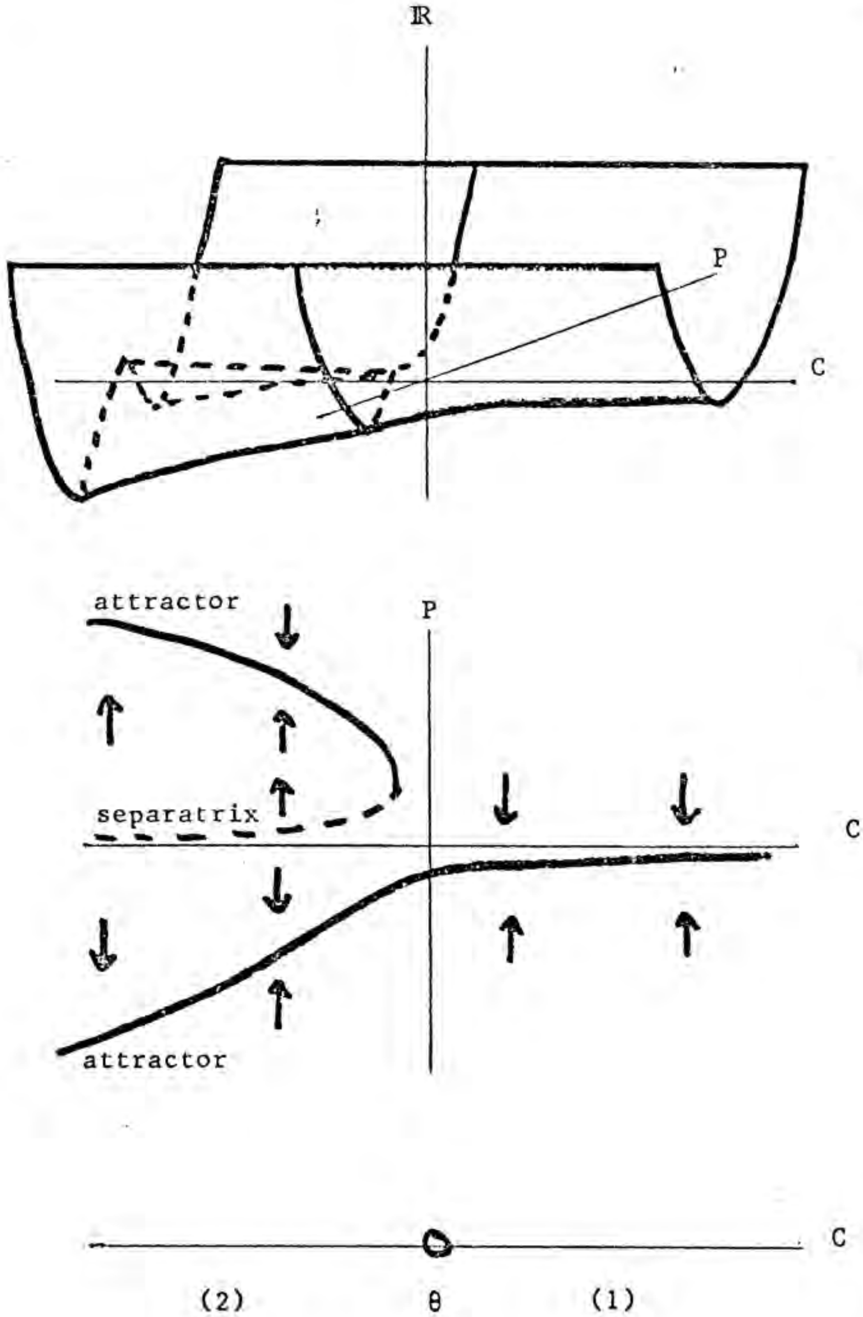

Catastrophe

FIGURE 9-6 : STABLE PARABOLIC CATASTROPHE

Static f:eld, defined by $\sigma(c)(p) = \frac{1}{4}p^4 + \frac{1}{2}cp^2 + dp$, d>0 has no Maxwell :atastrophe, only the fold near the origin.

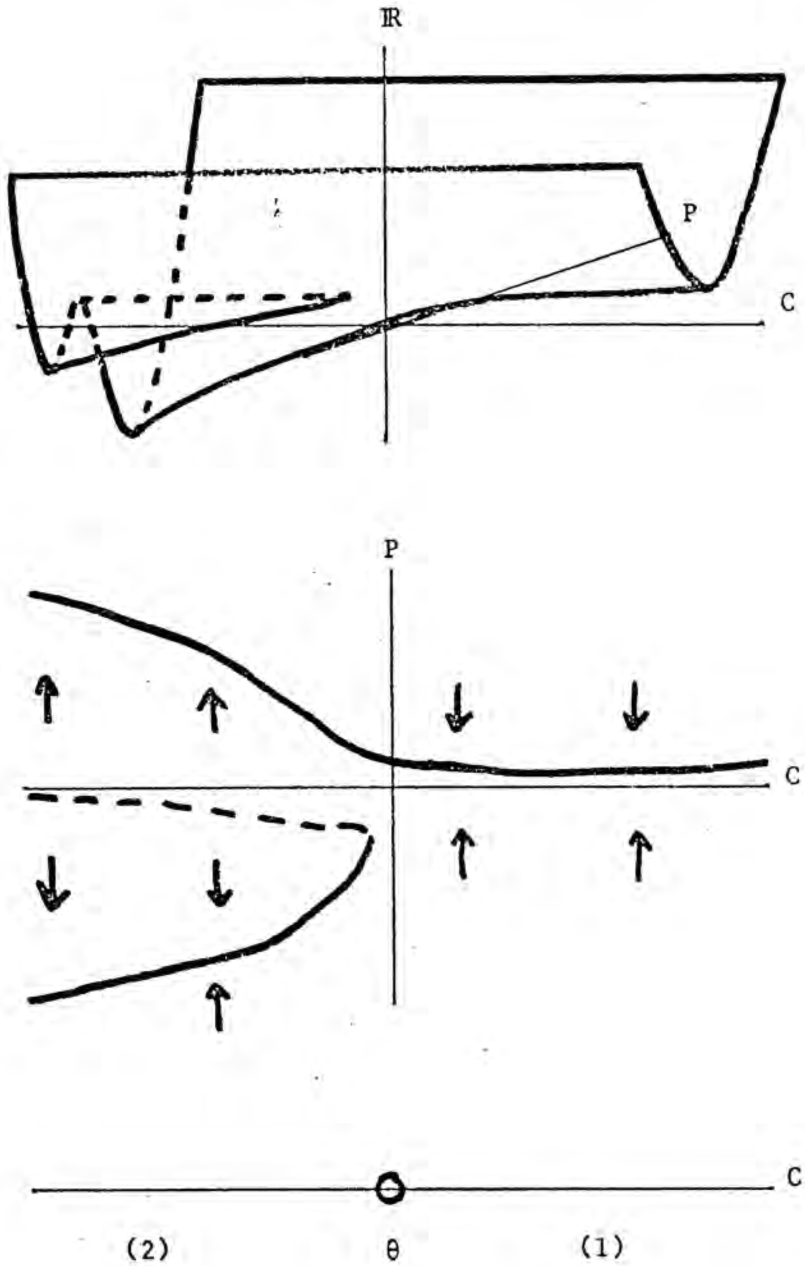

Graph

Logos

Catastrophe

FIGURE 9-7 : STABLE PARABOLIC CATASTROPHE

Static field, defined by $\sigma(c)(p) = \frac{1}{4} p^4 + \frac{1}{2} cp^2 + dp$, $d < 0$, is similar to the previous figure.

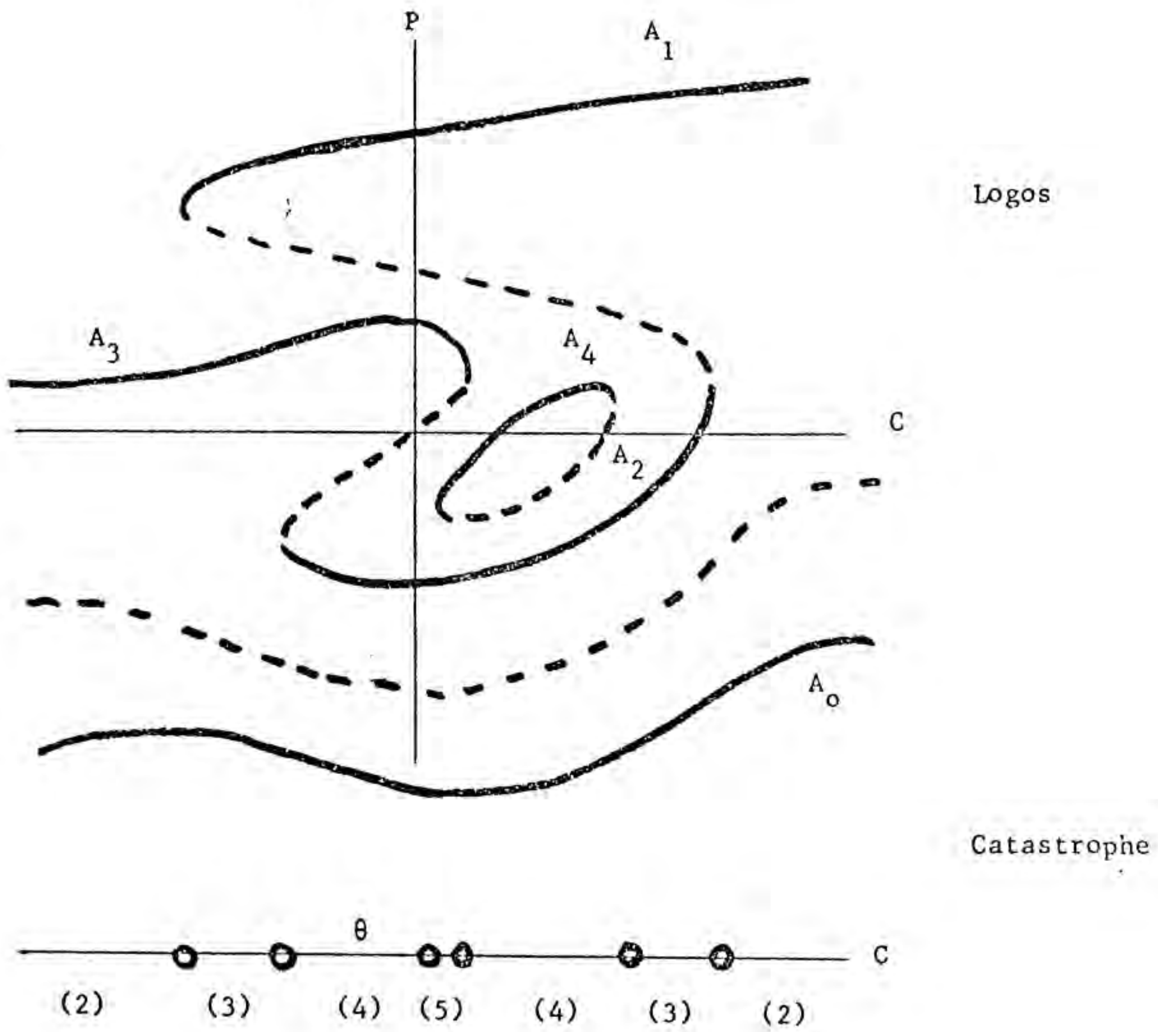

FIGURE 9-8 : TYPICAL MORPHOSTATIC LOGOS, $\dim(C) = 1$.

Structurally stable field, with a simple minimum and six folds. Attractors indexed according to (arbitrary) increasing hight, A_o lowest. In general, one could expect Maxwell catastrophes at additional isolated points.

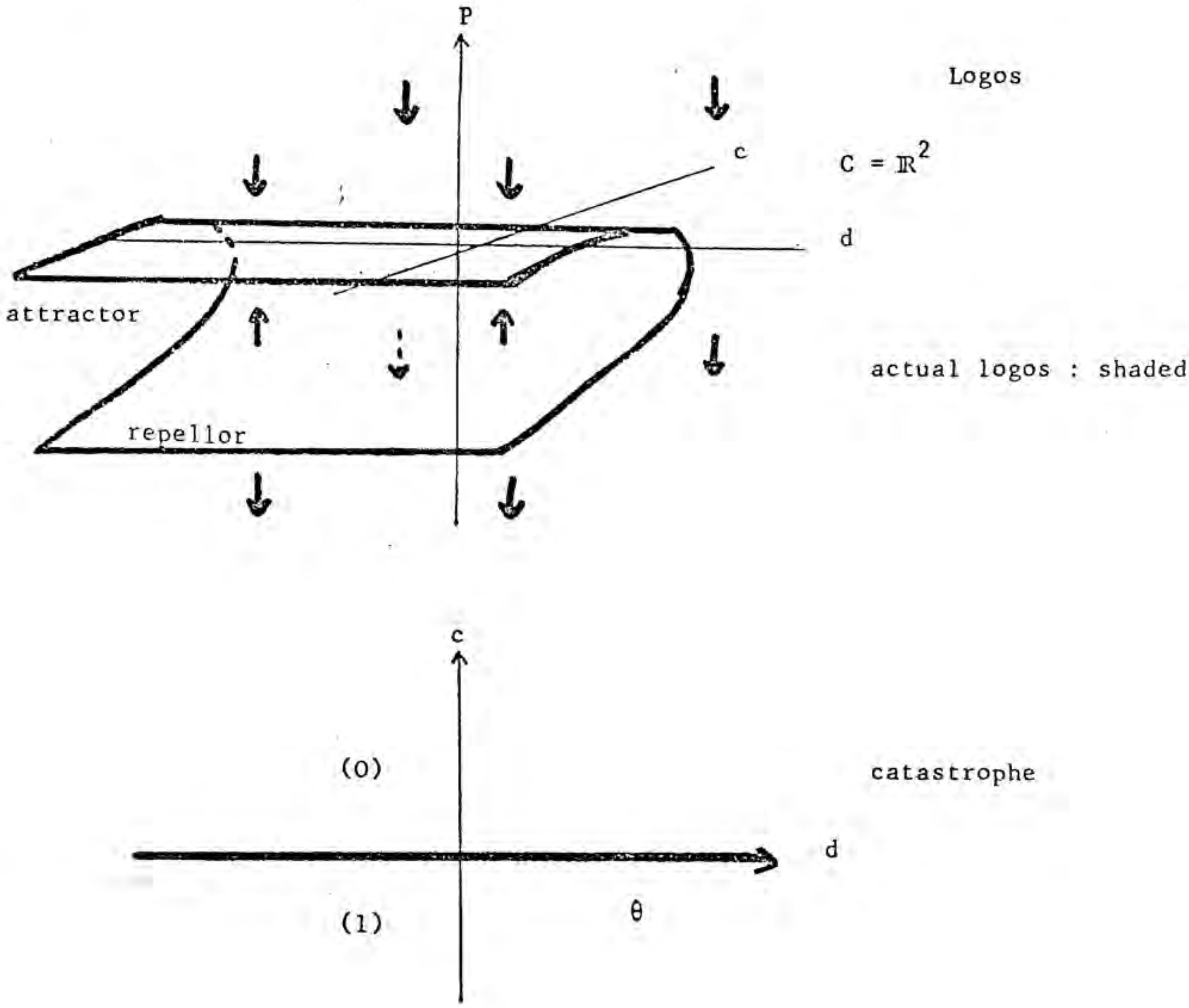

FIGURE 10-2 : THE FOLD

Static field defined by $\sigma(c,d)(p) = \frac{1}{3}\,p^3 + cp$

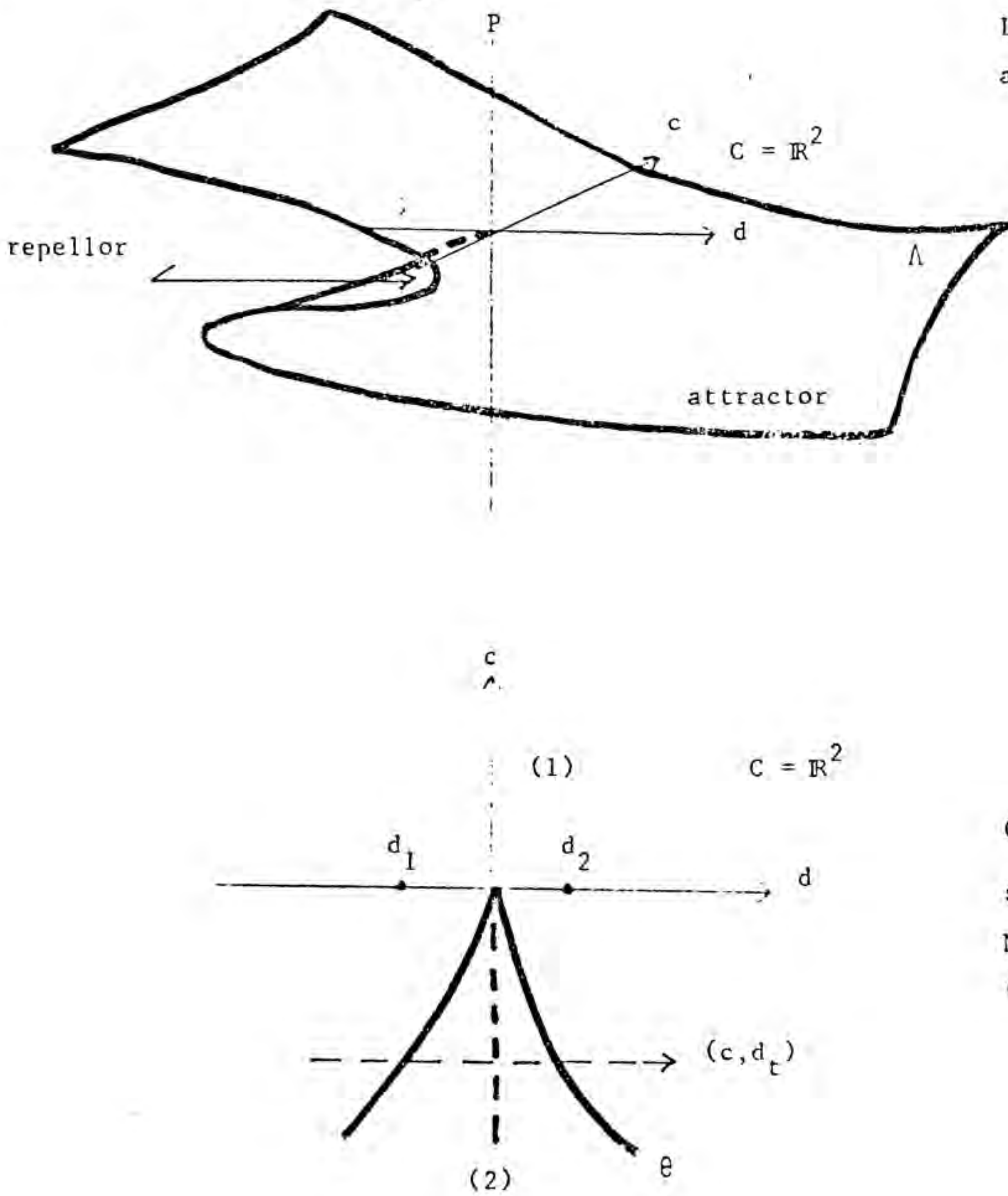

Logos

actual logos : shaded

Catastrophe

singular : solid

Maxwell : dashed

(no. of attractors)

FIGURE 10-2 : THE CUSP

Static field, defined by $\sigma(c,d)(p) = \frac{1}{4}p^4 - \frac{1}{2}cp^2 + dp$. The virtual logos is the separatrix of the two basins of attraction, within the cusp.

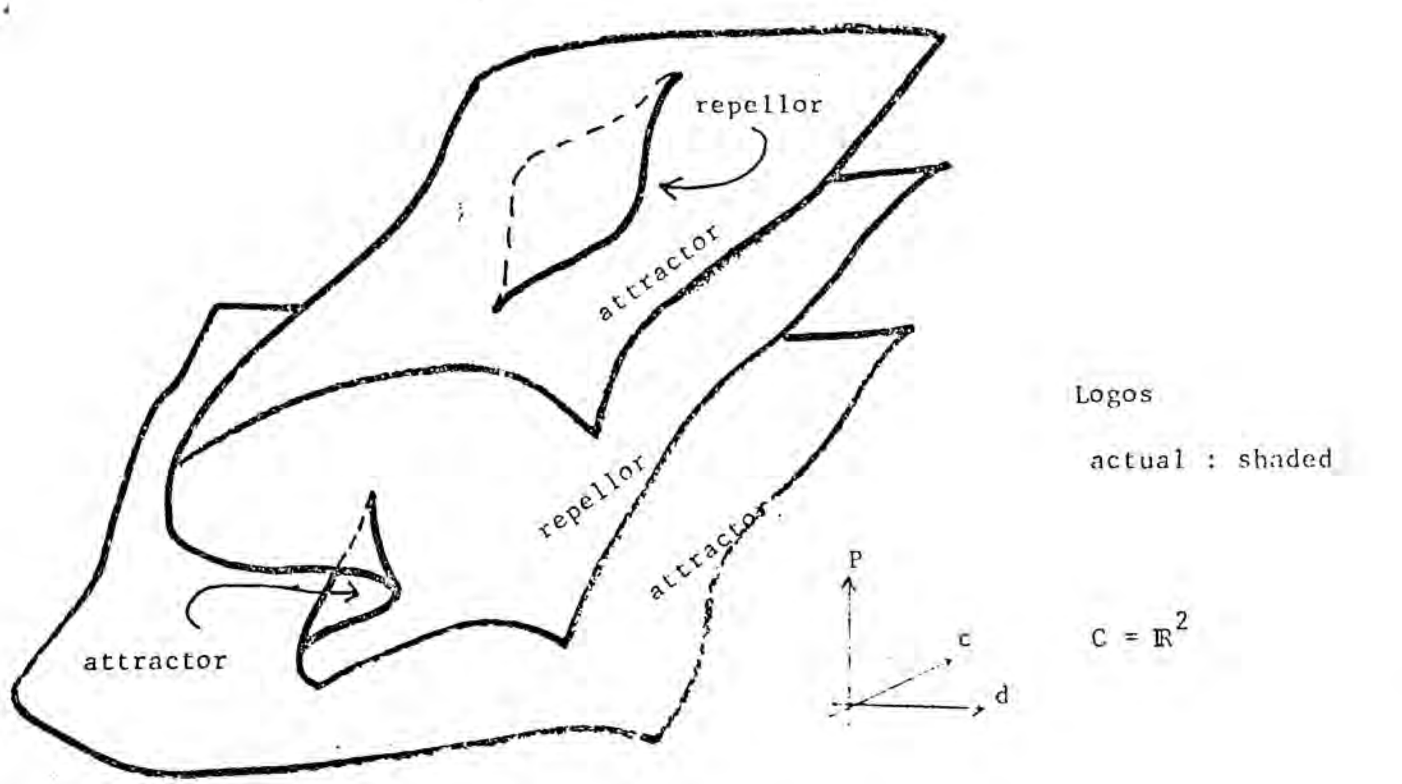

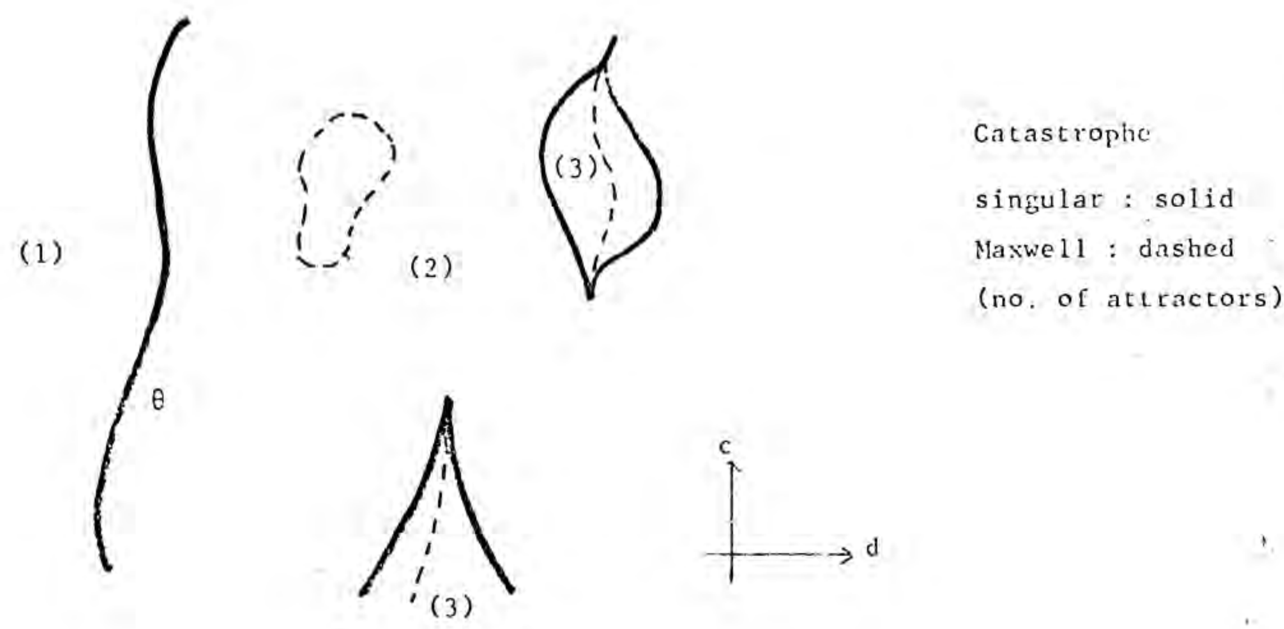

FIGURE 10-3 : TYPICAL LOGOS, dim(C) = 2 .

Structurally stable field, with simple minima, folds, and cusps, in a typical global configuration. Note the isolated cycle of Maxwell catastrophes. Fold cycles without cusps can also occur. Classification of global static logoi, for control spaces of low dimension , is feasible now, but has not been done.

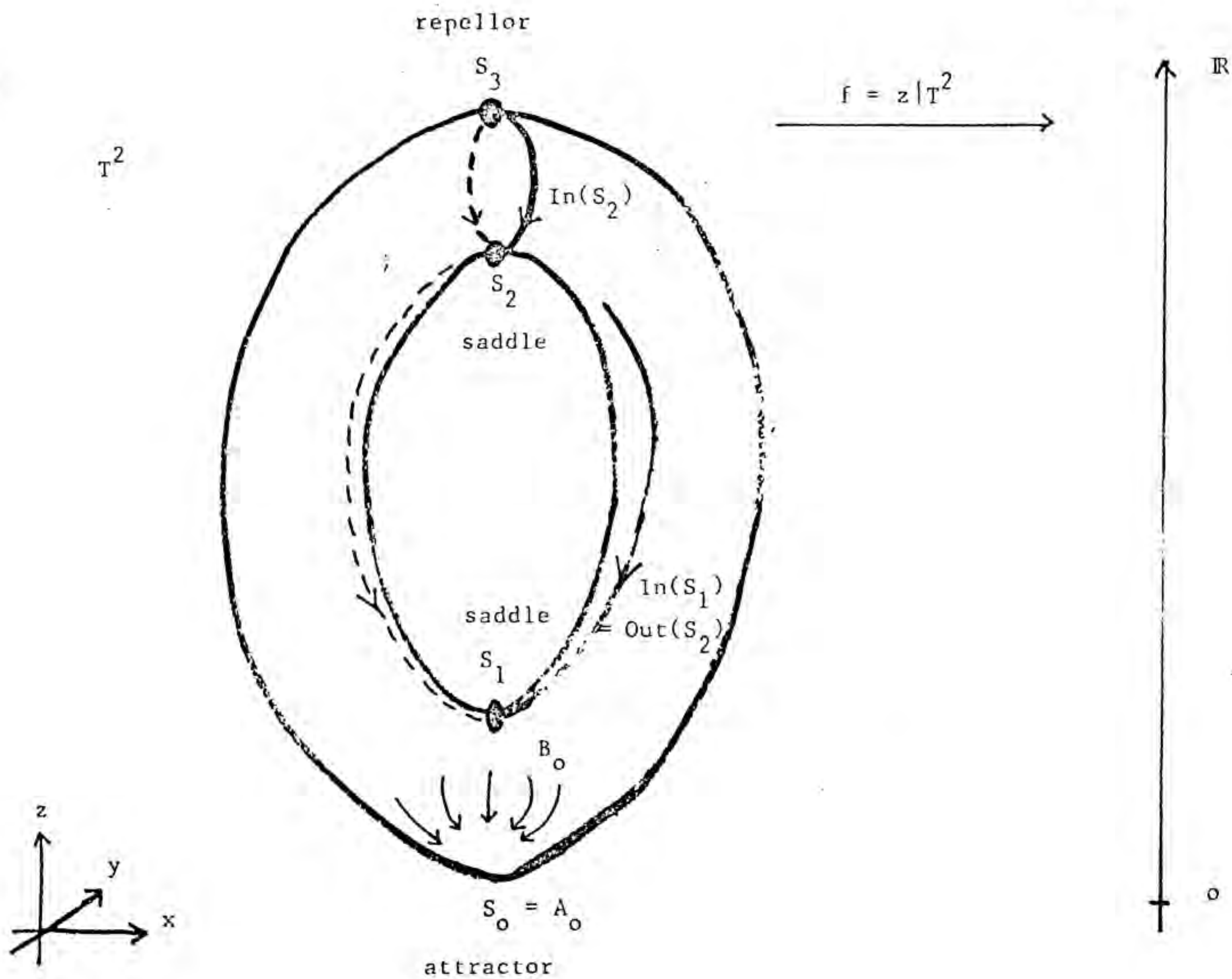

FIGURE 11-1 : STANDARD HIGHT FUNCTION ON TORUS

This function is statically stable , $f \in \Sigma_s \setminus \Theta_s$, but unstable as a vectorfield, $\nabla f \in \Theta_d$, because $In(S_1)$ meets $Out(S_2)$ non-transversally.

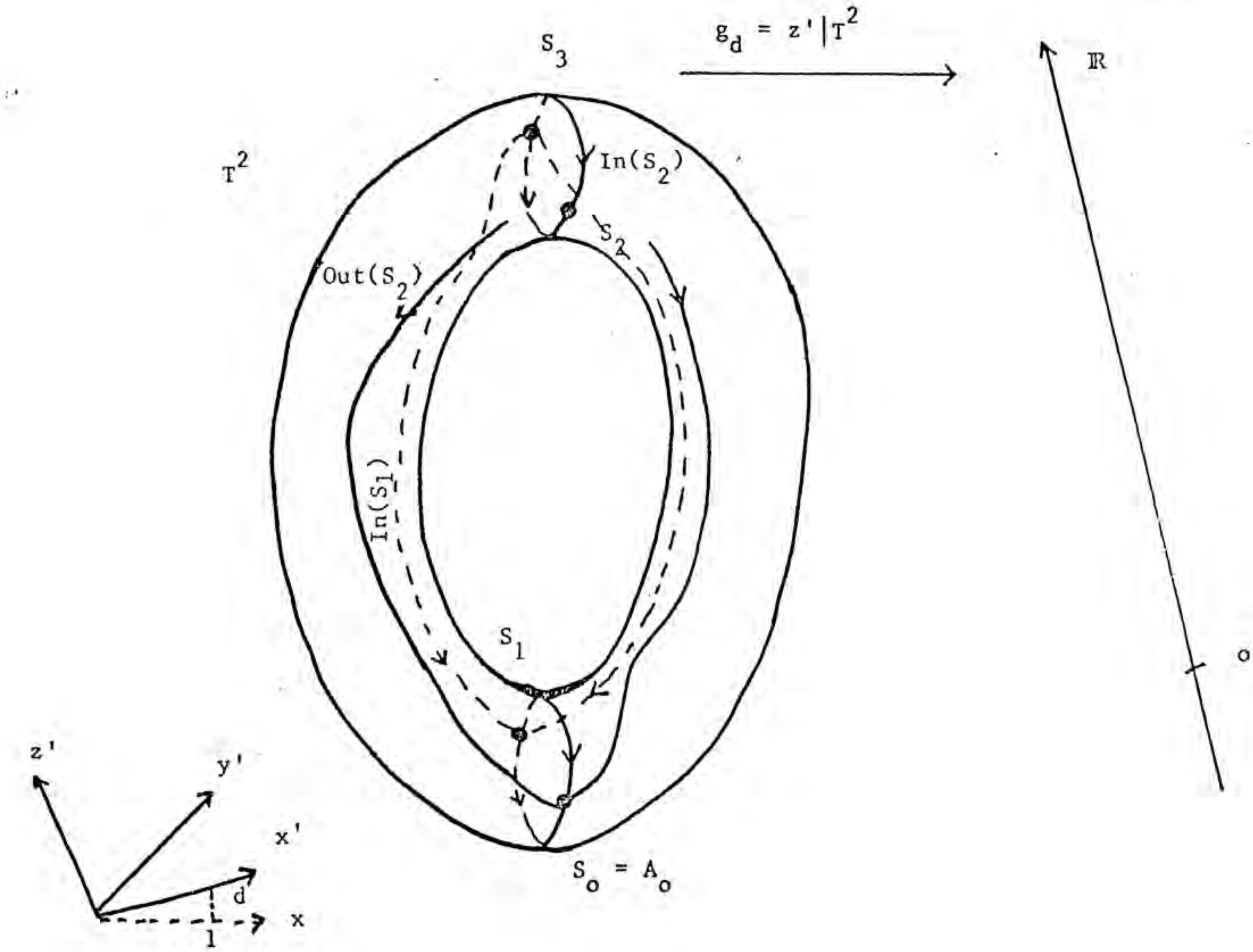

(d)

FIGURE 11-2 : TILTED HIGHT FUNCTION ON TORUS

(d) This function is stable statically and dynamically, as $\nabla g_d \in \Sigma_d \setminus \Theta_d$. The outset, $Out(S_2)$, is on the right side of the torus, and tends to S_o instead of S_1 . The inset, $In(S_1)$, is on the left, coming from S_3 rather than S_2 . They do not intersect.

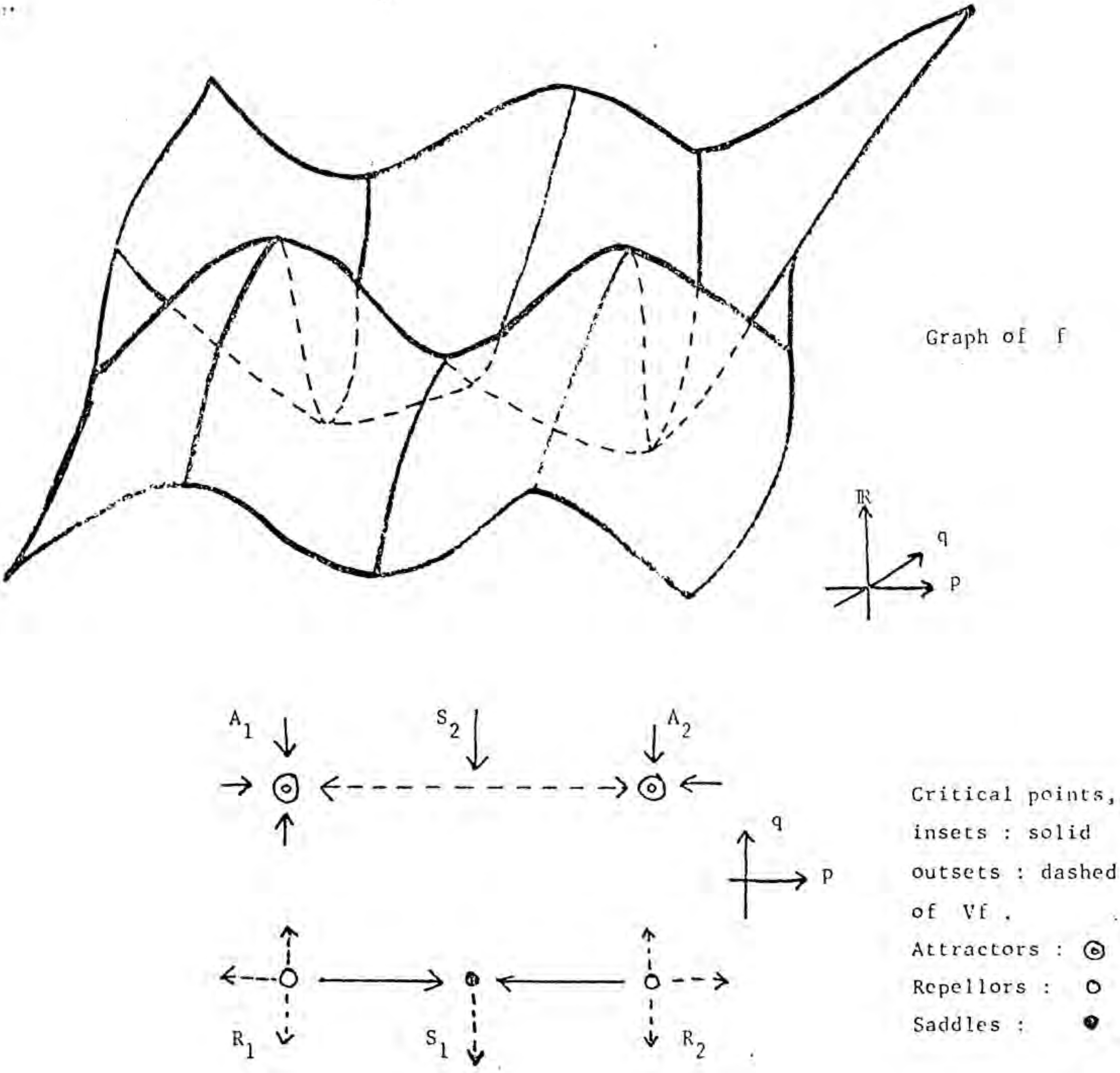

FIGURE 11-3 : STANDARD TWIN SADDLE FUNCTION

Another function, statically stable but dynamically unstable, due to non-transversal intersection of $Out(S_1)$ and $In(S_2)$.

A(d > 0)

B(d = 0)

C(d < 0)

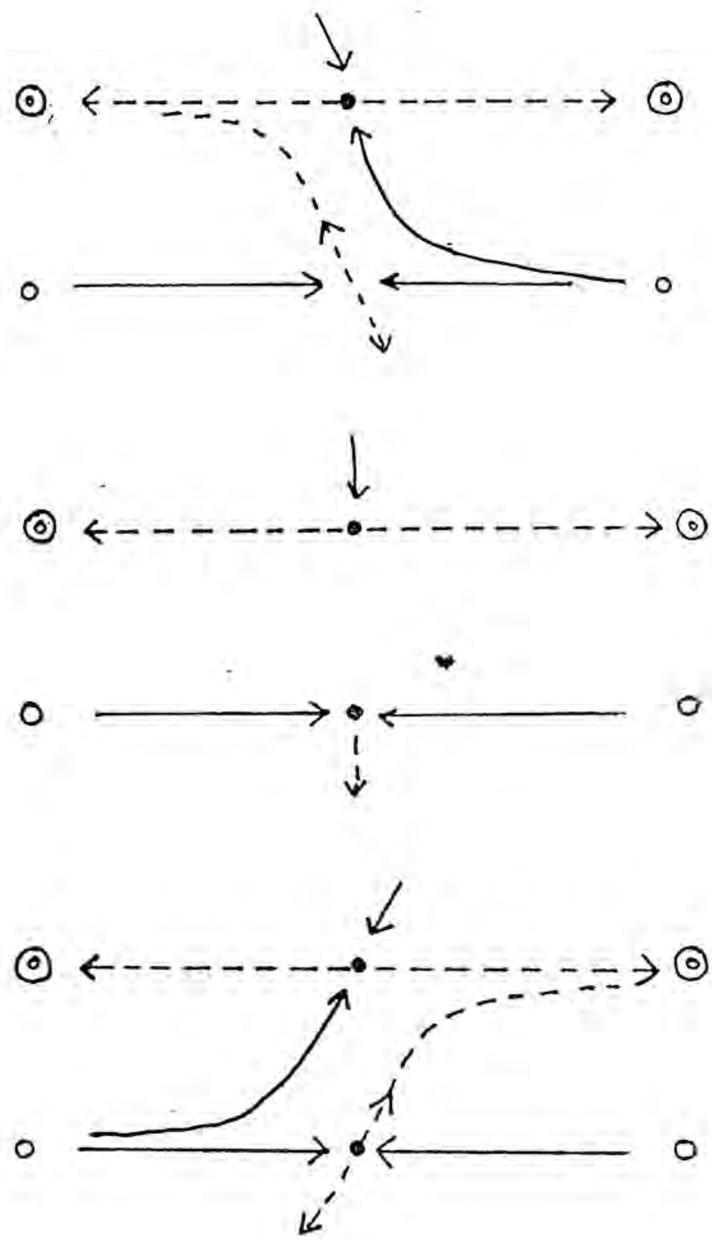

Insets : solid outsets : dashed

Repellor : O attractor : ⊙ saddle : •

FIGURE 11-4 : BASIN CATASTROPHE

Successive phase portraits of ∇g_d , where g_d is the tilted twin saddle function. The catastrophe is $d = 0$. The basin of A_1 is shown shaded in each case.

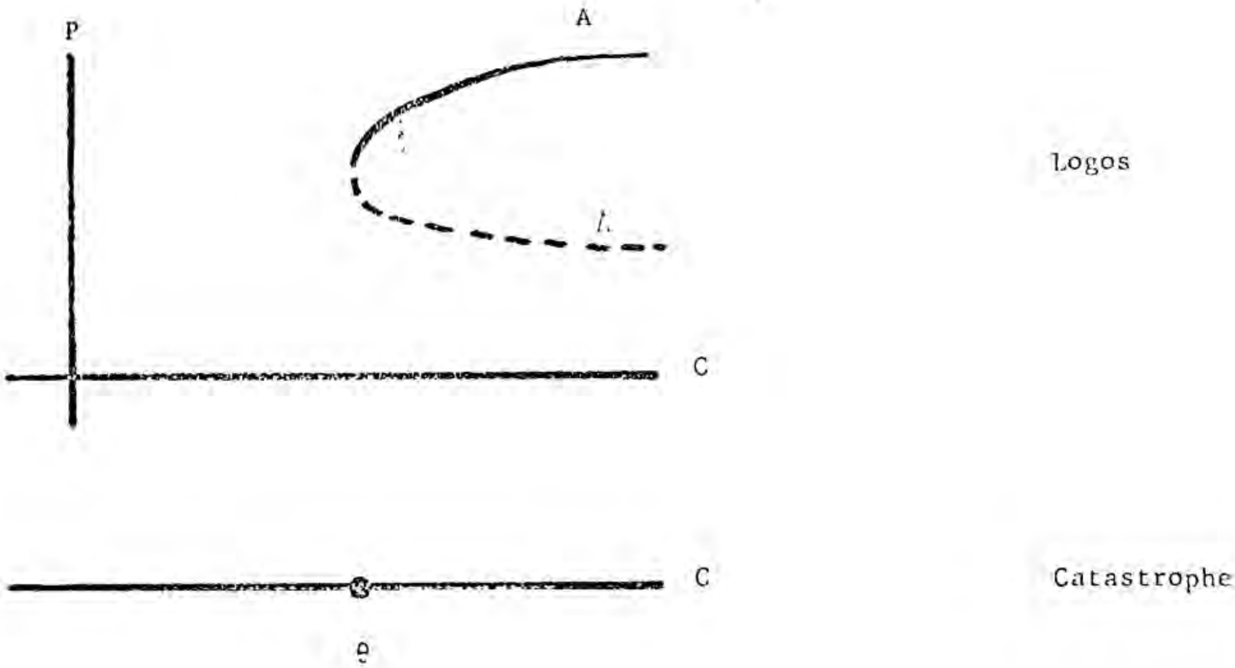

FIGURE 12-1 : STATIC CREATION

Here, $C = \mathbb{R}$, $P = \mathbb{R}$, or any manifold, $\theta \subset C$ is a single point, and as c moves to the right past θ , a pair of critical points is created, whose insets differ in dimension by one. In the case shown, $\dim(P) = 1$, so an attractor (solid line) and a repellor (dashed line) appear, contributing to the actual and virtual logoi, respectively. Each has a real CM approaching $+1$ as c tends to θ from the right. This is identical to the fold catastrophe of morphostatics.

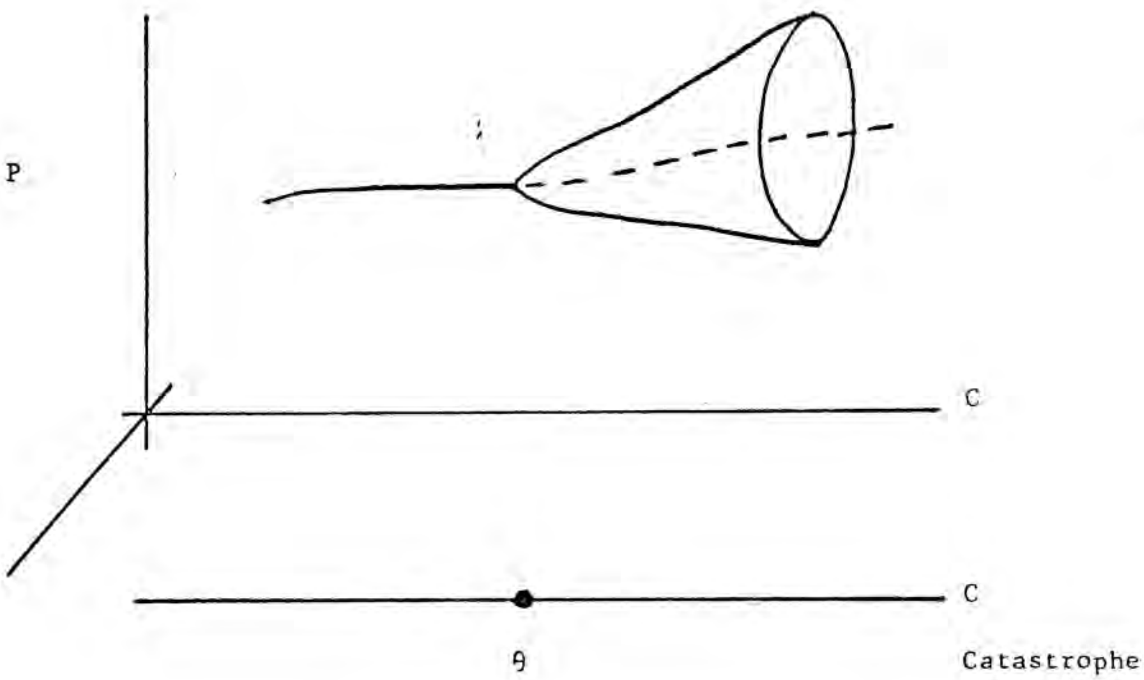

FIGURE 12-2 : HOPF EXCITATION

Here, $C = \mathbb{R}$, $P = \mathbb{R}^2$, or any manifold of dimension ≥ 2 . $\partial \subset C$ is a single point, and as c moves to the right past $\mathfrak{g}$, the inset of the critical point decreases its dimension by two - shown here is the most interesting case, an attractor changing to a repellor - and a closed orbit is born, with possibly a large frequency, but very small amplitude. The change in the inset is caused by a complex conjugate pair of CM's passing through the unit circle. In the case shown, the created closed orbit is an attractor, so the actual logos consists of the bell and tail (solid lines). This catastrophe is observed in triode oscillators and hydrodynamical instability.

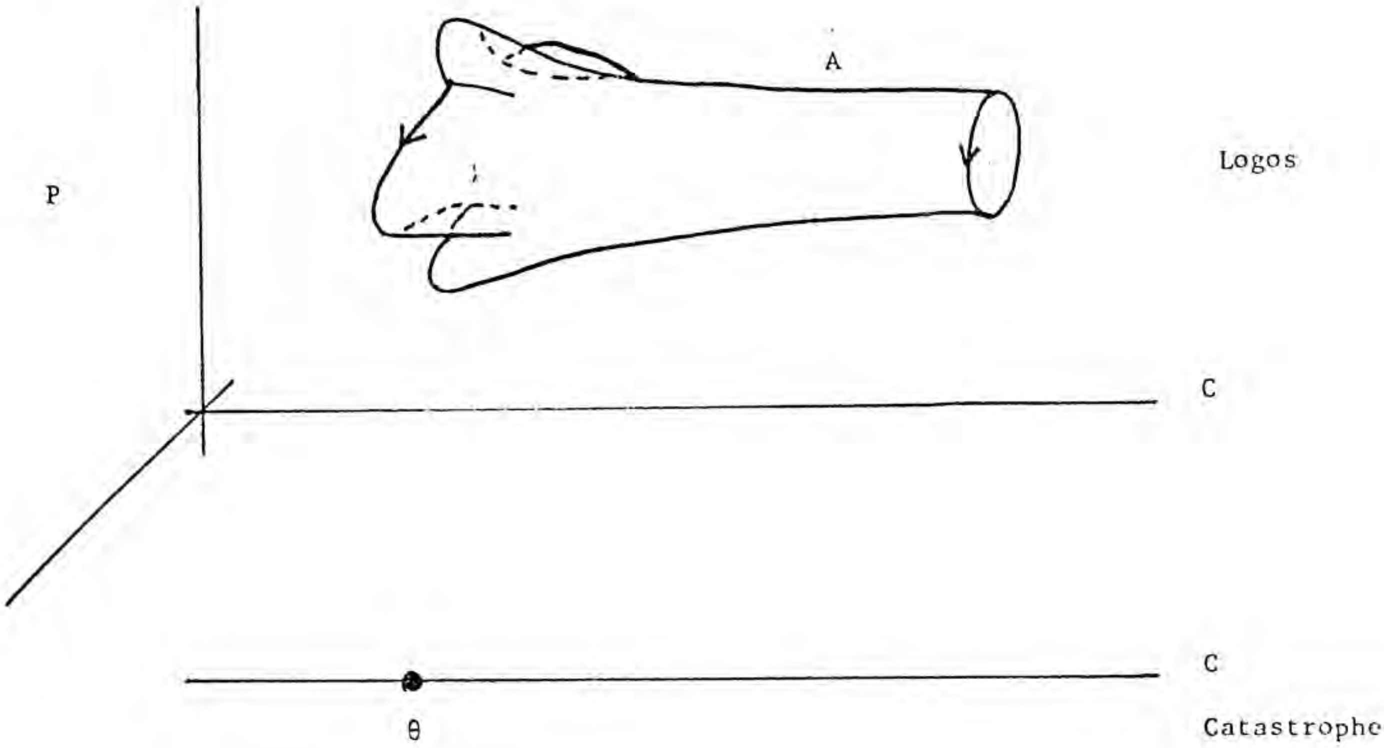

FIGURE 12-3 : BLUE SKY CATASTROPHE

Here, $C = \mathbb{R}^2$, $P = \mathbb{R}^2$, θ is a single point, and as c moves to the left, the period of the closed orbit tends to infinity. At θ , there is no closed orbit, it has dissappeared into the blue. Here, the closed orbit is shown as an attractor, so a piece of the actual logos ends at θ . When the control moves to the right, an attractor suddenly appears out of the blue, and probably is not noticed. When the control moves to the left, if the process is in the state identified by this part of the actual logos, the behavior of the process becomes increasingly erratic, then jumps to another state at $c = \theta$. I suppose this can also occur in a Hamiltonian system, with energy as control.

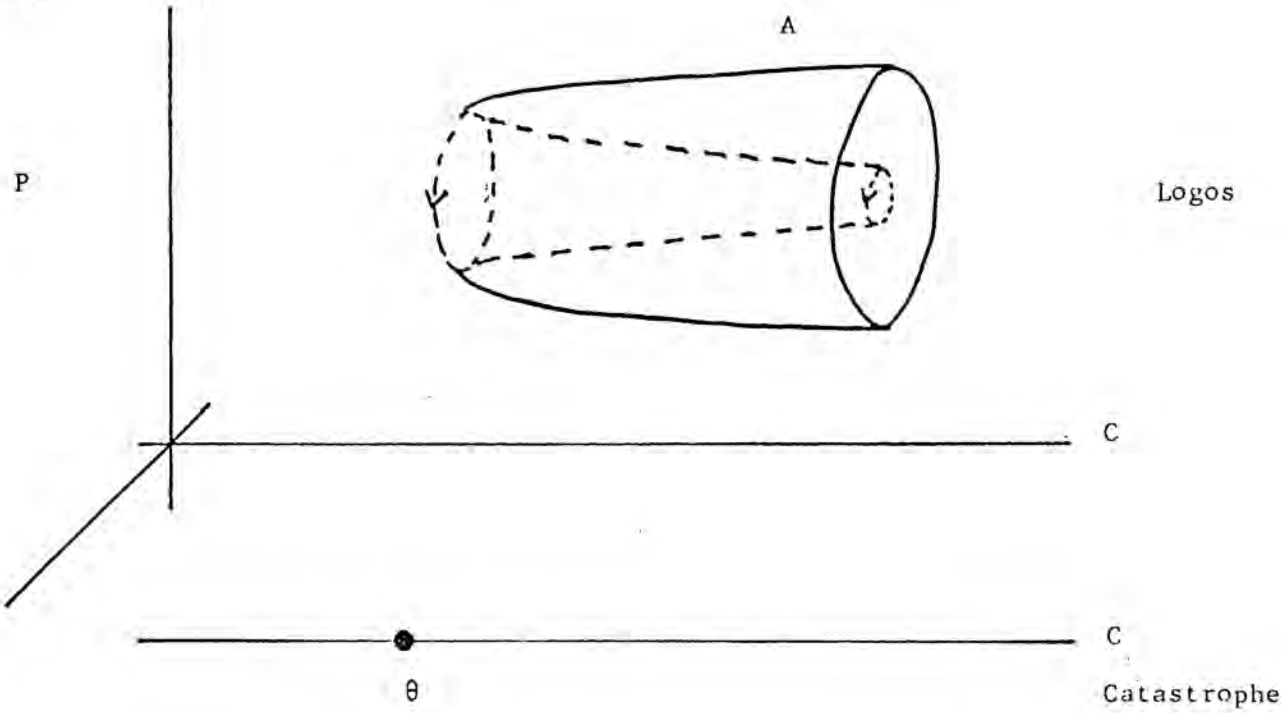

FIGURE 12-4 : DYNAMIC CREATION

Two closed orbits, their insets differing in dimension by one, are created (or annihilated) at θ . Shown here are an attractor and a repellor, with dim(P) = 2 . As c moves to the left, the CM of each approaches +1. This catastrophe occurs also in Hamiltonian systems, with energy as the control parameter. The behavior of a process, through this case, is similar to the blue sky catastrophe, but the motion is steady until the catastrophe, when the system jumps to another attractor.

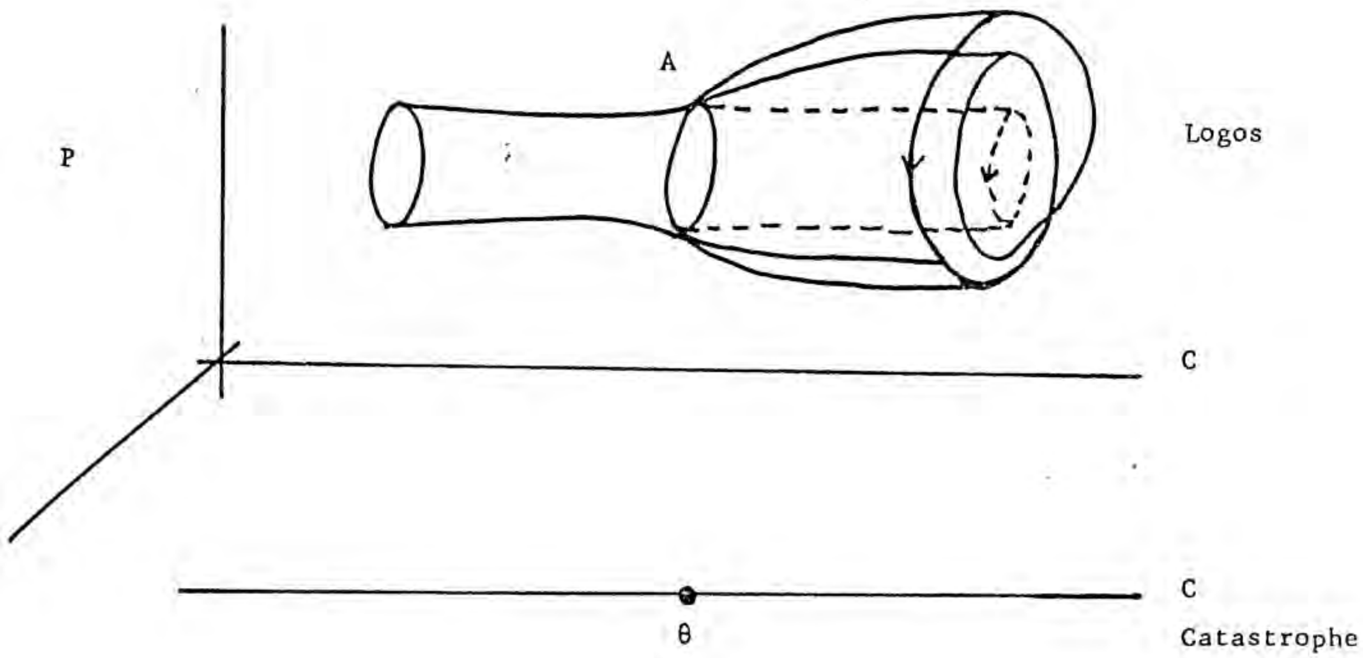

FIGURE 12-5 : SUBTLE DIVISION

A closed orbit changes the dimension of its inset by one, as a real CM passes -1, here shown as an attractor changing to a repellor, with dim(P) = 2 . At the catastrophe, another attractor, of half the frequency, is emitted. The actual logos becomes branched. The behavior of a process, observed in this catastrophe, is changed in a subtle, barely perceptible way, which becomes obvious when the control is moved sufficiently far to the right, as a halving of the frequency of the motion : two oscillations are required to return to the initial condition. This catastrophe occurs also in Hamiltonian systems.

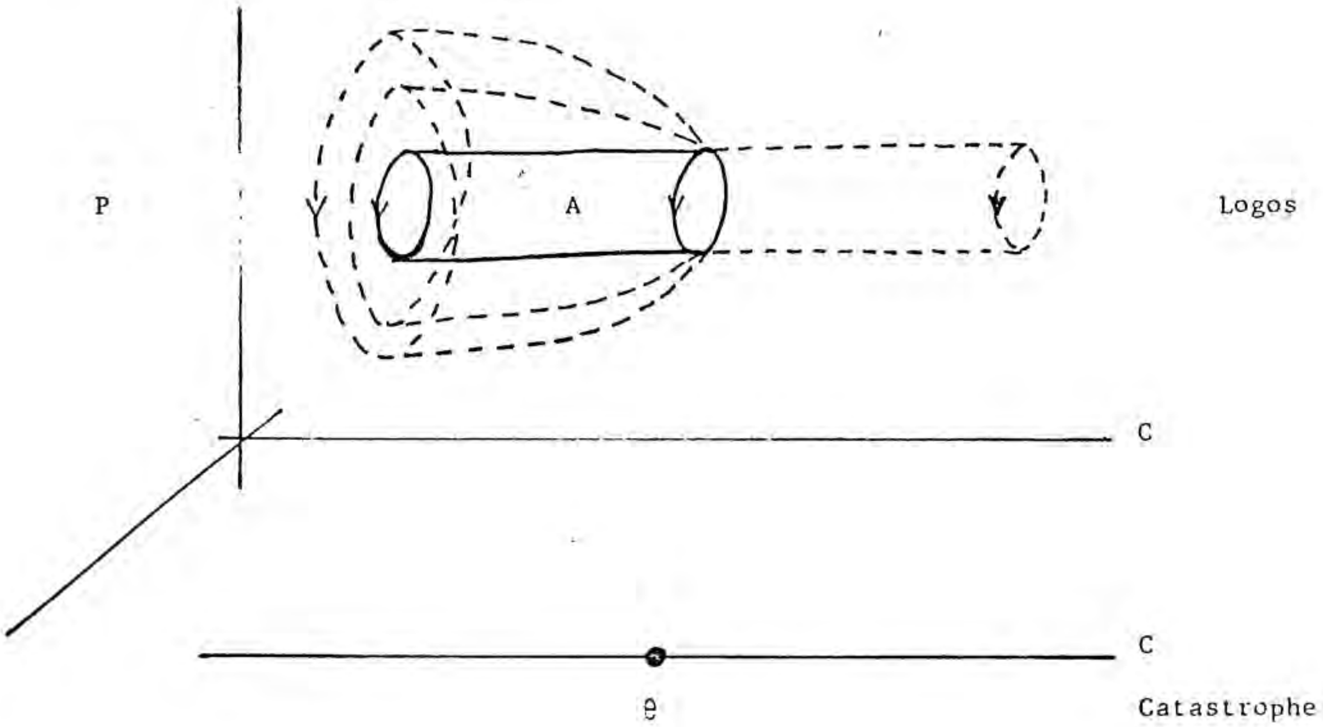

FIGURE 12-6 : MURDER

A closed orbit changes exactly as in subtle division, but a repellor is absorbed, rather than an attractor emitted. The actual logos ends in this case, as in dynamic creation, and the blue sky catastrophe. This also occurs in Hamiltonian systems.

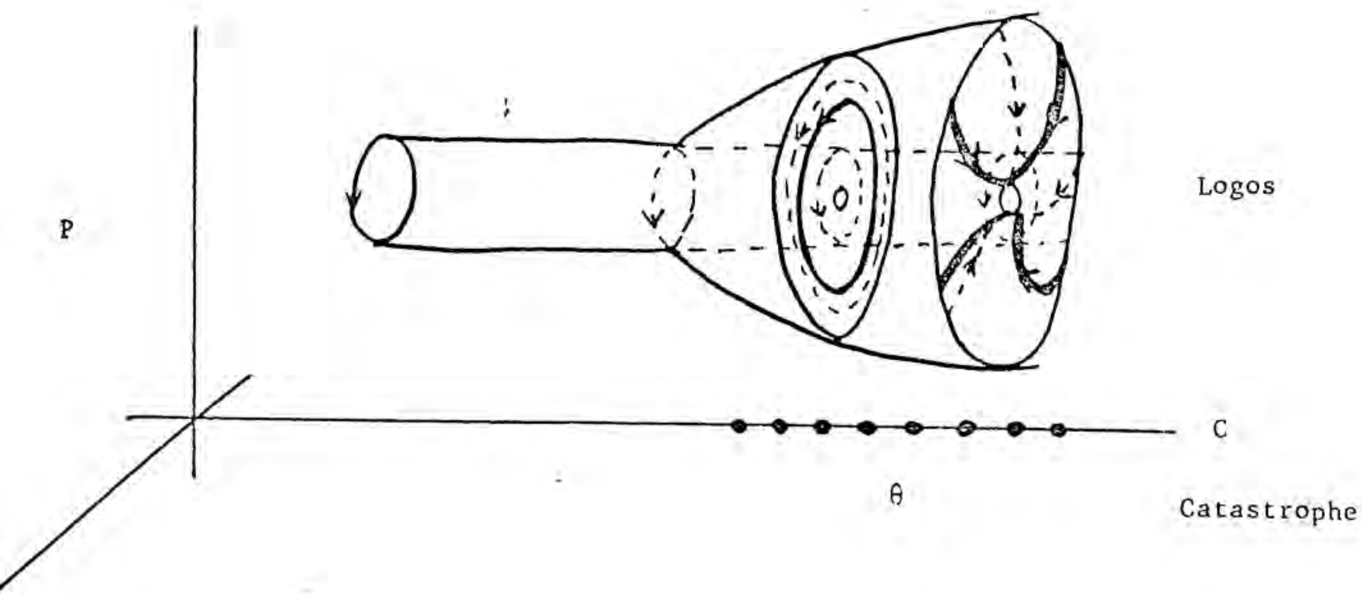

FIGURE 12-7 : NEUMARK EXCITATION WITH SOTOMAYER VASCILLATIONS

This is similar to Hopf excitation but begins with a closed orbit instead of a critical point, and ends with an invariant torus instead of a closed orbit. In Takens excitation, a torus T^K becomes a T^{K+1} , $K \geq 2$. All of the excitation catastrophes are subtle, like division, in that the change of behavior is obvious only after the control is moved well past the catastrophic value. But unlike Hopf excitation, the catastrophe in this case consists of many points, as the flow on the invariant T^2 may undergo rapid Sotomayor catastrophes. Here, one is shown. It is very difficult to visualize the actual logos in this situation, which is observed in hydrodynamical instability.

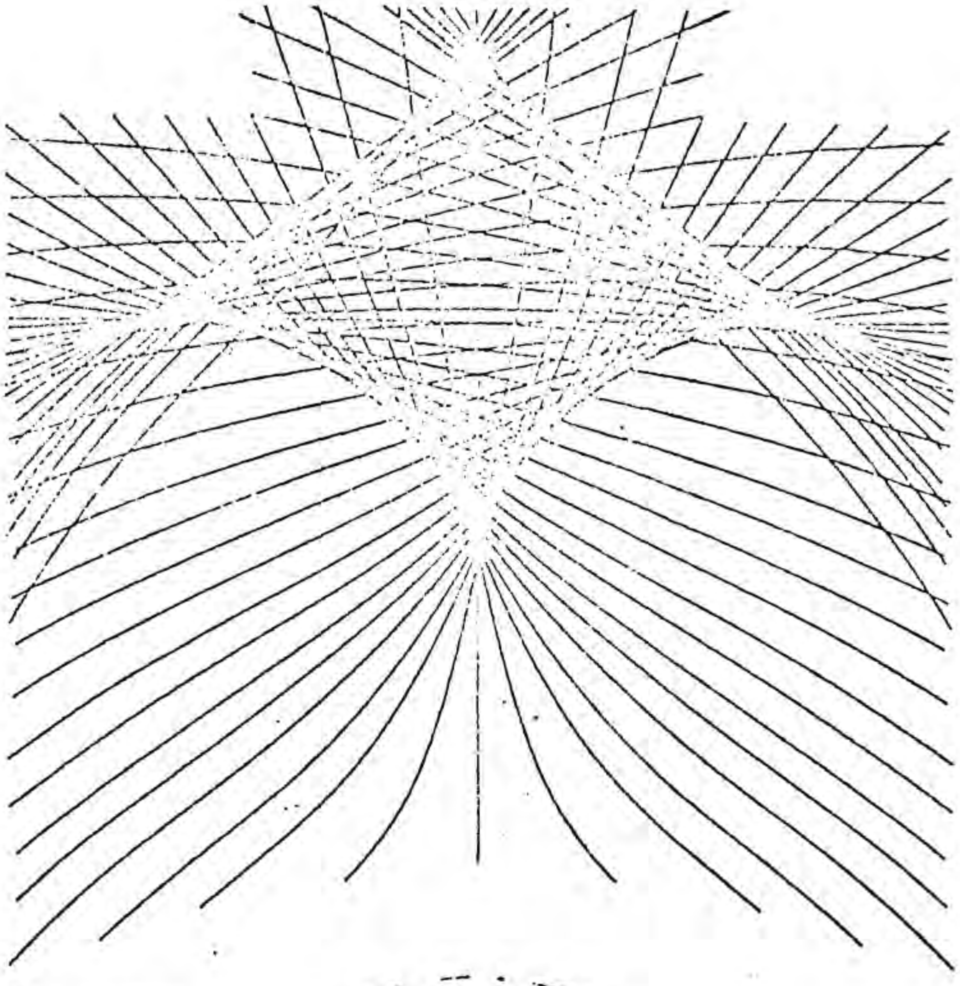

The state of this system (i.e. the angle of the wheel) is controlled by the position in the plane of the free end C of the elastic, but not uniquely. If C is inside the ⟡ region, there are two stable states of equilibrium; outside, there is only one.

Experiment with the machine will verify this, and explain (i) what decides which state it will occupy, if there is a choice, and (ii) what the computer-drawn lines represent.

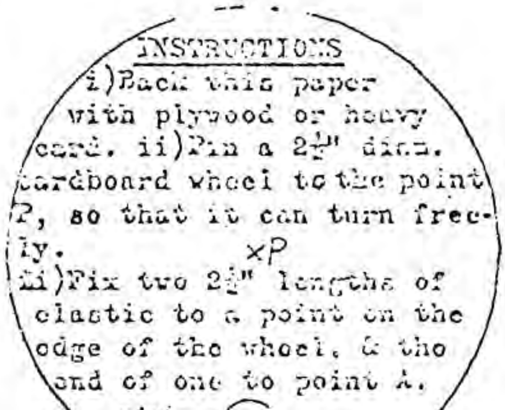

FIGURE 13-0 : ZEEMAN'S CATASTROPHE MACHINE

Courtesy of the Mathematics Institute, University of Warwick, England.

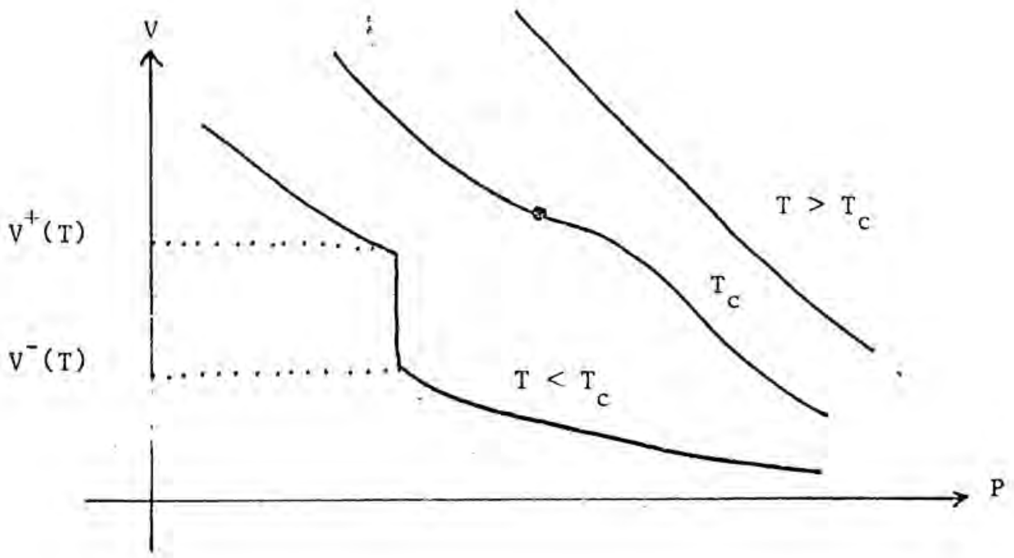

FIGURE 13-1 : ISOTHERMS OF PHASE TRANSITION

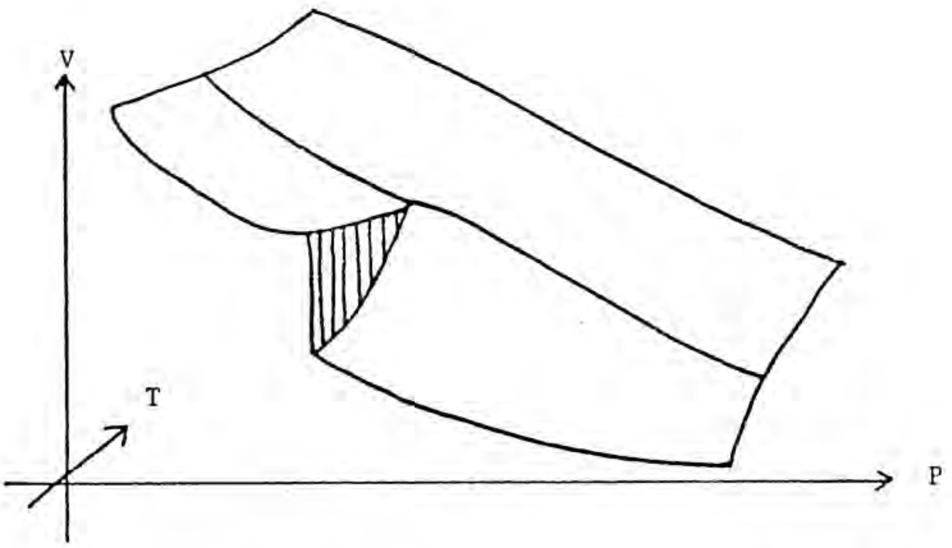

FIGURE 13-2 : STATE SURFACE OF PHASE TRANSITION

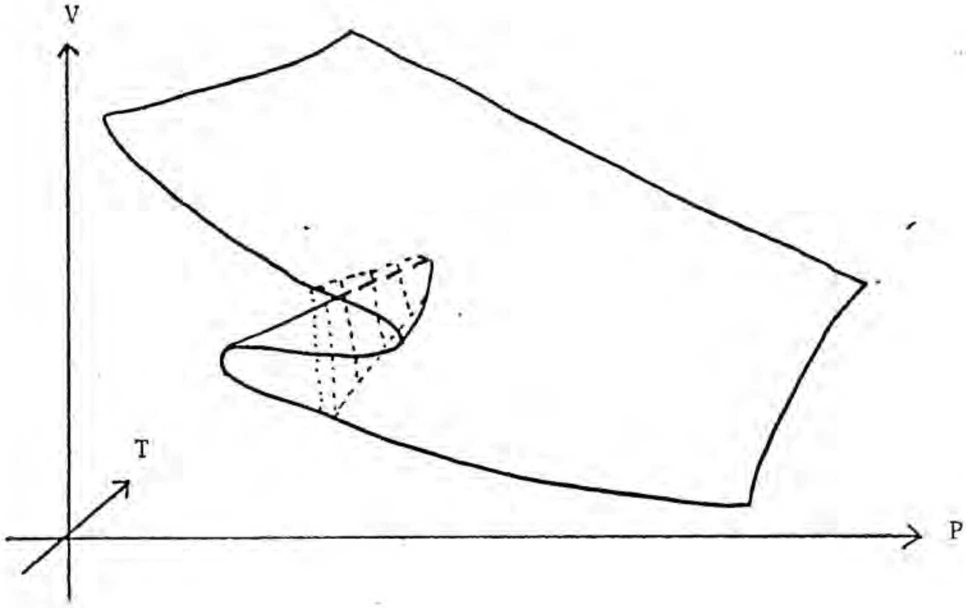

FIGURE 13-3 : VAN DER WAAL'S MODEL

The observed cliff is superimposed in dotted lines

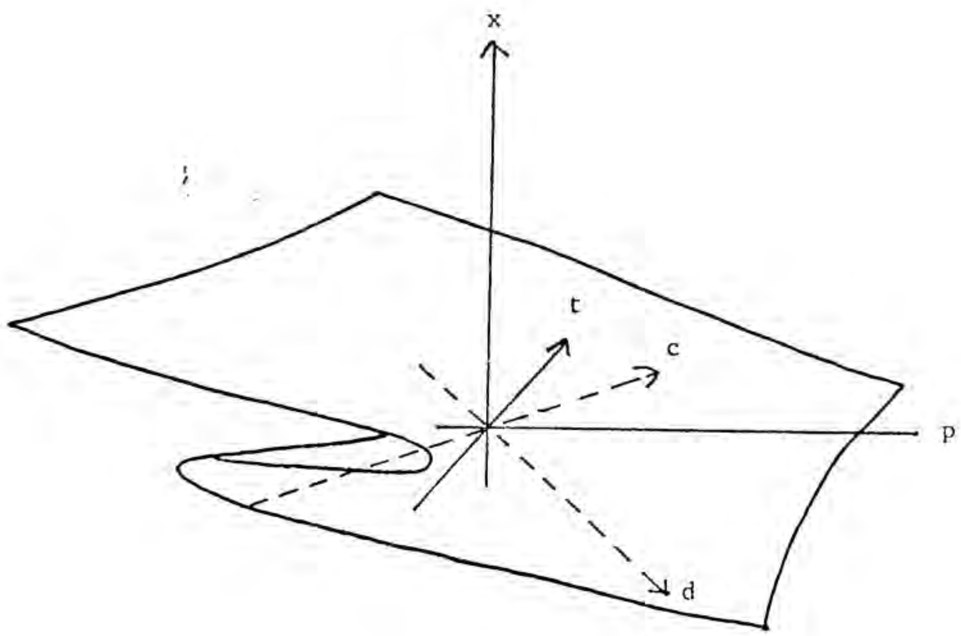

FIGURE 13-4 : VAN DER WAAL'S MODEL IN FOWLER COORDINATES

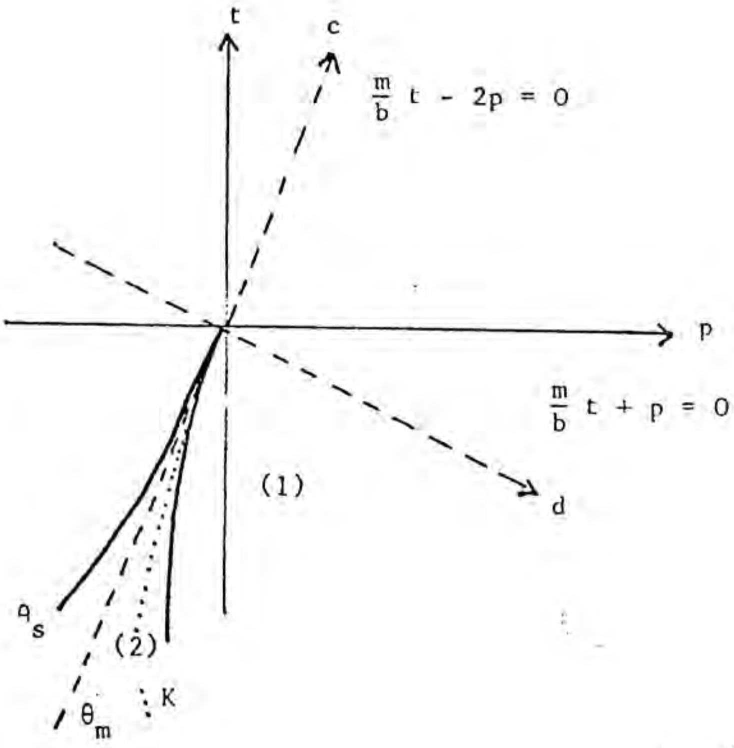

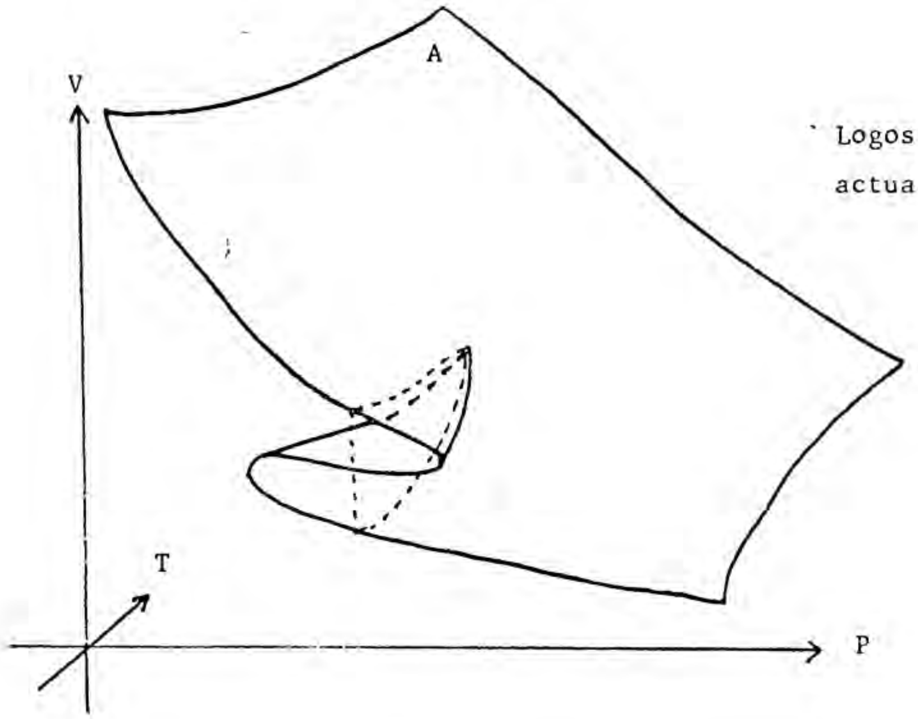

Logos
actual : shaded

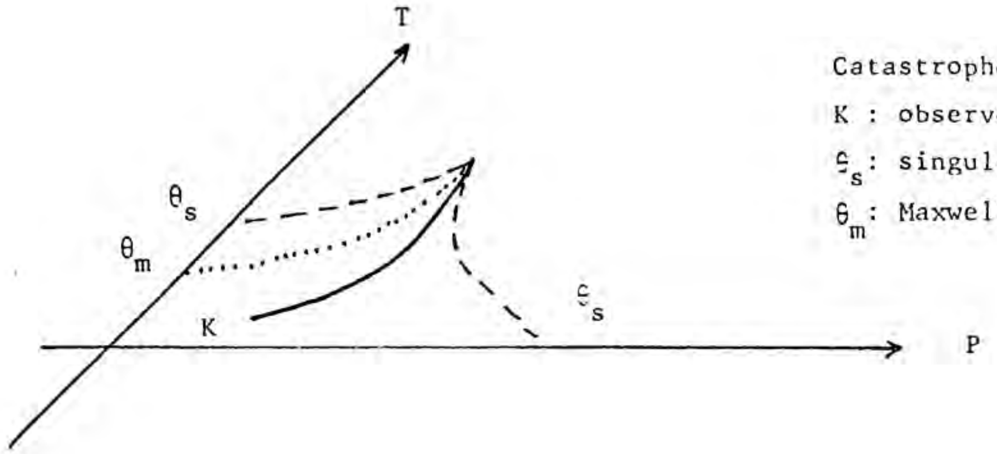

Catastrophe
K : observed
θ_s: singular
θ_m: Maxwell

FIGURE 13-6 : LOGOS AND CATASTROPHE IN PHYSICAL COORDINATES

The catastrophe convention relates K to θ_m (but $K \neq \theta$) and defines $A \subset \Lambda$. A better choice of morphostatic field (or change of coordinates) would provide $K = \theta_m$.

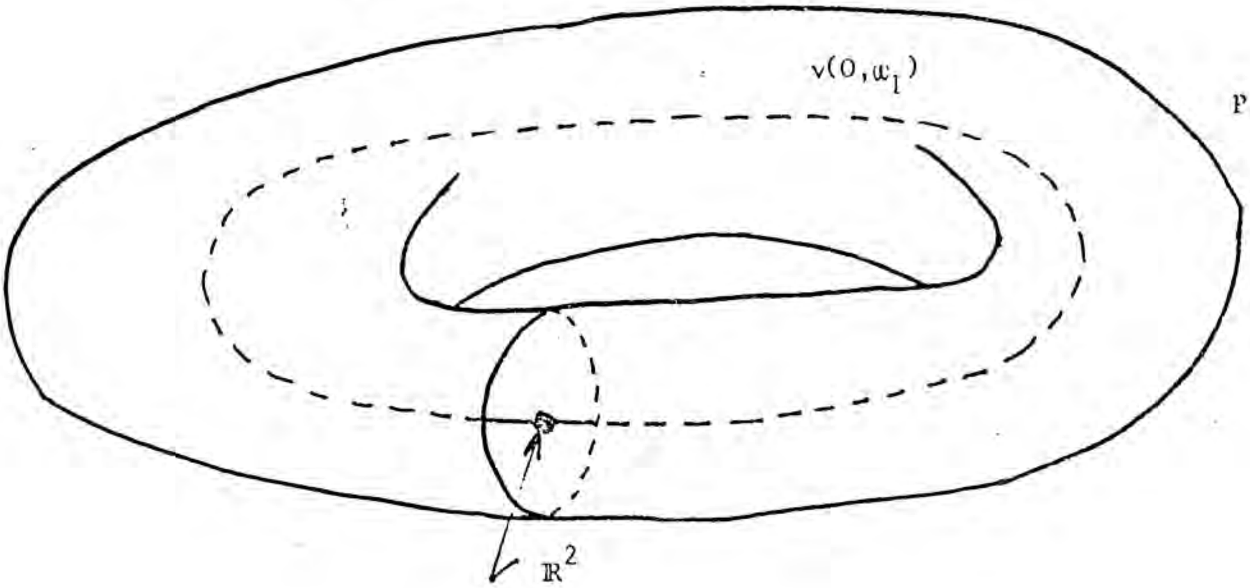

A. The catastrophe closed orbit

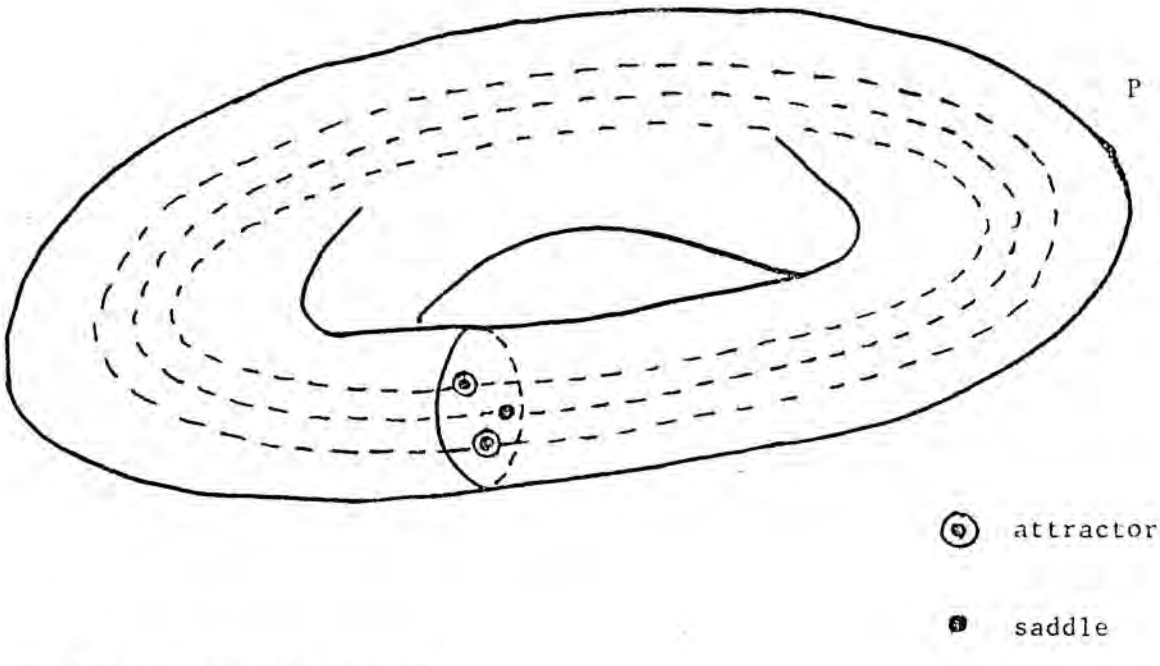

B. The trifurcated orbits.

FIGURE 14-1 : ZEEMAN CATASTROPHE, $P = \mathbb{R}^2 \times S^1$

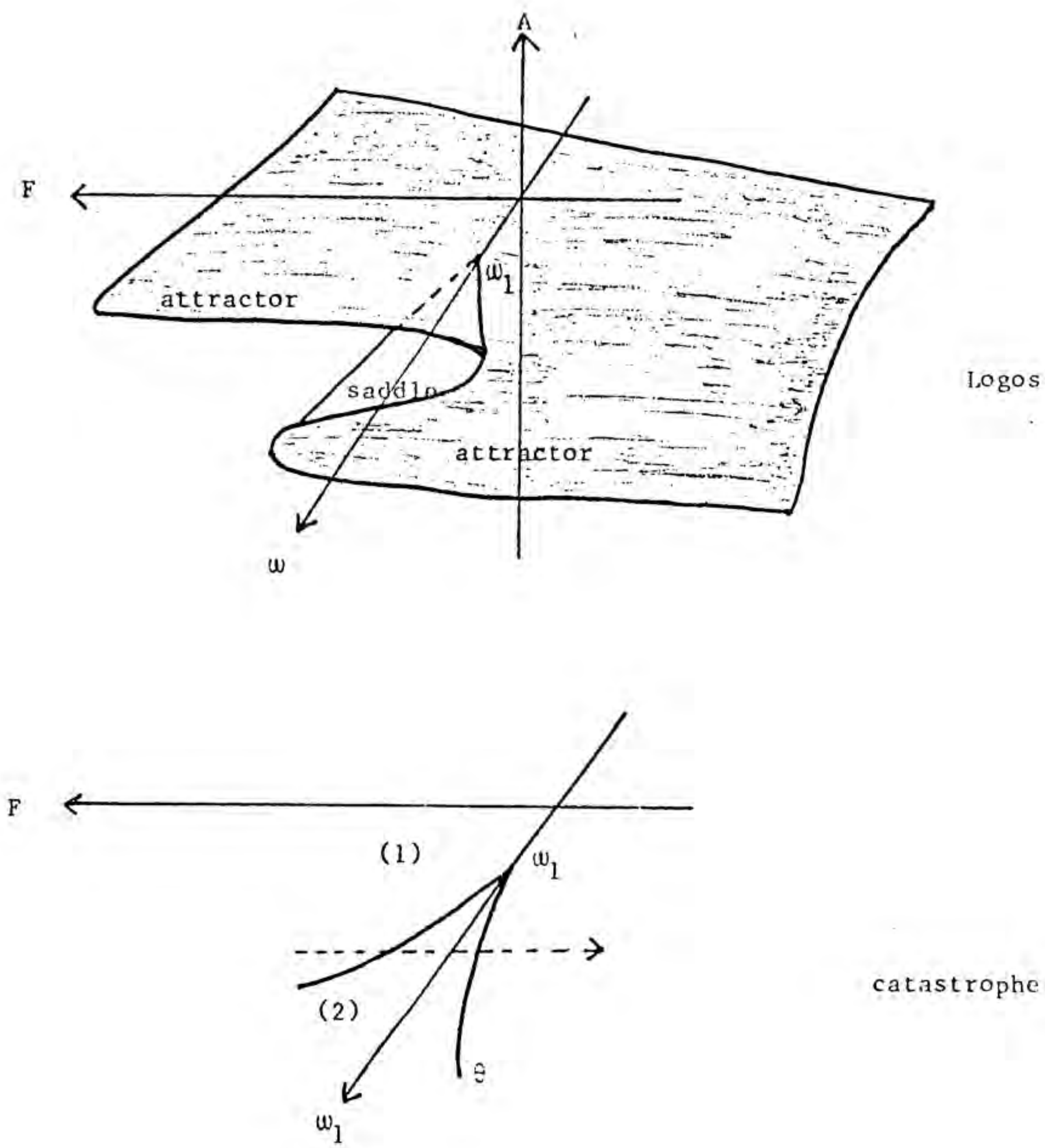

FIGURE 14-2 : AMPLITUDE LOGOS, ZEEMAN CATASTROPHE

Here, A denotes the amplitude of the closed orbits shown in Figure 14-1. The actual logos (shaded) indicates the delay convention of the dynamic interpretation.

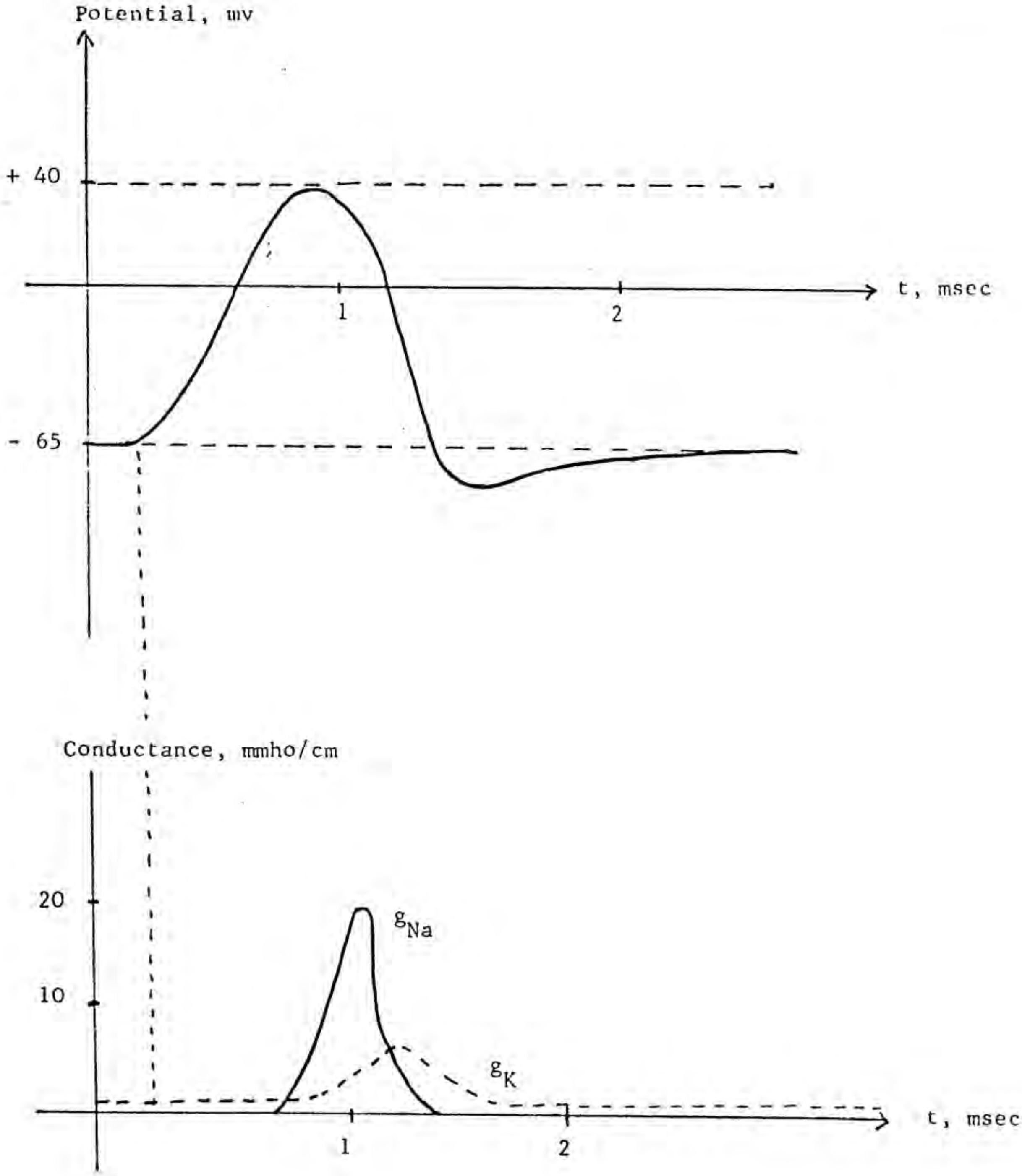

FIGURE 16-1 : THE NERVE IMPULSE

The spike of activity in potassium conductivity, voltage across the axon, b , and sodium conductivity, -x , form Zeeman [622].

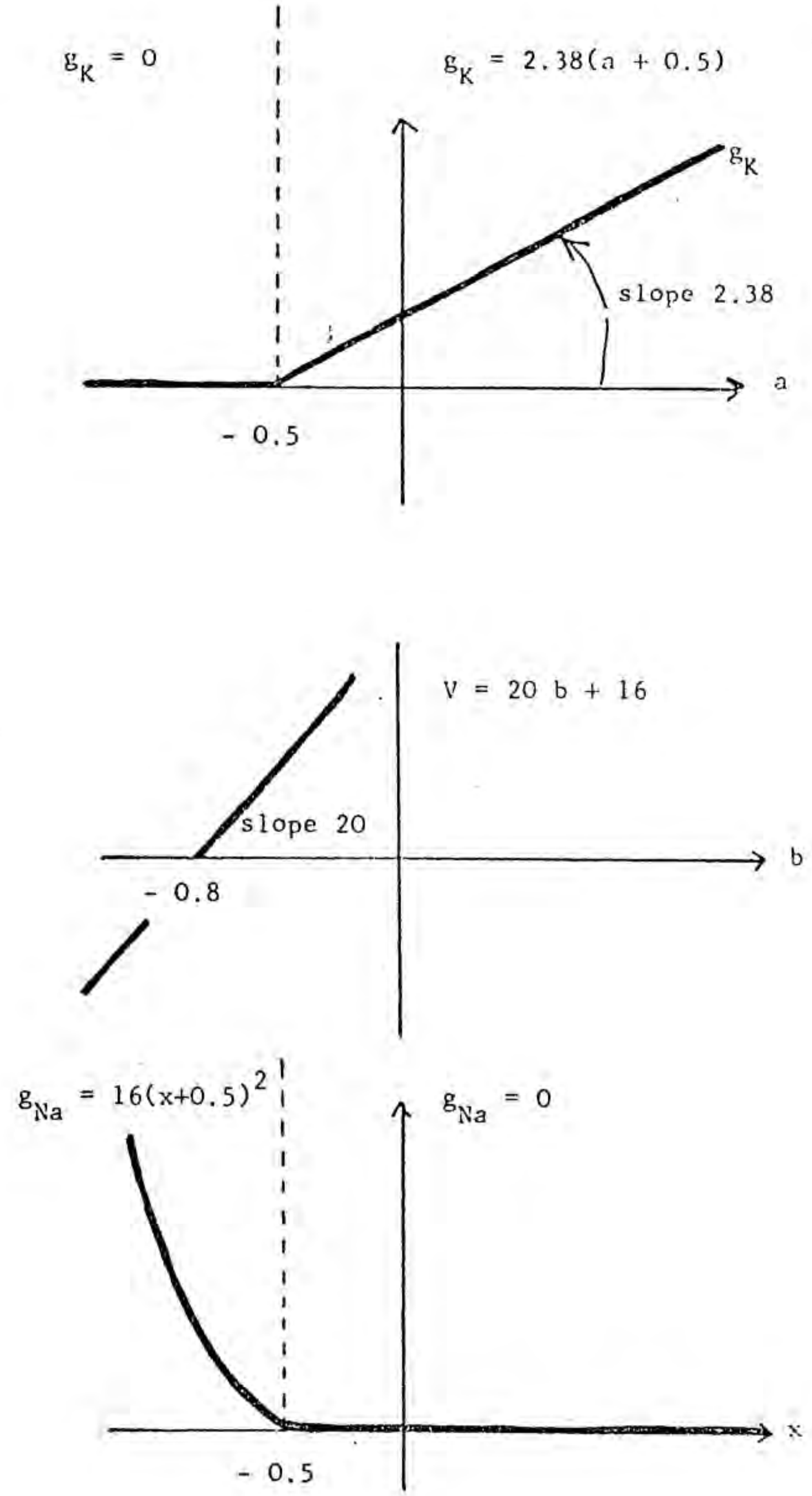

FIGURE 16-2 : DEFINITION OF ZEEMAN COORDINATES

Here are shown the graphs of the functions $g_K(a)$, $V(b)$, and $g_{Na}(x)$. The corners in the conductance functions could be smoothed.

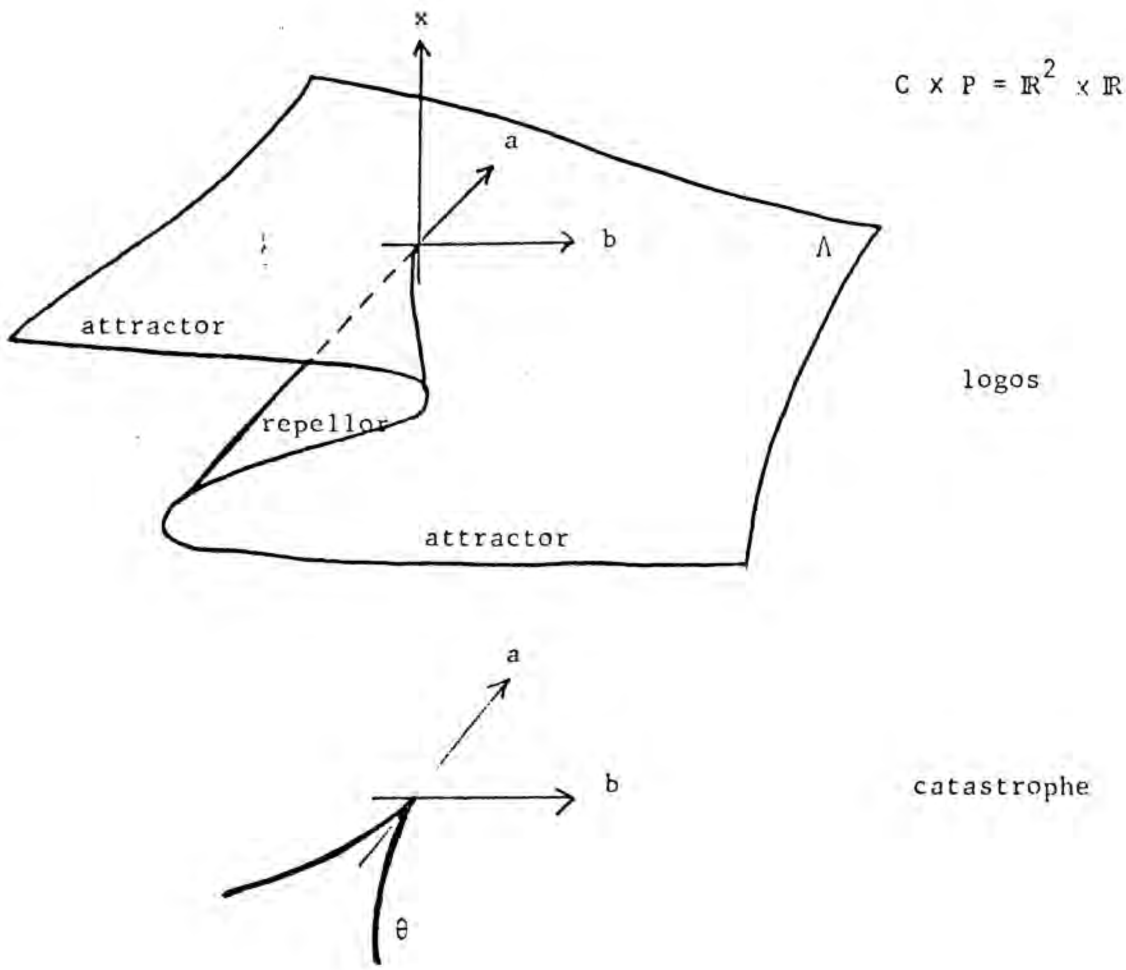

FIGURE 16-3 : MODEL FOR ZEEMAN'S FAST EQUATION

The virtual logos is a separatrix for the basins of attraction of the two attractors over the interior of the cusp. Here a is the potassium conductance, b is the action potential, and x the sodium conductance of the axon.

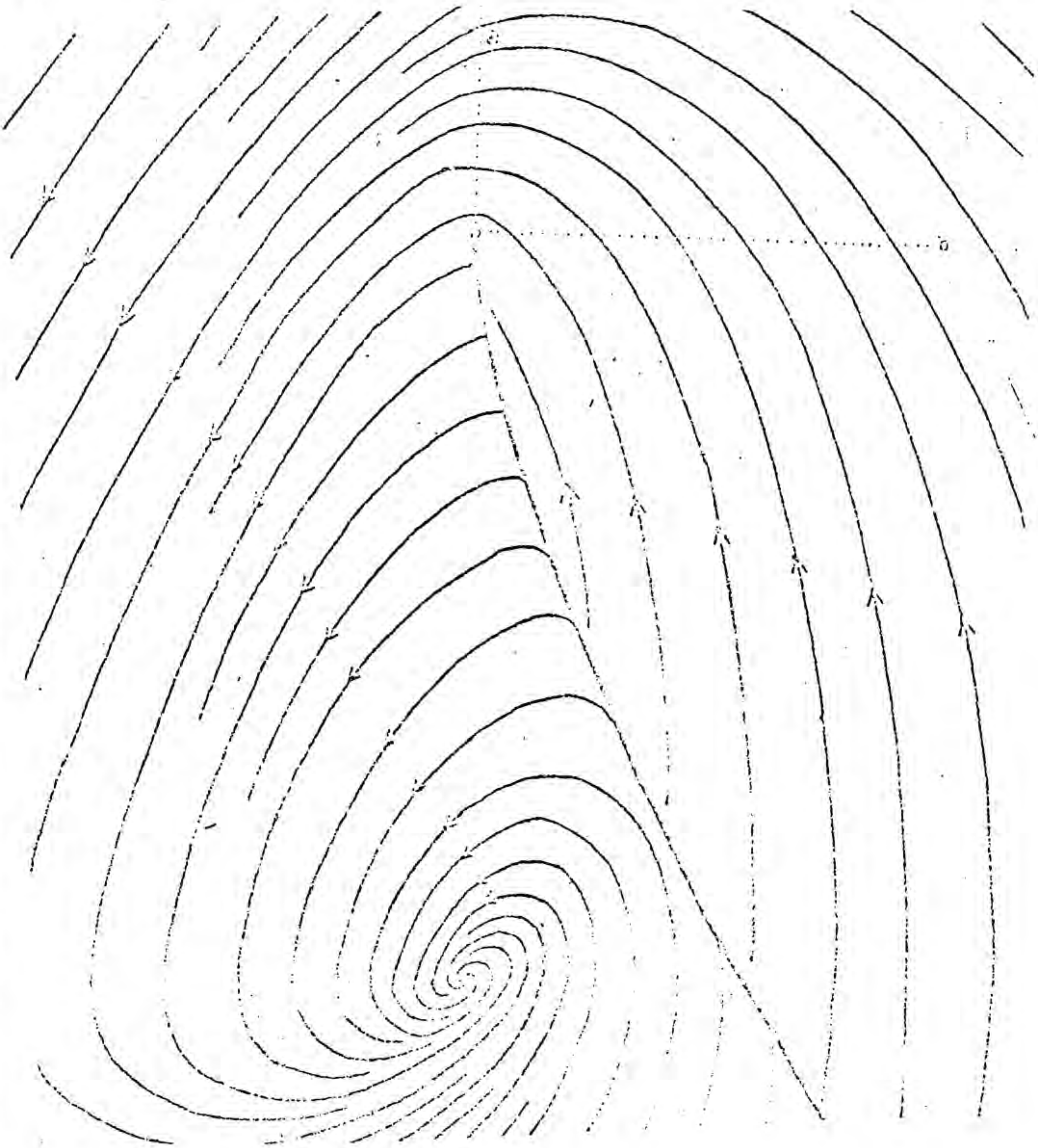

FIGURE 16-4 : SLOW ACTION OF SIMPLECTIC MODEL

Trajectories near the slow manifold of Example 8, from Zeeman [422, p. 36], seen from above.

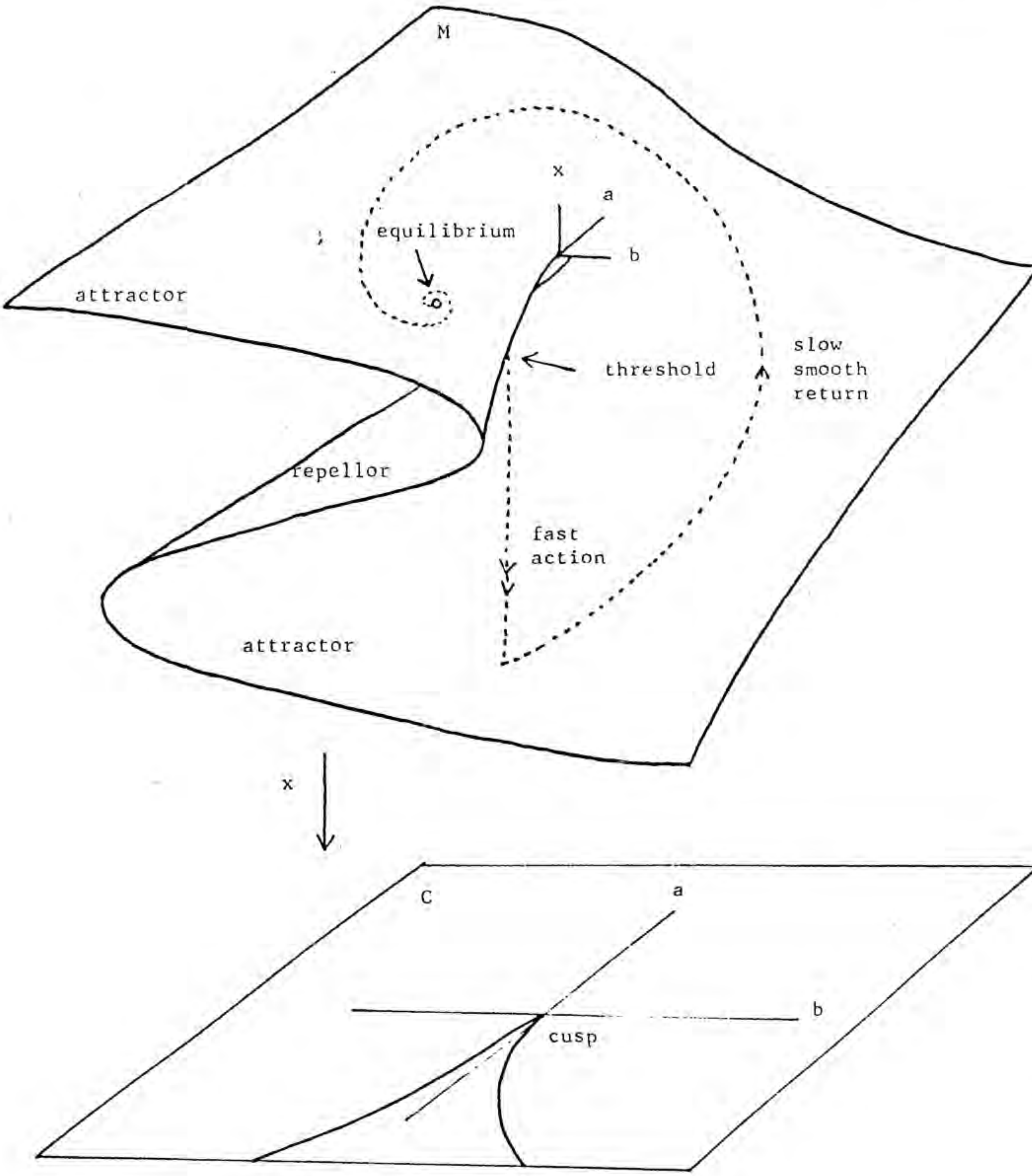

FIGURE 16-5 : NERVE IMPULSE, SIMPLISTIC MODEL

Trajectory of the neuron parameters in Example 8, after a trigger to threshold voltage by the experimentalist, from Zeeman [422, pp. 28].

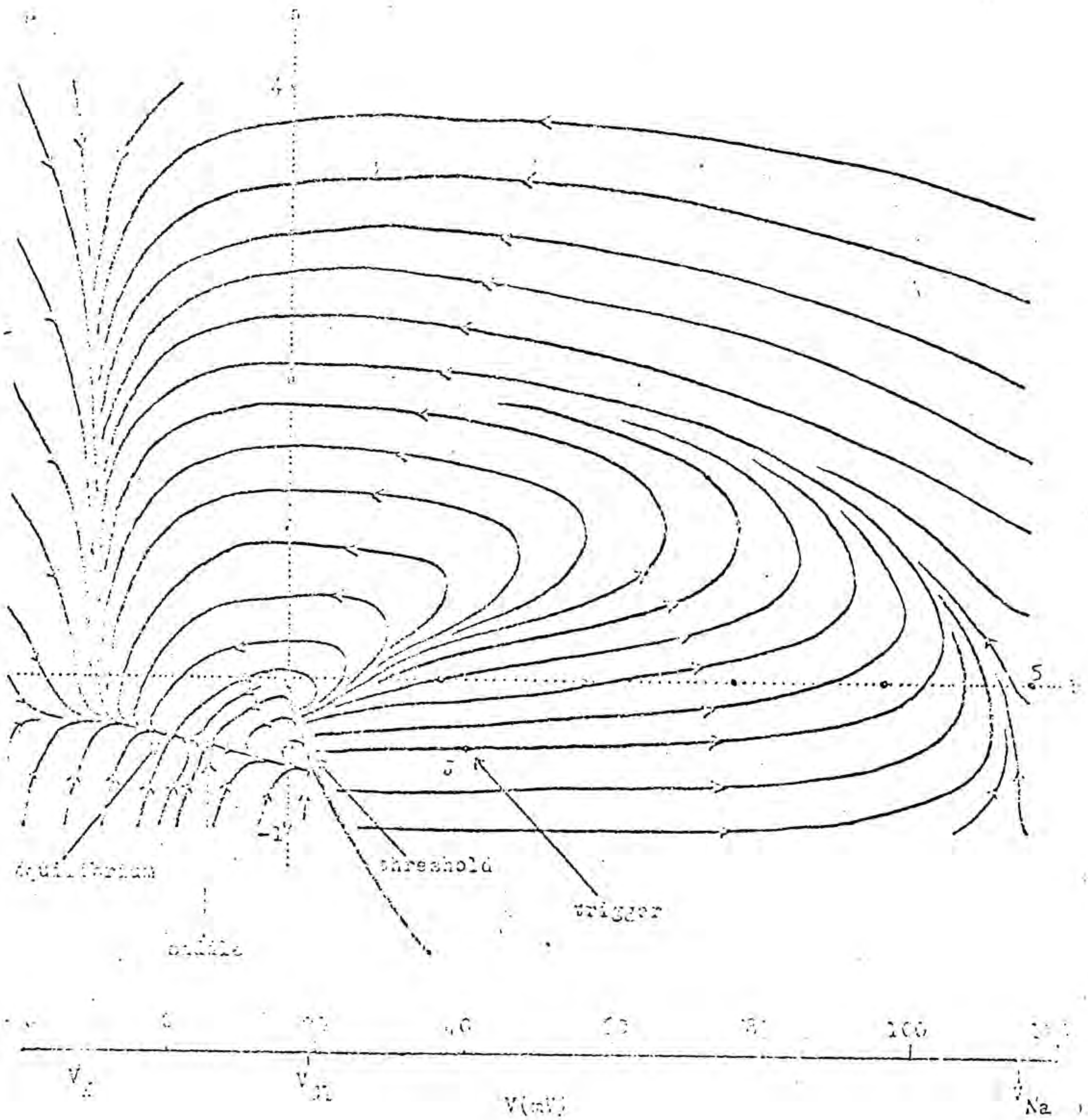

FIGURE 16-6 : SLOW ACTION OF ZEEMAN MODEL

Orbits near the slow manifold, seen from above, for the precise model, from Zeeman [422, p. 70].

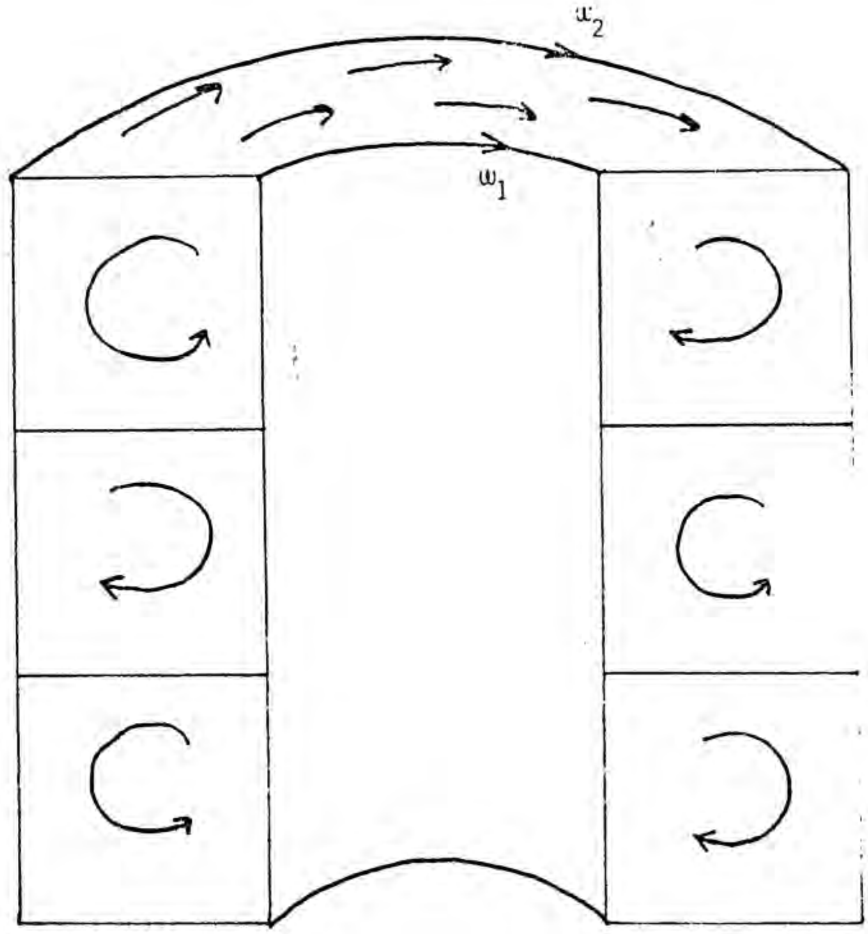

FIGURE 17-1 : CROSS-SECTION OF COUETTE FLOW

These are Taylor cells, and the flow within, which must be imagined superimposed on a cylindrical rotation.

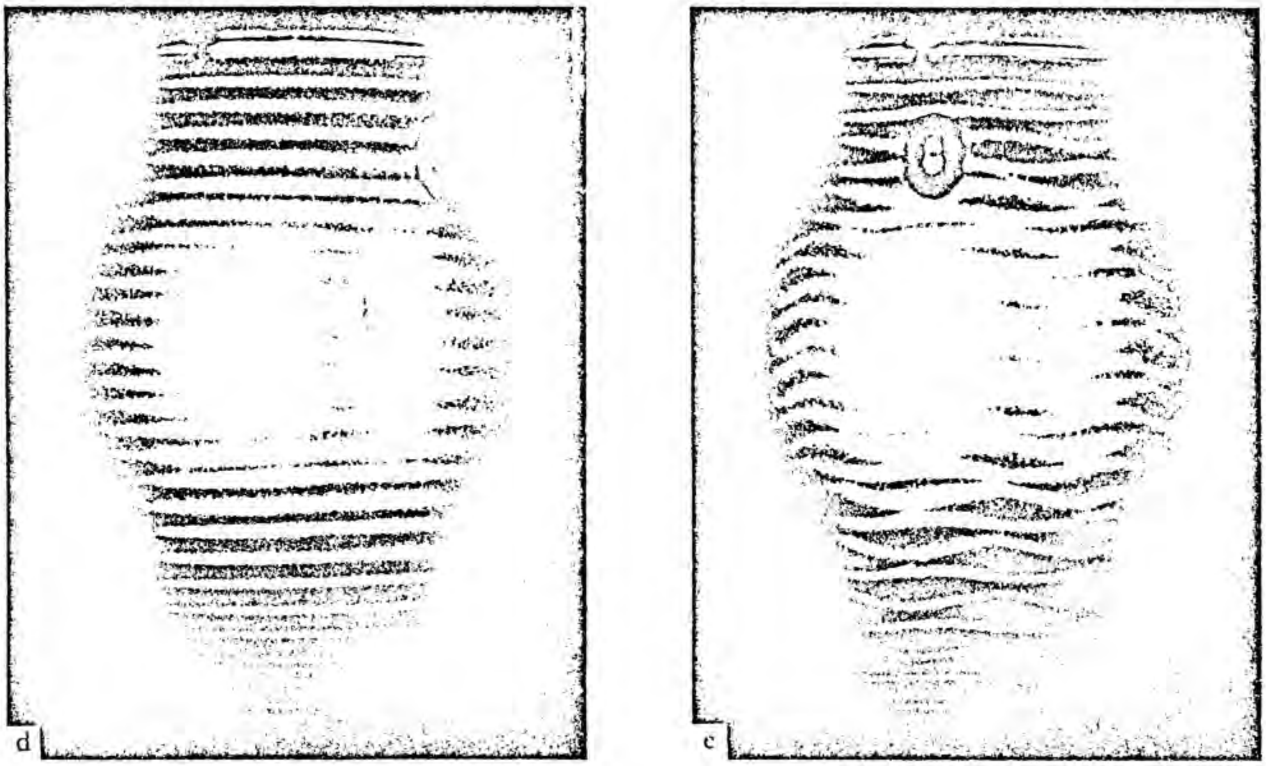

FIGURE 17-2 : TAYLOR CELLS IN COUETTE FLOW
Photographs of taylor cells through the transparent cylinder, before and after the first catastrophe, from Coles [401] .

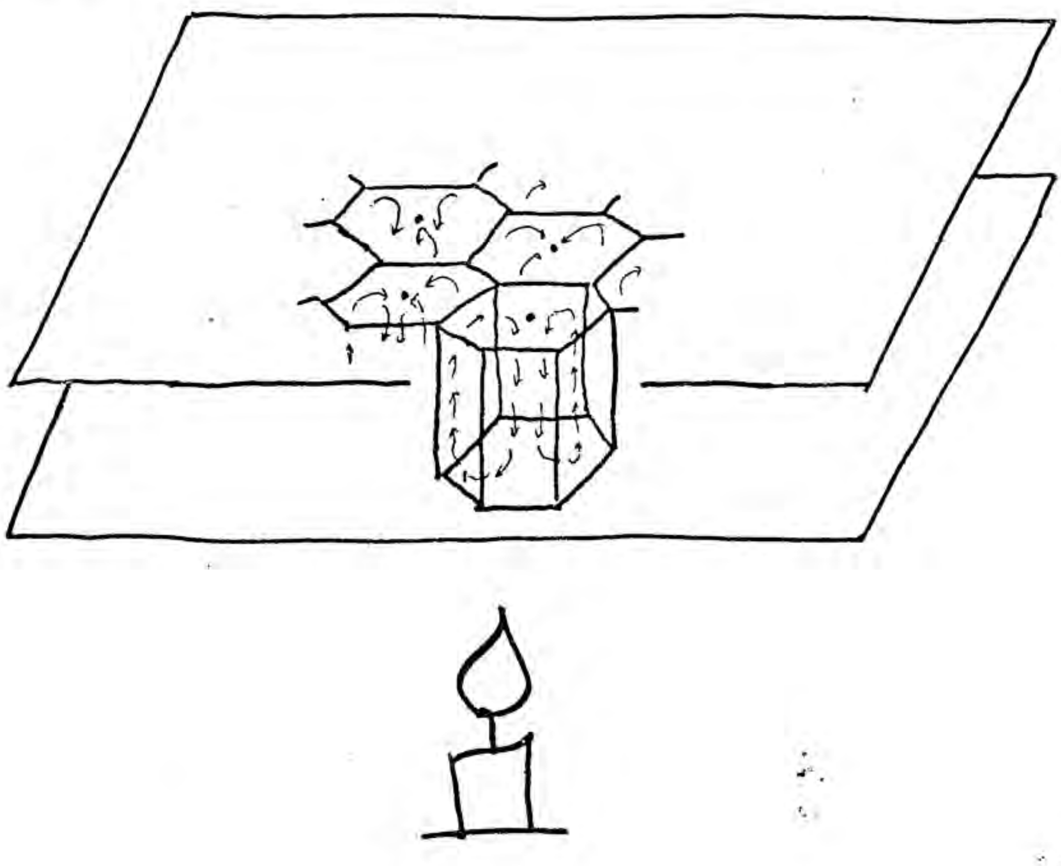

FIGURE 17-3 : (Same picture)

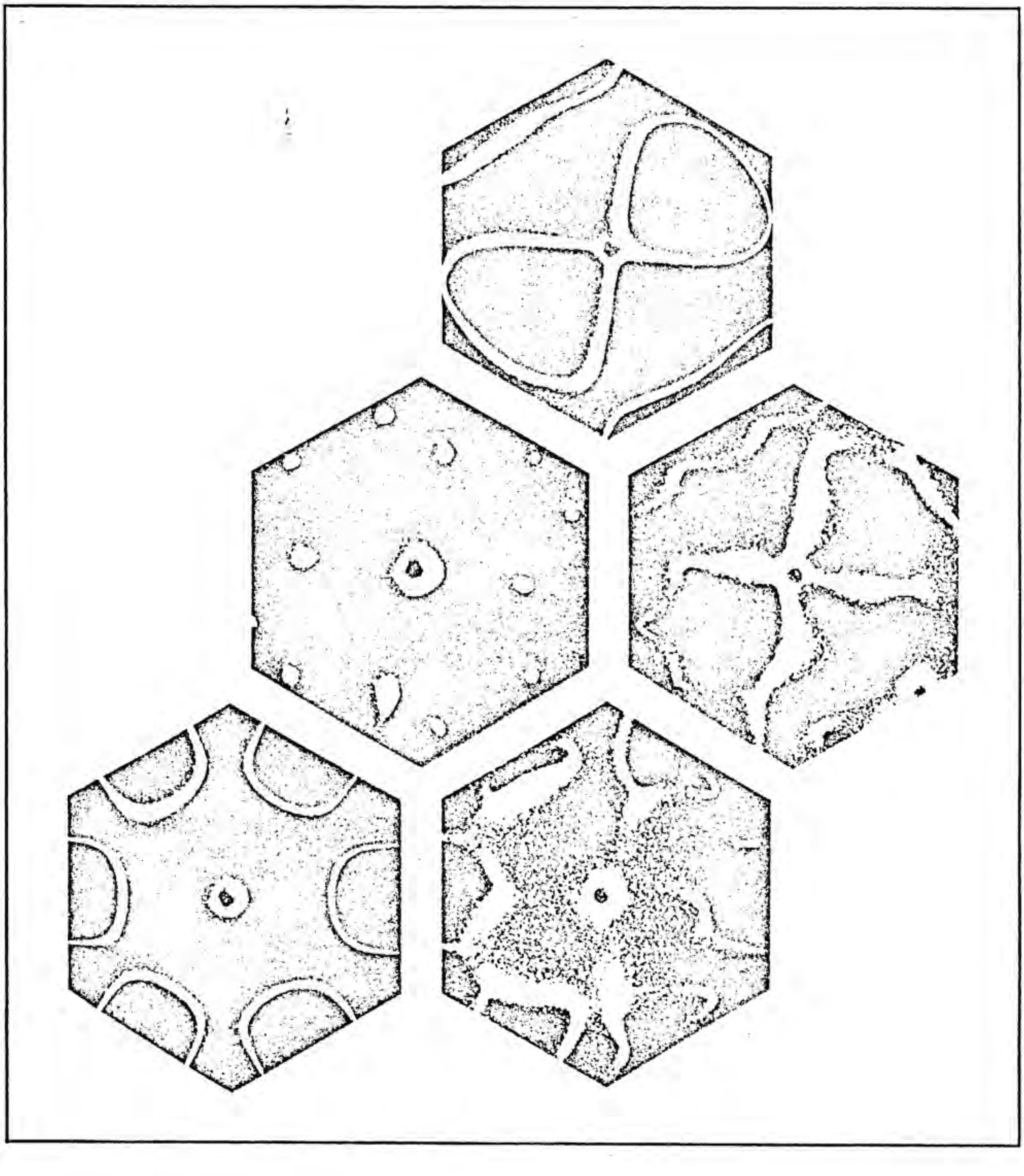

FIGURE 18-1 : KYMATIC CATASTROPHES
A sequence of photographs of sand on a vibrating plate, showing two successive catastrophes of the Chaldni nodal lines, as the frequency is changed. From Jenny [103] .

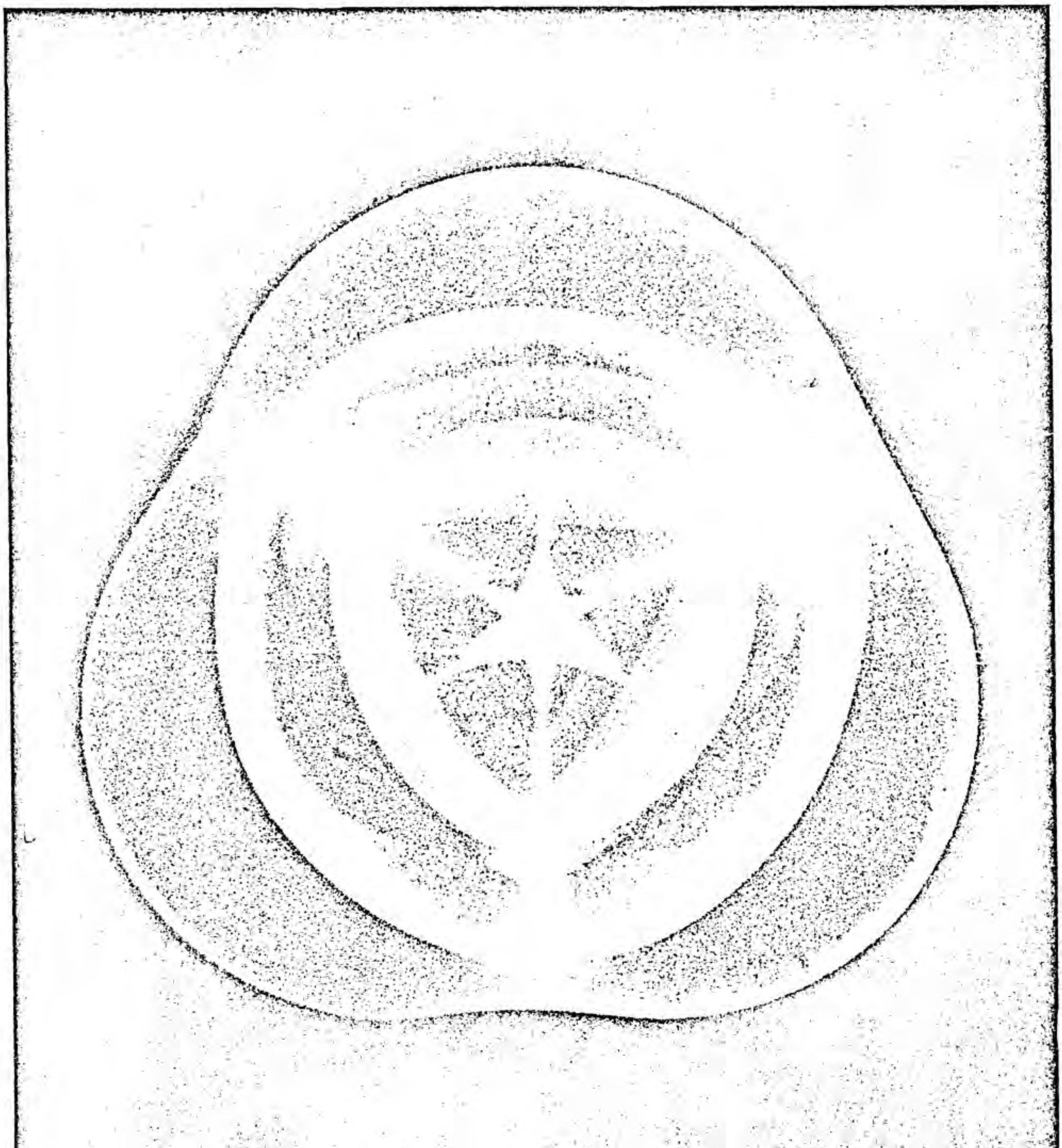

FIGURE 18-2 : KYMATIC MORPHOLOGY
Photograph of a drop of water on a vibrating plate, courtesy of Hans Jenny and Christiaan Stuten. The form changes penodically with the vibration, and changes to other forms as the frequency and amplitude are changed.

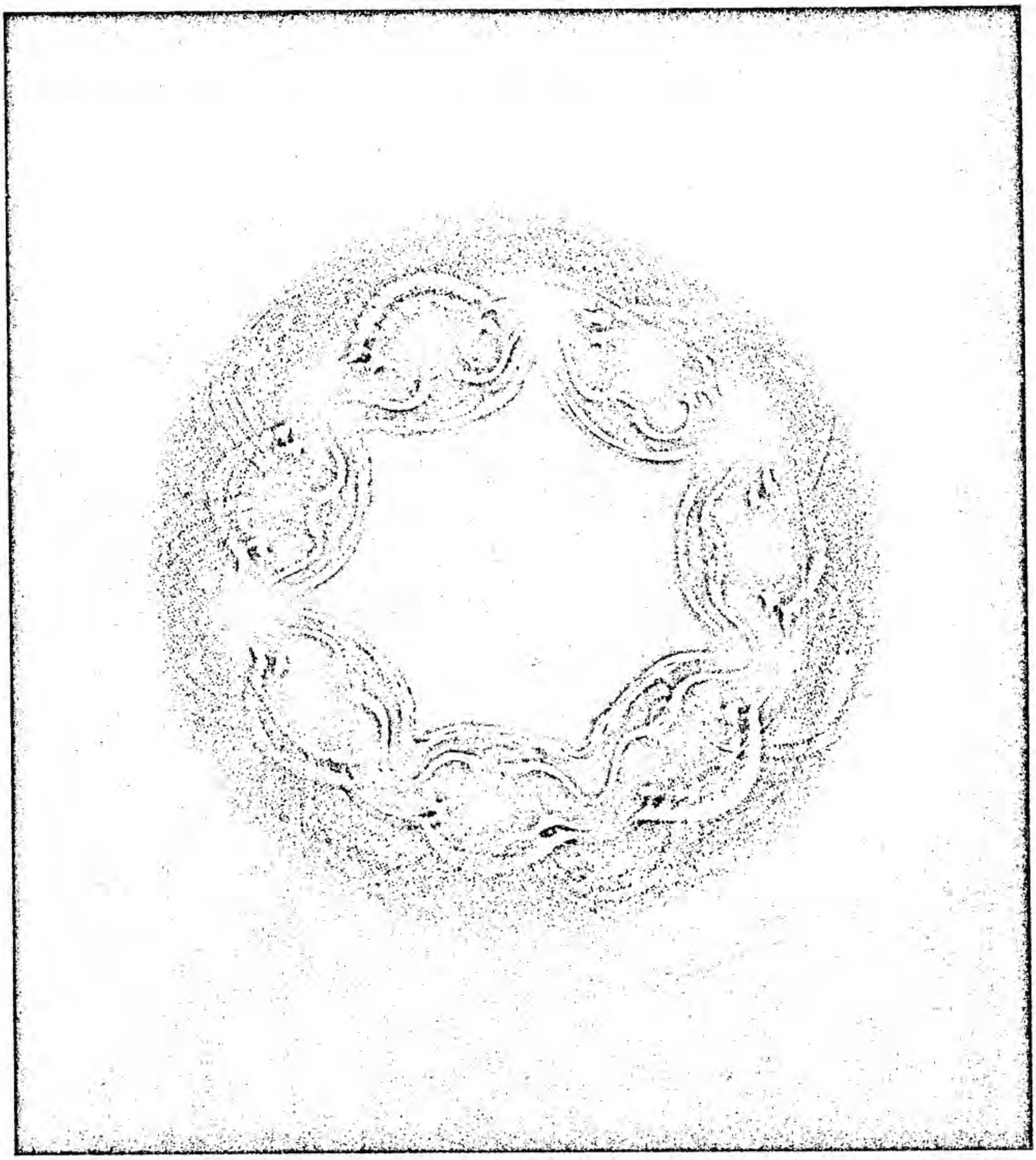

FIGURE 18-3 : VORTEX RING, TOP VIEW
Photograph of the fluid layer from above, a moment after the droplet has penetrated the upper surface, showing the density variation produced by the flow. From Schwenk [112] .

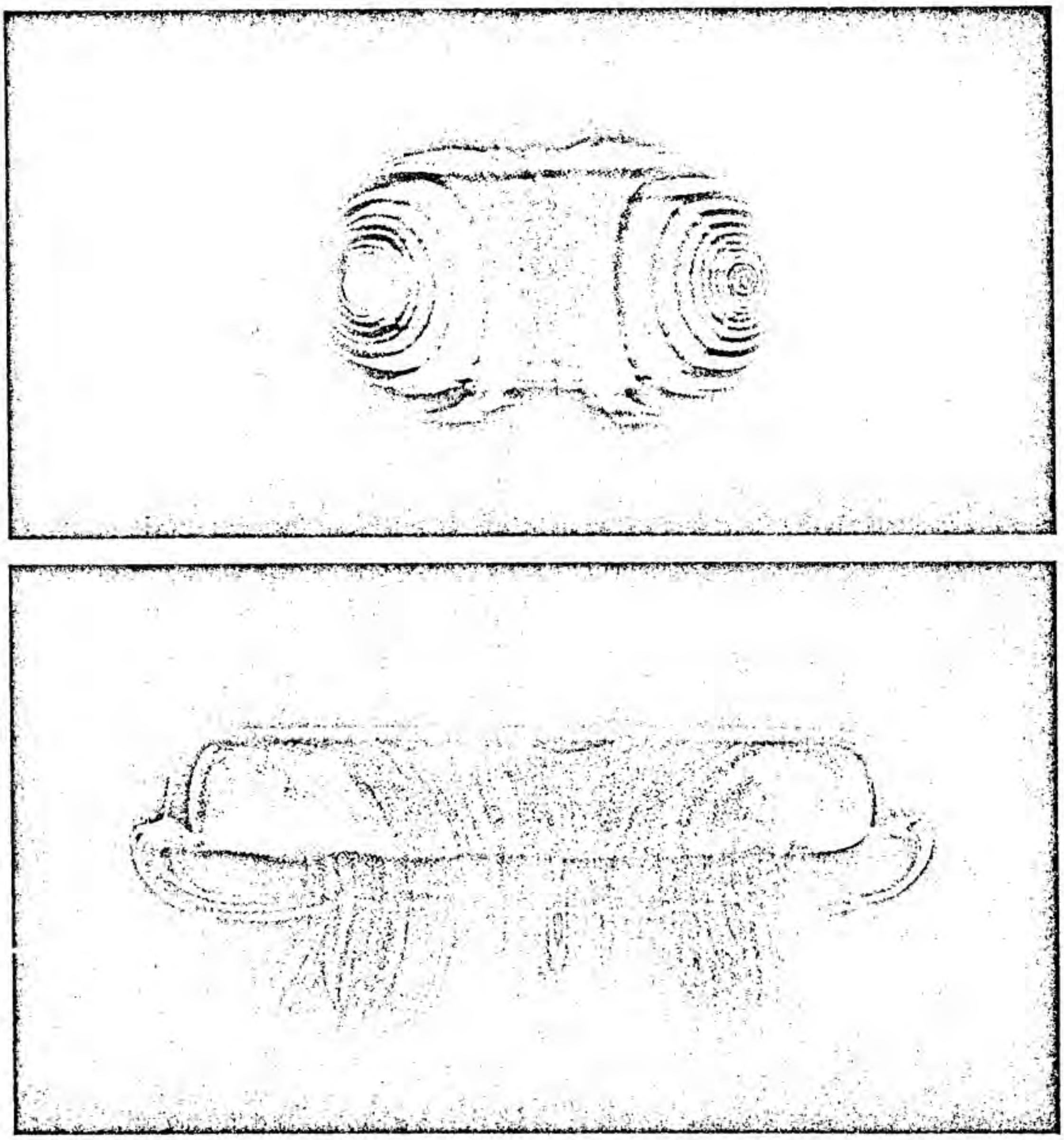

FIGURE 18-4 : VORTEX RING, SIDE VIEWS
Two successive views of the event shown from above in Figure 18-3. From Schwenk [112] .

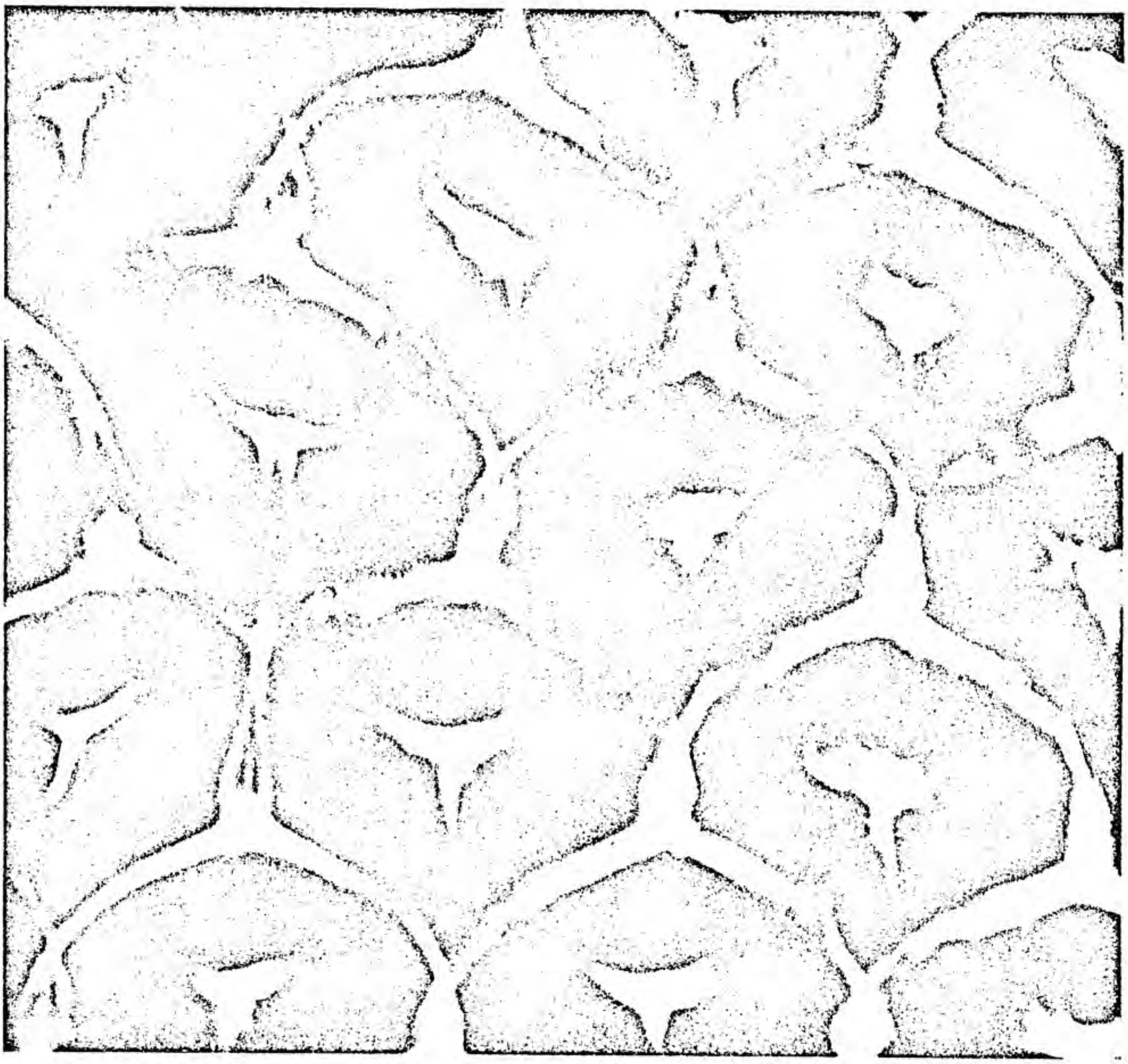

FIGURE 19-1 : THE WILLIAMS EFFECT
Electrostatic convection cells in a nematic liquid crystalline material. Photographed by the Liquid Crystal Group, Université de Paris-Sud (Orsay).

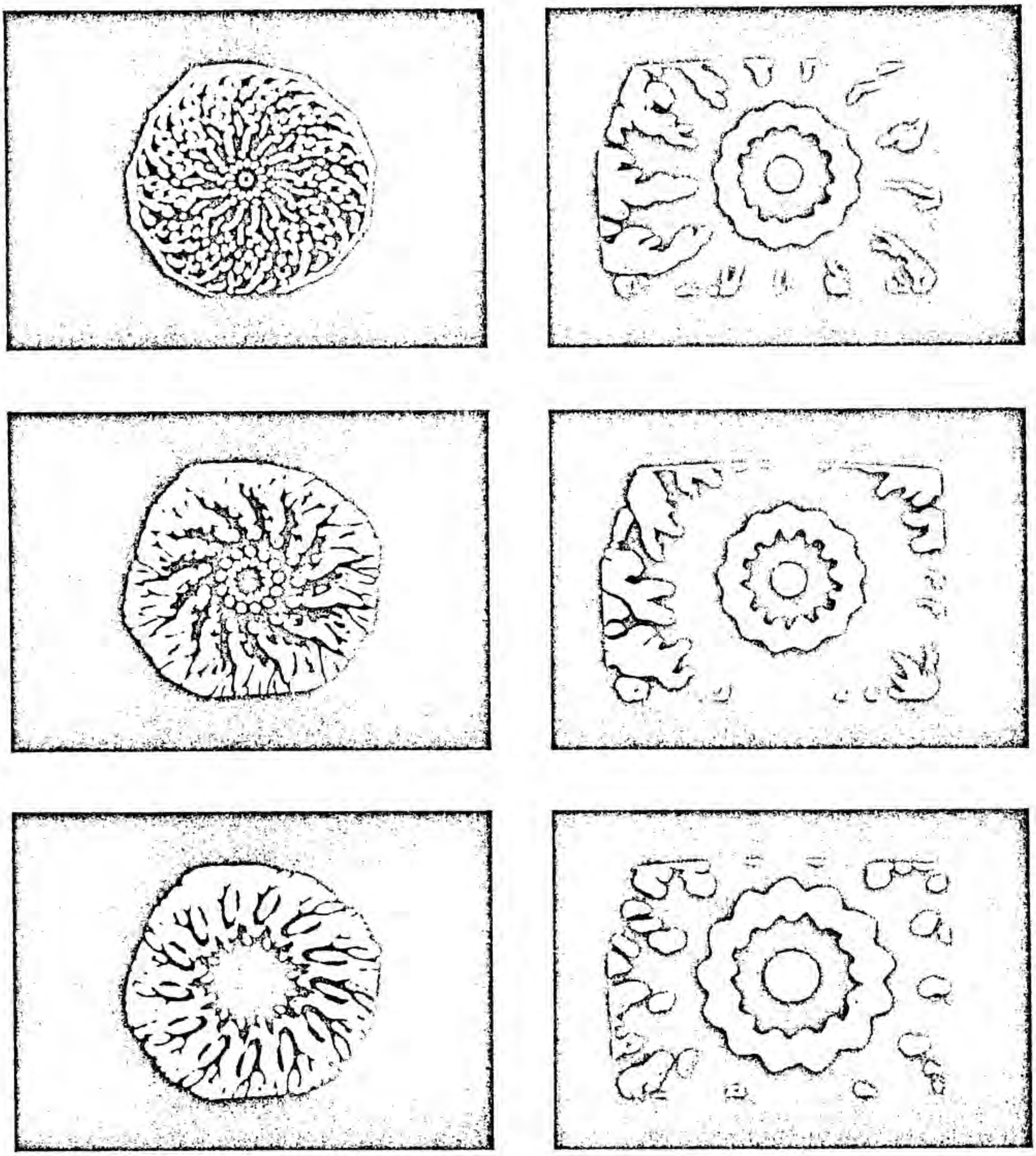

FIGURE 20-1 : VIDEO FEEDBACK
When the video camera looks at its own image on the monitor, with a slight angular misalignment, a morphogenesis in self-regulation is revealed on the screen. Here are shown two sequences from a videotape by Brian Woods.